General Disclaimer

One or more of the Following Statements may affect this Document

- This document has been reproduced from the best copy furnished by the organizational source. It is being released in the interest of making available as much information as possible.

- This document may contain data, which exceeds the sheet parameters. It was furnished in this condition by the organizational source and is the best copy available.

- This document may contain tone-on-tone or color graphs, charts and/or pictures, which have been reproduced in black and white.

- This document is paginated as submitted by the original source.

- Portions of this document are not fully legible due to the historical nature of some of the material. However, it is the best reproduction available from the original submission.

Princeton University

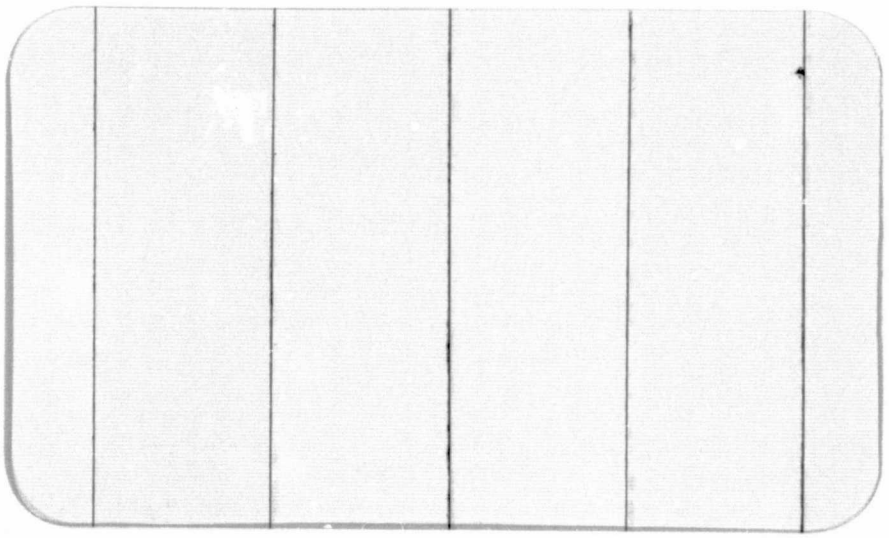

Department of Aerospace and Mechanical Sciences

National Aeronautics and Space Administration
NGL 31-001-005

PULSED ELECTROMAGNETIC GAS ACCELERATION

1 July 1974 to 31 December 1974

Semi-annual Report 634x

Prepared by: Robert G. Jahn

Robert G. Jahn
Dean, School of Engineering and
Principal Investigator

and

W. von Jaskowsky

Woldemar F. von Jaskowsky
Sr. Research Engineer and
Lecturer

Kenn E. Clark

Kenn E. Clark
Research Engineer

January 1975

School of Engineering and Applied Science
Department of Aerospace and Mechanical Sciences
PRINCETON UNIVERSITY
Princeton, N.J. 08540

ABSTRACT

Terminal voltage measurements with long cathodes in a high power, quasi-steady MPD discharge show that the critical current for the onset of voltage fluctuations, which was previously shown to be a function of cathode area, approaches an asymptote for cathodes of very large surface area. Floating potential measurements and photographs of the discharge luminosity indicate that the fluctuations are confined to the vicinity of the cathode and hence reflect a cathode emission process rather than a fundamental limit on MPD performance.

Photoelectric measurements of particular argon neutral and ion transitions show that the higher electronic states are populated more heavily than would be calculated on the basis of Saha-Boltzmann equilibrium at the local electron temperature and number density. Preliminary optical depth measurements show that for a current of 4 kA and an argon mass flow of 12 g/sec, a population inversion exists between the upper and lower states of the 4880 Å argon ion transition.

Measurements of current distributions in large hollow cathodes show that for a current of 7 kA and a mass flow of 4 g/sec, the cavity diameter and shape have little effect on the distribution of current within it. However, for a fixed cathode configuration, the current conduction pattern is sensitive to both the current and mass flow. For a given current, there is a well-defined range of mass flows for which the current penetrates deeply into the cavity, with the extent of current penetration increasing even further as the current decreases. Spectroscopic and photographic studies of AII radiance and electron densities within the cavity indicate a corresponding distribution of highly conducting plasma.

TABLE OF CONTENTS

	Page
Title Page	i
Abstract	ii
Table of Contents	iii
List of Illustrations	iv
Current Student Participation	v
I. INTRODUCTION	1
II. QUASI-STEADY MPD DISCHARGE	3
III. PLASMADYNAMIC LASER STUDIES	19
A. Plasma Species and Optical Depth Measurements	19
B. MPD Discharge in a Laser Cavity	36
IV. HOLLOW CATHODE STUDIES	42
PROJECT REFERENCES	71
GENERAL REFERENCES	89
APPENDIX: Semi-annual Statement of Expenditures	92

LIST OF ILLUSTRATIONS

		Page
1.	Cathode geometries	5
2.	Enclosed current contours	6
3.	Voltage-current characteristic	8
4.	4880 Å radiance patterns	9
5.	Onset current J*	11
6.	Onset voltage V*	12
7.	Voltage-current characteristics, 13.6 cm cathode	
	a. 6 g/sec	14
	b. 12 g/sec	15
8.	Voltage-current characteristics, 26.3 cm cathode	
	a. 6 g/sec	17
	b. 12 g/sec	18
9.	Calculated population inversions	22
10.	Optical arrangement	25
11.	PM response	27
12.	0.7503 μ (AI) radiance	30
13.	Optical depth measurements	33
14.	Two-dimensional discharge apparatus	37
15.	Optical cavity structure	41
16.	Hollow cathode facility	44
17.	Discharge apparatus	45
18.	Discharge current	47
19.	Cathode configurations	49
20.	Current and potential profiles	52
21.	Electric field in insulated channel	53
22.	Potential distribution	54
23.	Enclosed current in HC VI	56
24.	Hollow cathode VIII	57
25.	Spectra of HC discharges	59
26.	HC XII discharges	61
27.	Cavity potential dependence on external flow	63
28.	Current distributions in HC XII	64
29.	Active zone length	66
30.	HC operating regimes	68

CURRENT STUDENT PARTICIPATION

Student	Period	Degree	Thesis Topic
CAMPBELL, Edward M.	1972-	Ph.D. Cand.	Plasmadynamic Laser Studies
DUTT, Gautam S.	1971-	Ph.D. Cand.	Stimulated Emission of Argon Ion Lines in High Current Discharges
KRISHNAN, Mahadevan	1972-	Ph.D. Cand.	Hollow Cathode Discharges
NG, Charles	1974-	B.S.E. Cand.	Spectroscopic Study of Ionization in the MPD Exhaust Flow
PAULINE, Terri	1974-	B.S.E. Cand.	Cathode Emission Processes in MPD Discharges
RUDOLPH, L. Kevin	1973-		Cathode Studies in MPD Discharges
VILLANI, Daniel D.	1969-	Ph.D. Cand.	Power Deposition in MPD Discharges

I. INTRODUCTION

Following the move of the Electric Propulsion Laboratory from the Forrestal Campus to the Engineering Quadrangle in the spring of 1974, and the modifications to the experimental facilities which accompanied this move, full-time staff and student effort returned to the study of MPD discharges, plasmadynamic lasers and hollow cathodes. In the MPD portion of the program, one graduate student, M. Boyle, finished his Ph.D. thesis work, and will be presenting a summary paper of this work at the AIAA 11th Electric Propulsion Conference, March 19-21, 1975 at New Orleans, Louisiana. With his departure, one graduate student and one undergraduate student continue in this area. In one project, the influence of the cathode on arc performance and possible performance limitations are under investigation and are presented in Section II of this report. The other project is focused on cathode emission mechanisms and will be reported at a later date.

Three students are presently participating in the study of plasmadynamic lasers, using the quasi-steady MPD accelerator to generate a rapidly expanding dense plasma flow. Of the two Ph.D. programs, one of these includes optical depth measurements in the conventional three-dimensional MPD configuration and is discussed in detail in this report. The other doctoral program utilizes a two-dimensional geometry to produce a greater extent of uniform active plasma transverse to the flow. Since this latter project was reviewed in the previous semi-annual report, only a brief status report is included here. The undergraduate project in this area, recently begun, involves spectroscopic determination in the exhaust plume of the presence and distribution of excited and ionized species relevant to the collisional-radiative recombination model.

Significant progress has been made in the investigation of large hollow cathodes. Following an earlier series of tests that revealed an insensitivity of the current distribution to the hollow cathode configuration, one cathode was selected for study over a wide range of operating conditions. The large changes in the measured current distribution that are reported here will also be the subject of a second paper to be presented at the AIAA 11th Electric Propulsion Conference. Earlier results have been presented in a paper entitled "Hollow Cathode Physics" at the Third European Electric Propulsion Conference in Hinterzarten, Germany in October, 1974.

II. QUASI-STEADY MPD DISCHARGE

Cathode Studies (Rudolph)

Recent measurements of terminal voltage and potential distribution in the MPD discharge chamber have established the importance of the cathode region in determining the optimum accelerator performance. Earlier experiments in other laboratories showed that for a given propellant and mass flow, there appeared to be a maximum current that could be driven through the arc, beyond which erratic arc operation resulted.[A-1,A-2] This maximum current translated into a maximum thrust and specific impulse and thus put an upper limit on anticipated MPD performance. However, Boyle has recently shown that the erratic arc operation is related to the cathode surface area, and that for cathode surface areas up to 40 cm^2, the maximum current and hence the maximum attainable performance continues to increase.[159,163]

To verify this trend, a larger cathode (length, ℓ = 13.6 cm; surface area, A_c = 75 cm^2) was examined and a higher limiting current was observed.[159] More recently, a still larger cathode (ℓ = 26.3 cm, A_c = 158 cm^2) has been studied. In addition to terminal measurements to determine the maximum current for this cathode, current and potential distributions have been mapped in the vicinity of both the 13.6-cm and 26.3-cm-long cathodes to ascertain whether the erratic operation still originates near the cathode surface for these larger cathodes.

A second way in which the cathode influences accelerator performance derives from the intense plasma which forms immediately downstream of the cathode tip. The role of this cathode tip plasma in the overall acceleration process is unclear since it is a source of both a high pressure region on

the cathode face which leads to a positive thrust increment ("pumping"), and a high temperature which generates excited states in the plasma with consequent radiation and frozen flow losses. With the new long cathode, it is anticipated that the axial current components, which produce the cathode tip plasma via radial Lorentz forces, will be minimized, and hence the operation of an accelerator dominated by purely axial Lorentz forces can be studied.

The electron configuration with the 26.3-cm-long cathode is shown in Fig. 1 compared to the previous configuration with the 13.6-cm-long cathode. The 26.3-cm cathode is a 1.9-cm-diameter, stainless steel cylinder with a hemispherical tip. The upstream beveled edge of the cathode serves as the inner wall of a mass injection annulus at the base of the cathode.[163] Unless otherwise noted, the mass flow, $\dot{m}$, is 6 g/sec of argon equally divided between the cathode base annulus and 12, 0.32-cm-diameter injection ports equally spaced at a radius of 3.80 cm in the backplate of the discharge chamber.

To determine whether a significant radial "pumping" force exists for this electrode configuration, the local magnetic field distribution was measured at a total current, J, of 16 kA. The resulting enclosed current contour plot is shown in Fig. 2. Two features of this current distribution are immediately apparent. The first is that the current does not completely cover the cathode surface, in contrast with all previous cathodes where current was observed to attach over all of the cylindrical surface as well as the downstream end of the cathode. Since it is the axial component of current associated with this tip attachment that produces the radial "pumping" force, the resulting cathode tip plasma should be absent with this long cathode. The second feature is that despite the attainment of a current distribution that

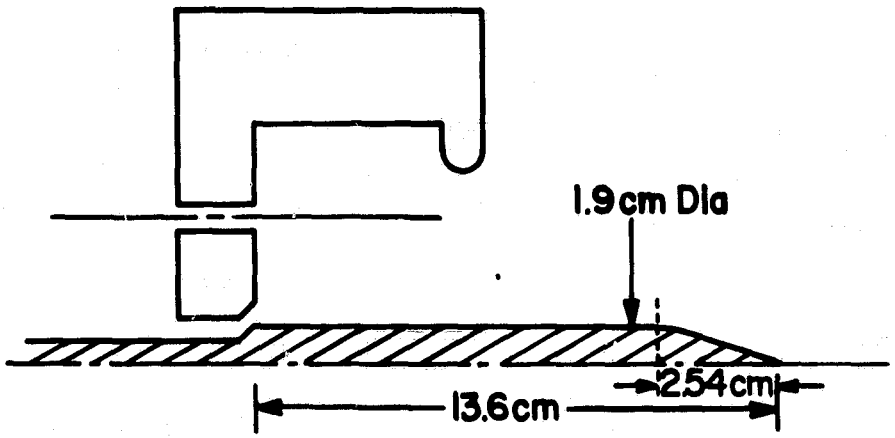

a) 13.6 cm CATHODE

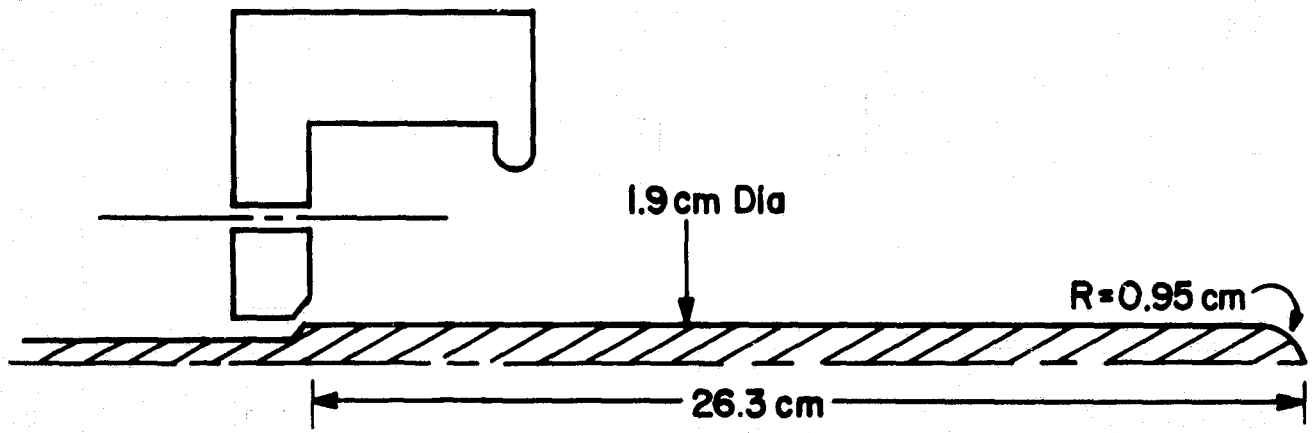

b) 26.3 cm CATHODE

CATHODE GEOMETRIES

FIGURE 1
AP25-5071

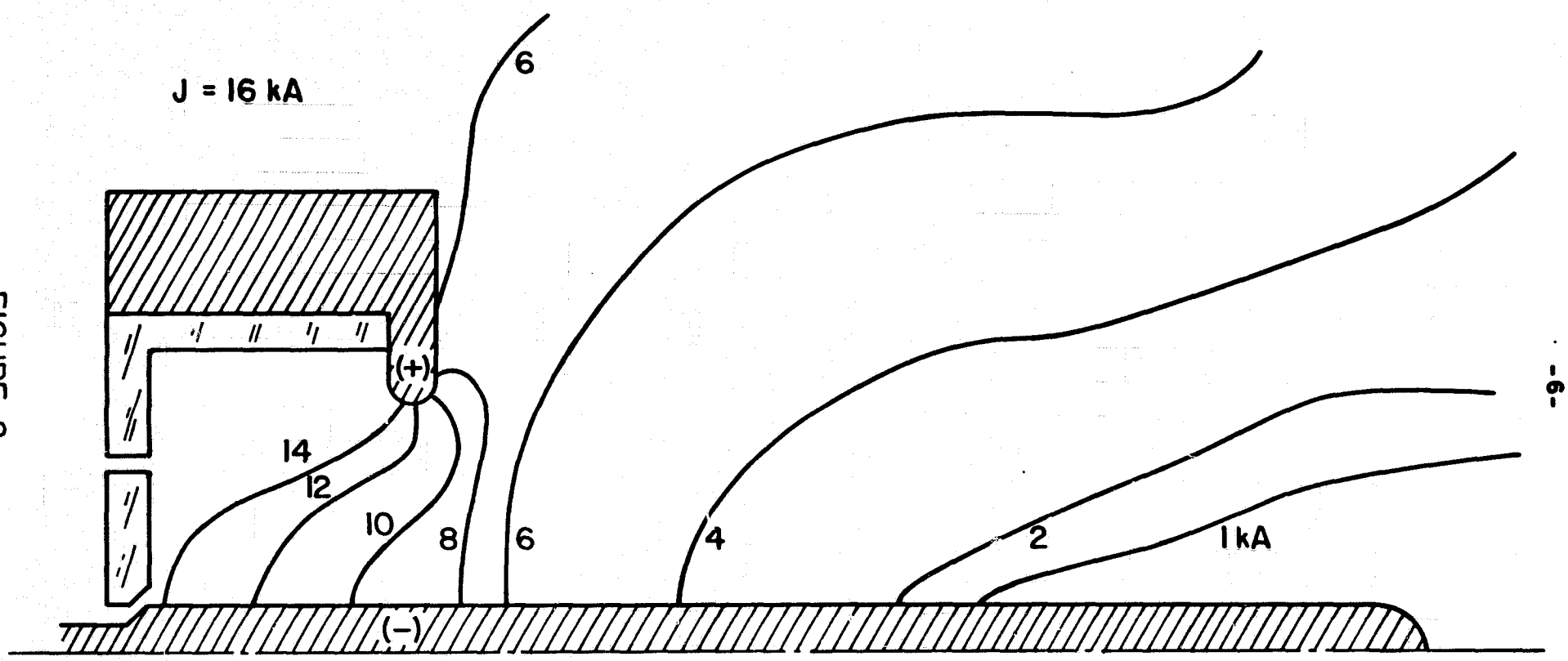

ENCLOSED CURRENT CONTOURS

FIGURE 2
AP 25-5123

does not cover the cathode tip, a significant axial current component still exists near the cathode surface for the furthermost downstream 4 kA. This component of current compresses the plasma against the cathode surface thereby converting some fraction of the kinetic energy into thermal energy and obscuring the analysis of the purely "sweeping" type accelerator. It thus appears that for this type of cathode, it is not possible to produce a current distribution which is only radial in the vicinity of the cathode. Further study of the cause of the axial current components, although interesting, has been delayed until after the effect of these large cathodes on the terminal properties of the arc and thus on the maximum practical current has been determined.

Spurious or erratic arc operation is most easily detected by fluctuations in the arc terminal voltage. Figure 3 shows a typical voltage-current characteristic for the 26.3-cm long cathode at a mass flow of 6 g/sec. The onset of voltage "hash" is seen to occur at a critical or onset current J* of 25 ± 2 kA for which the terminal voltage V* is 160 ± 25 V. Similar voltage-current characteristics obtained with this same cathode at other mass flows indicate a critical current which scales such that the parameter $J^{*2}/\dot{m}$ is a constant. For this configuration, the constant is 96 ± 10 $kA^2 \cdot sec/g$, which lies considerably above the value of 40 originally proposed as a fundamental limit for an accelerator operating with argon.

The changes in the discharge radiance and structure as the onset current J* is reached are clearly displayed in the two perspective photographs shown in Fig. 4. These photos were taken through a 4880 Å (AII) narrow bandpass filter and show the 26.3-cm cathode at a mass flow of 6 g/sec for a subcritical current of 17 kA (Fig. 4a) and the critical current of 25 kA (Fig. 4b). The flow in these photographs is from

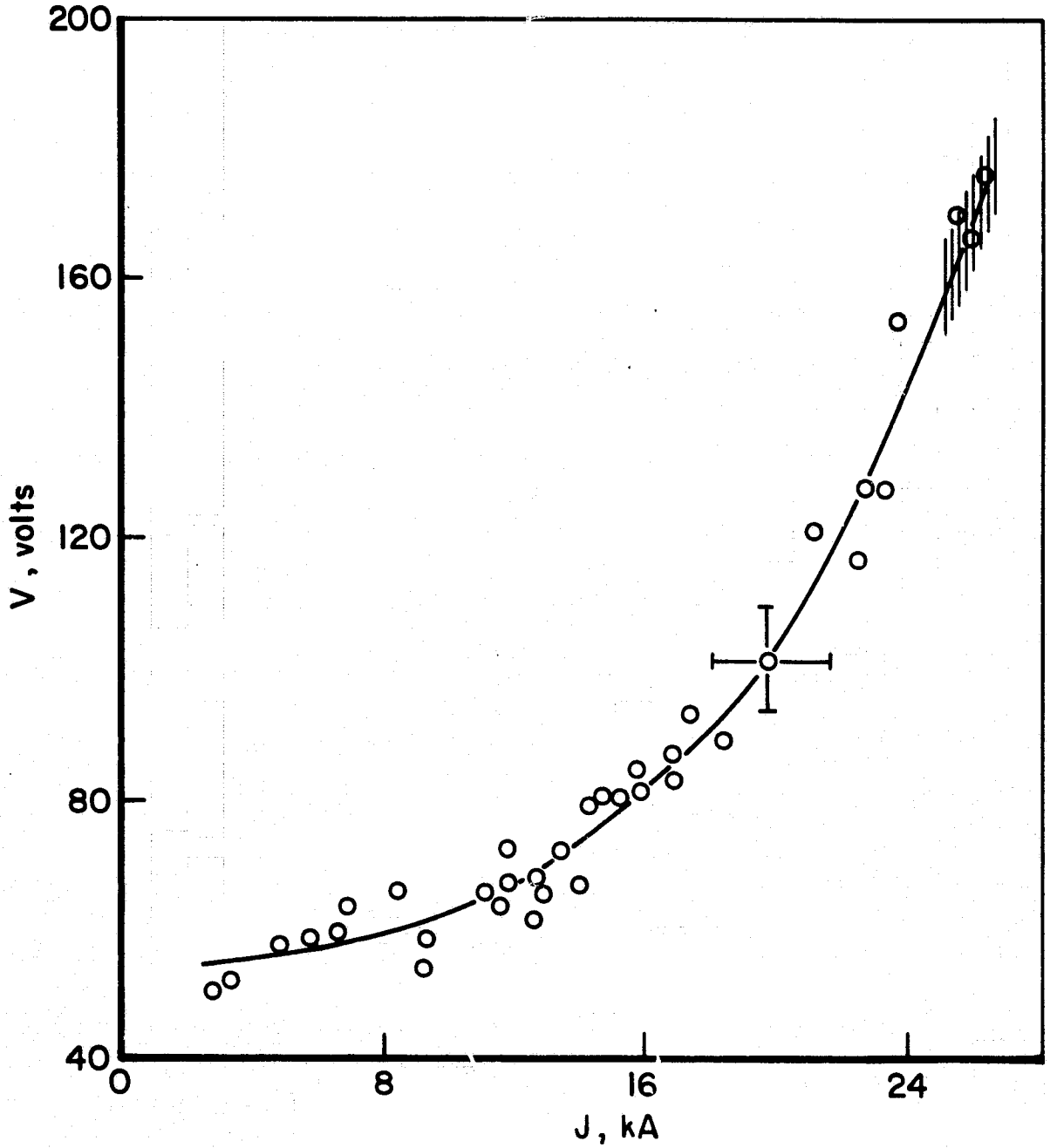

VOLTAGE-CURRENT CHARACTERISTIC

FIGURE 3
AP 25-5124

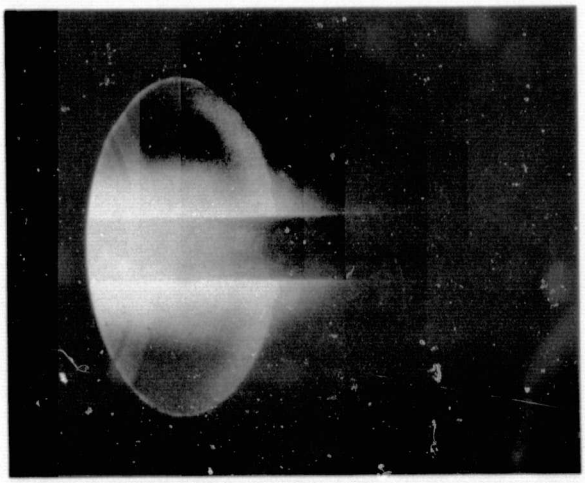

a) J = 17 kA

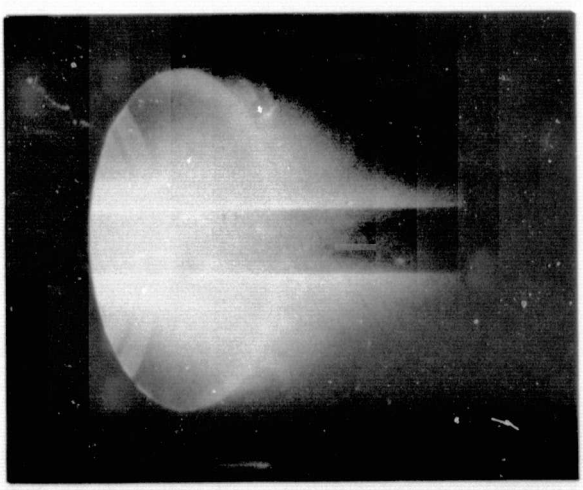

b) J = 25 kA

4880 Å - RADIANCE PATTERNS

FIGURE 4

left to right with the tip of the cathode extending downstream approximately one anode diameter beyond the field of view. For currents below the critical current, the argon ion luminosity is seen to be diffuse and symmetric about the cathode axis. However, at the critical current, a well-defined luminous shell has formed approximately 8 mm away from the cathode surface. The tendency for this shell to increase in diameter at the more downstream locations suggests a magnetic nozzle effect which has been used previously to explain the plasma acceleration downstream of the arc chamber for shorter cathode configurations.[159,162] Another feature of the photographs worth noting is the increased incidence of intensely luminous cathode spots at the critical current.

The values of the onset current and voltage for both the 13.6 and 26.3-cm cathodes are plotted against cathode area in Figs. 5 and 6, respectively. Also shown in the figures are the critical values measured by Boyle for a similar configuration but using tungsten cathodes instead of stainless steel,[159] and the values measured by Villani using stainless steel cathodes and a 20-cm-long cylindrical aluminum anode whose inner diameter of 10.2 cm equals the orifice diameter of the anode plate used to obtain the present data.[165] Referring to Fig. 5, the results show that increases in the cathode surface area can greatly increase the maximum current achievable before voltage fluctuations ensue. However, the effect is not unlimited, and at the larger cathode areas, an asymptotic value of the onset current is reached: approximately 25 kA for the present anode orifice plate configuration and about 31 kA for the cylindrical anode. These two distinct asymptotic values indicate that care must be taken in attributing the "hashy" voltage onset to cathode effects alone.[163]

In Fig. 6, the terminal voltage at which fluctuations first appear is shown to be a weakly varying function of cath-

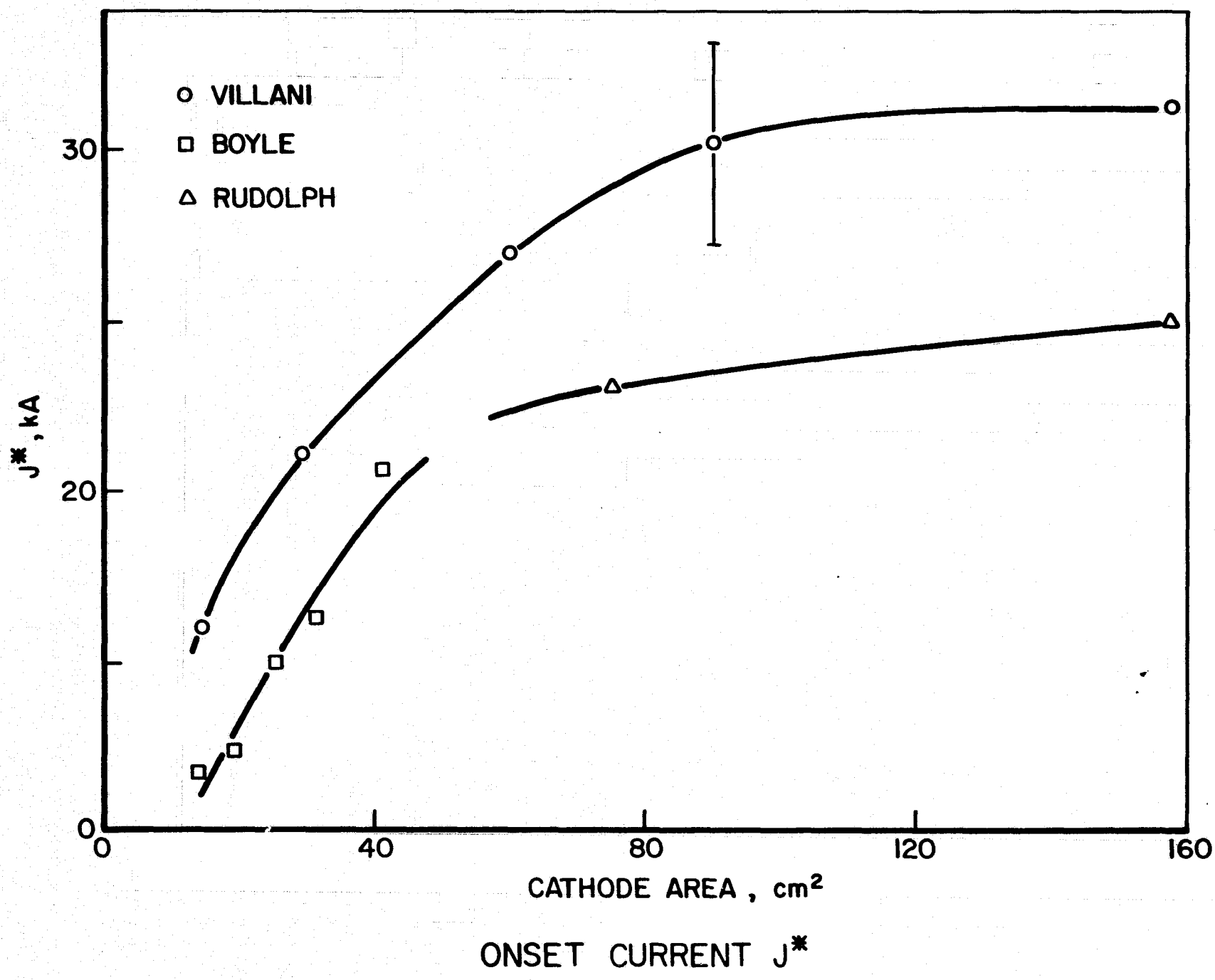

FIGURE 5
AP25-5125

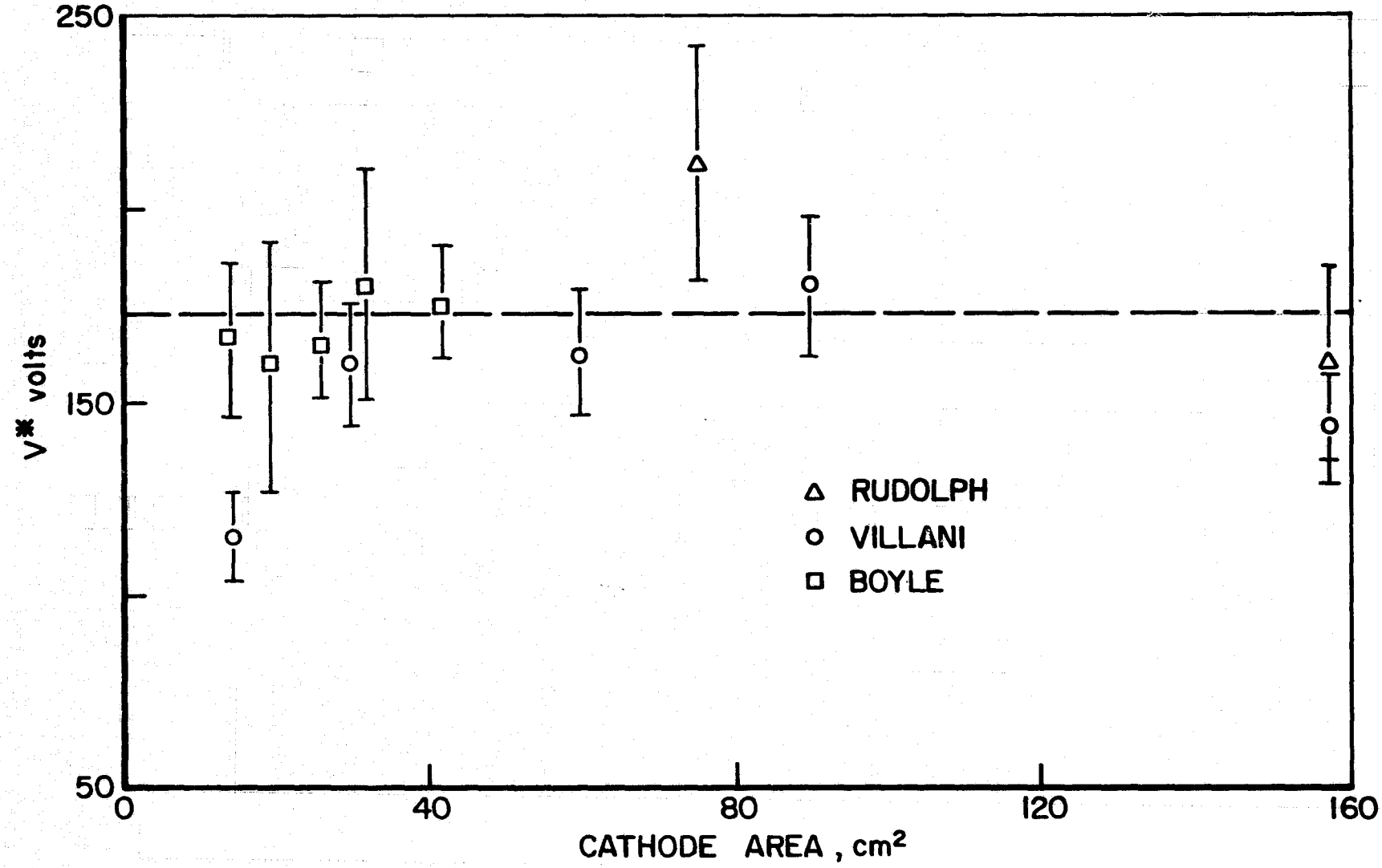

FIGURE 6
AP 25-5137

ode area, even with the large changes in anode configuration and cathode material. To first order, this onset voltage can be approximated by a constant value of 170 V. This suggests that if the fractional distribution of potential does not change greatly with cathode configuration, then the voltage fluctuations may originate in one specific region of the discharge when the local electric field exceeds a particular critical value.

Following experiments by Boyle which showed that the voltage fluctuations appeared to originate at or near the surface of the smaller cathodes,[163] floating potential measurements were made in the vicinity of both the 13.6 and 26.3-cm cathodes. The floating potential probe consists of a 0.25-mm-diameter tungsten wire of which 2 mm is exposed to the plasma. Tektronix P-6007 voltage probes were used to measure the differential potential drop between the cathode and the probe, V_c , and between the anode and the probe, V_a. The floating potential was measured a few millimeters off the cathode surface, and at each location the sum of V_c and V_a was shown to agree with the terminal voltage within experimental error. Since the potential was found to be only weakly dependent on axial position, the data presented here were obtained with the probe at a fixed position in the anode plane.

The cathode voltage and terminal voltage for the 13.6-cm cathode are compared in Figs. 7a and 7b for mass flows of 6 and 12 g/sec, respectively. Like the terminal voltage, the cathode voltage also displays a transition to a hashy signature as the current is increased. The regions where voltage fluctuations were observed are shown in the figure for both the cathode voltage and the terminal voltage. At each mass flow, the cathode voltage is seen to become hashy at approximately the same current as the terminal voltage indicating that the fluctuations in the terminal voltage probably orig-

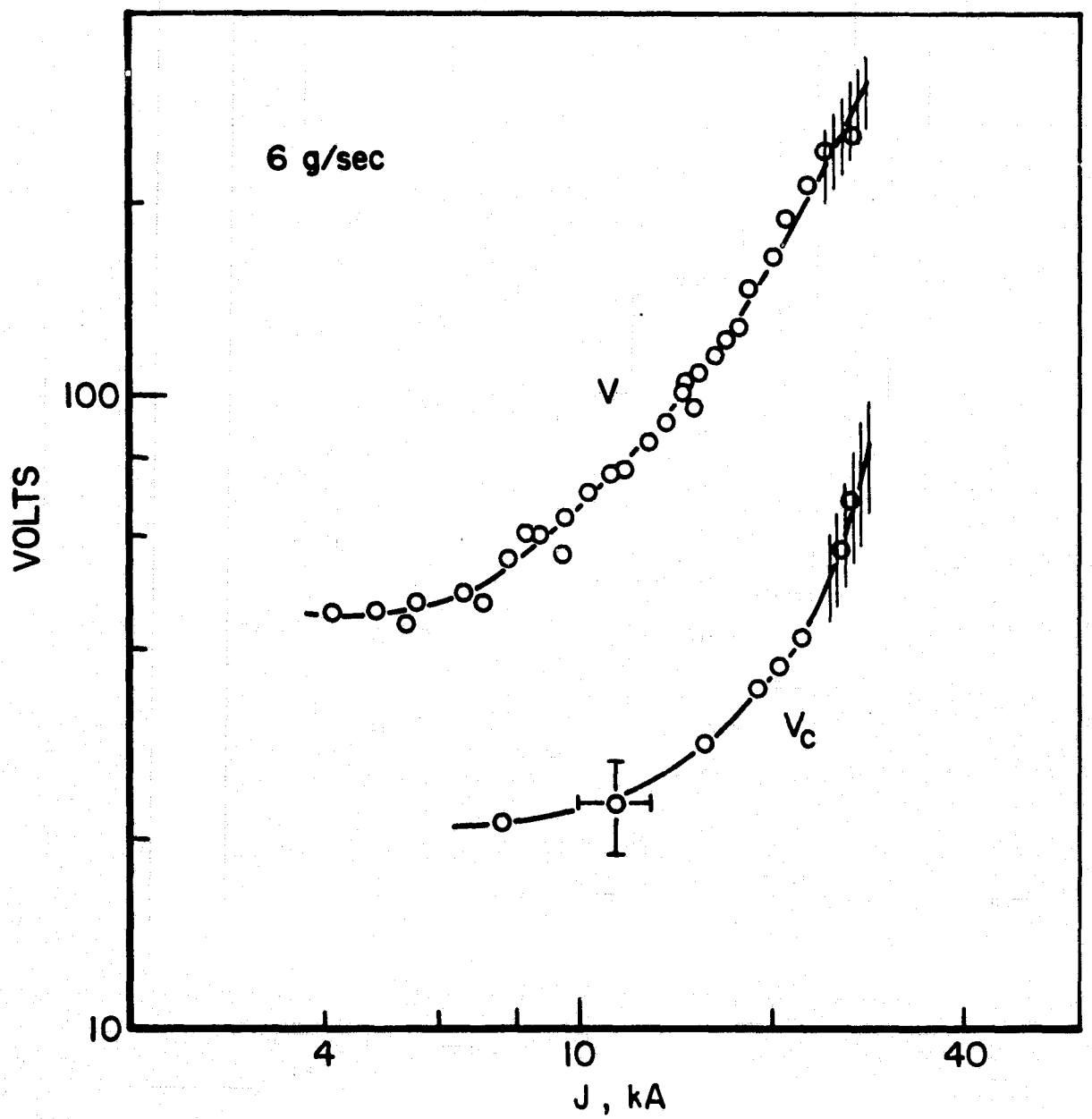

VOLTAGE-CURRENT CHARACTERISTICS , 13.6 cm CATHODE

FIGURE 7a

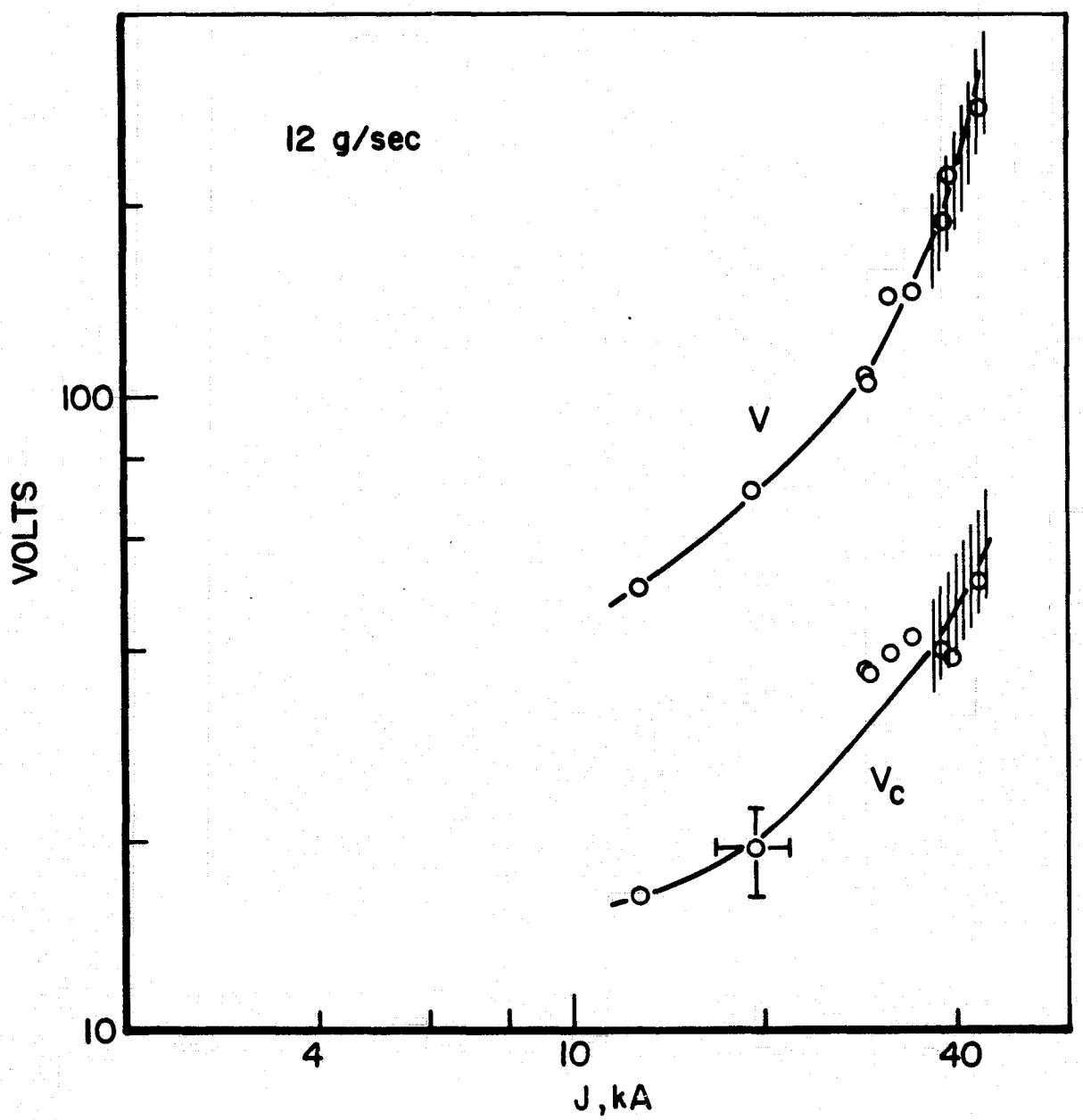

VOLTAGE-CURRENT CHARACTERISTICS, 13.6 cm CATHODE

FIGURE 7b

inate in the vicinity of the cathode. The data for the 26.3 cm cathode, shown in Figs. 8a and 8b, lead to a similar conclusion.

It is also interesting to note that the cathode onset voltages are not all the same. Thus, based on these data alone, it does not appear that there is a particular value of the electric field near the cathode, beyond which voltage fluctuations occur regardless of the cathode configuration.

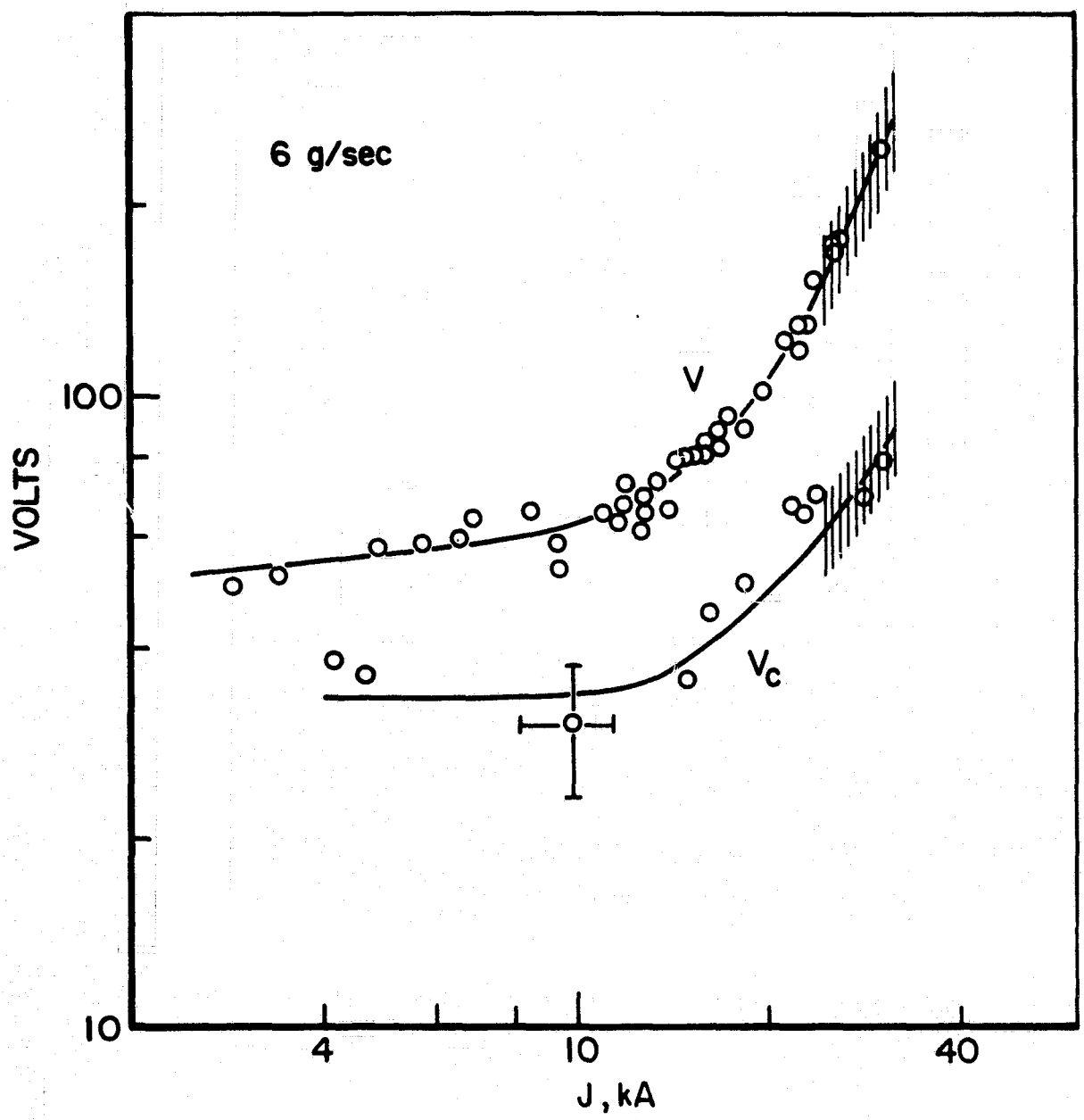

VOLTAGE - CURRENT CHARACTERISTICS, 26.3 cm CATHODE

FIGURE 8a

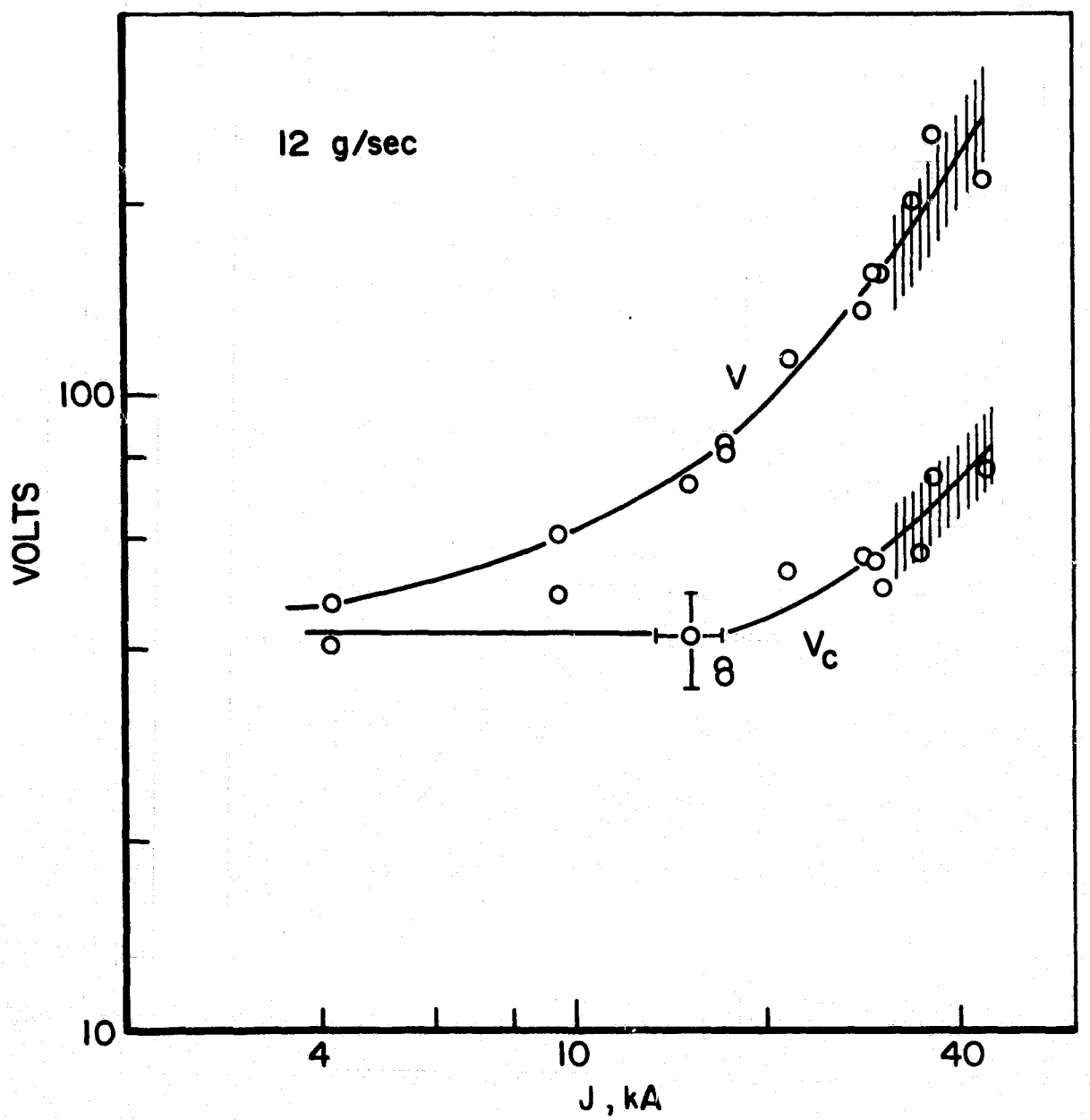

VOLTAGE-CURRENT CHARACTERISTICS , 26.3 cm CATHODE

FIGURE 8b
AP25-5130

III. PLASMADYNAMIC LASER STUDIES

A. Plasma Species and Optical Depth Measurements (Campbell)

The development of laser systems capable of producing high power, coherent radiation in the visible and shorter wavelength regions of the spectrum has recently begun to generate considerable interest. The attractiveness of such a device results from its many potential applications: Raman scattering studies, isotope separation and other wavelength selective chemical syntheses, space communications, basic studies in the electronic structure of atoms and molecules, non-linear optics, and laser fusion.

At present, gaseous laser systems with output in the visible are primarily of the electric discharge type ($I < 100$ amps, fill pressure $\approx$ 0.5 torr). These lasers are limited to relatively modest CW output power ($< 10^3$ W, multimode) due to material problems associated with the large energy flux from the lasing medium to the electrodes and enclosing walls.[A-3] A more fundamental limitation may exist however, since it has not been conclusively established that output power increases monotonically with power input to the working gas; saturation effects may result from the particle kinetics which establish and maintain the inversion.

CW operation in the ultraviolet ($\lambda < 0.4\ \mu$) has been obtained with noble gases in low pressure electric discharges with considerably lower output power ($\approx$ 10 W, multimode).[A-4] The limitations on these systems are basically the same as for the visible lasers. Pulsed operation in the UV using high current electric discharges (e.g. the TE N_2 laser at 0.337 μ) and relativistic e-beams (e.g. molecular xenon at 0.174 μ) has produced output powers of 10^6 W for pulse durations of 10^{-9} to 10^{-6} sec.[A-4]

In all of these systems, pumping of the upper laser level arises predominantly from inelastic collisions between lower lying states and electrons or heavy particles. An alternate process for creating population inversions between electronic levels occurs in the recombination phase of a highly ionized, nonequilibrium plasma. In this scheme, pumping of the upper laser level initiates from higher lying energy states, i.e. the continuum, the bound states of the next higher ionization level, and the bound states of the ion or neutral in question. It is this latter mechanism which is discussed more thoroughly in the following section and is examined experimentally in the highly nonequilibrium expansion of the plasma flow from an MPD accelerator.

Theoretical Considerations

The complete description of a plasma which is not in local thermodynamic equilibrium requires a detailed knowledge of processes occurring on a microscopic scale. In such a description, the distribution of the neutral and ionic species over their internal energy states is not given by the familiar Boltzmann relation (with the kinetic temperature of the collision dominating species, the free electrons, as a parameter), but must be determined from a set of coupled differential equations encompassing all appropriate collisional and radiative processes. The free electron number density is not given by the Saha relation using the local value of the electron temperature, but must also be found from conservation considerations.

Because of the complexity of the problem and the large uncertainties in the various rate coefficients, no general solution appeared in the literature until 1962. In that year, Bates et al. developed a statistical theory which described the nonequilibrium phenomena of collisional-radiative

relaxation of hydrogenic plasmas.[A-5] The theory employs the fact that over a wide range of electron number density and temperature, the relaxation time for the excited states, τ_k, is much shorter than the relaxation times for both the ground state, τ_1, and for the free electrons, τ_e. It can be shown that for a fixed electron temperature, T_e,

$$\frac{\tau_k}{\tau_e} \sim \frac{n_k}{n_e} C \qquad (1)$$

where n_k is the number density of the k^{th} level ($k \geq 2$), n_e the number density of free electrons, and C a constant, at most of order 1. Thus, as long as $n_k \ll n_e$, the populations of the excited states can be assumed to adjust instantaneously to any change in the electron temperature without altering the free electron or ground state number densities. It follows that little error is incurred by setting the net production rate for the excited levels equal to zero. Using this "quasi-steady" assumption, the excited level populations and the collisional-radiative decay coefficient can be determined as a function of n_e, T_e and the ground state number density, n_1.

This type of calculation is illustrated in Fig. 9 in which the inversion ratio $g_2 n_4 / g_4 n_2$ is plotted against the recombination rate, $\dot{n}_e$, for an optically thin hydrogen plasma. It is seen that inversions occur if the incoming electron flux from the continuum to the bound levels is large enough to significantly perturb the bound-bound collisional and radiative processes (note the threshold behavior at $\dot{n}_e \approx 10^9$ cm^{-3} sec^{-1}). However, if the flux is too great, e.g. at large values of n_e, then collisional processes which tend to thermalize the excited level populations will dominate and the inversions will be destroyed. The figure also shows the strong dependence of

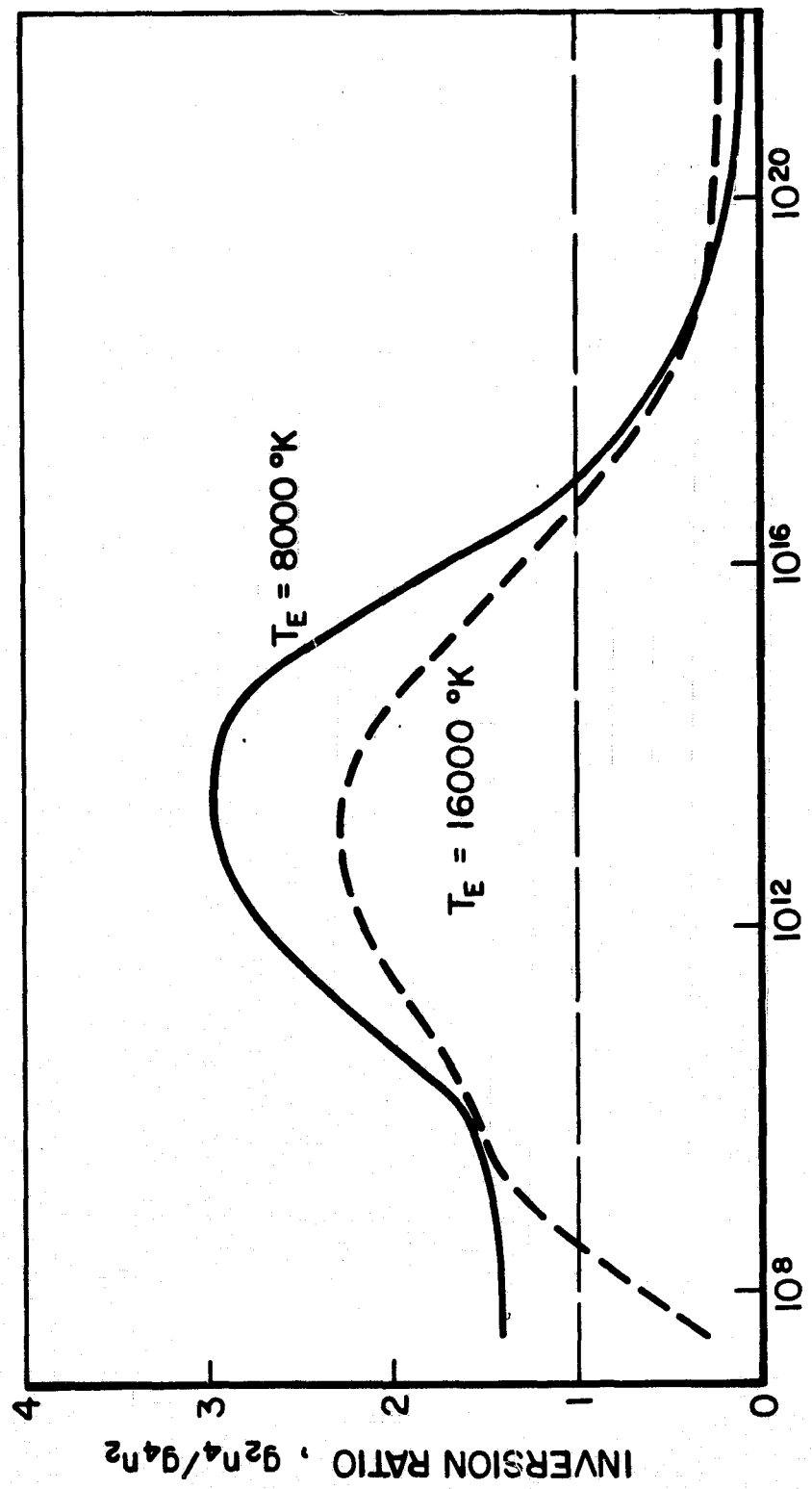

FIGURE 9
AP 25-5131

the recombination rate and thus the inversion ratio on the electron temperature.

A practical method of producing the rapid cooling necessary to generate inversions by this mechanism is the supersonic expansion of a highly ionized plasma into a region of reduced pressure. Because of the relatively long relaxation time for the free electrons as compared to the local flow residence time, ionizational nonequilibrium results, from which population inversions can be created by the collisional-radiative recombination processes. Bohn has proposed a plasmadynamic laser based on this mechanism which is capable of high power ($10^5 - 10^6$ W) CW operation in the visible and UV.[A-6] Other theoretical studies conducted by Gudzenko and Shelepin,[A-7] and Gol'dfarb and Lukyanov[A-8] for hydrogen plasmas, and Bowen and Park[A-9] for nitrogen plasmas have also indicated the feasibility of this process for creating inversions. Experimental verification using low power ($\approx 10^4$ W) steady-state arc facilities has been provided by Gol'dfarb et al in argon,[A-10] Bowen and Park in carbon at 0.248 μ,[A-11] Hoffman and Bohn in hydrogen,[A-12] and Irons and Peacock in C^{5+}.[A-13]

The quasi-steady MPD accelerator offers two advantages over the low power, steady-state plasma accelerator for studying the plasmadynamic flow processes which can lead to inversions. First, the quasi-steady MPD accelerator is capable of operating over a wide range of mass flows, arc currents and propellant species, making accessible the entire power spectrum from a few tens of kilowatts typical of the steady devices, up to 100 MW. Second, because of the pulsed nature of the MPD discharge ($\approx$ 1 msec), diagnostic probes can be used which are not generally suited to the hostile plasma environment in the steady devices. Using these diagnostics, it should be possible to establish the dependence of the inversions on various plasma parameters. Thus, the MPD accelerator may

provide a viable alternative to short-pulse, nonflowing systems for the development of high power visible and UV lasers.

Experimental Program

In order to examine the applicability of the relaxation model to the MPD exhaust plasma, photoelectric studies have been conducted in the near infrared, visible, and ultraviolet regions of the spectrum. From the measured intensity of line radiation from various neutral and ionic transitions, it should be possible to establish the deviation of the relative populations from that which would be calculated using the Saha relation at the local value of n_e and T_e. In addition, the optical depth of the 0.4880 μ AII line was measured to determine directly whether a population inversion occurs between the upper and lower states of this transition.

A schematic of the optical arrangement for studying the plasma flow is shown in Fig. 10. Radiation emitted by an elementary volume of the plasma at the centerline of the discharge is focused on the entrance slit of a Spex 3/4 m grating spectrometer whose exit is connected to a Hamamatsu R818 photomultiplier tube. A 1200 ruling/mm grating blazed for 0.7500 μ is the dispersing element in the spectrometer. Proper adjustment of the entrance and exit slits provides a resolution of approximately 1 $\mathring{A}$. Typical openings of the entrance and exit slits are 20 microns and 30 microns, respectively.

For the optical depth studies a concave mirror (radius of curvature = 67.5 cm) was placed on the opposite side of the vacuum tank to direct the radiance back through the plasma (Fig. 10). The focusing lens and variable iris were then adjusted so that the accepted cone of radiation was matched to that returned by the reflecting optics.

The MPD accelerator used in these experiments had a 10.2-cm-diameter anode orifice and a 1.9-cm-diameter tungsten

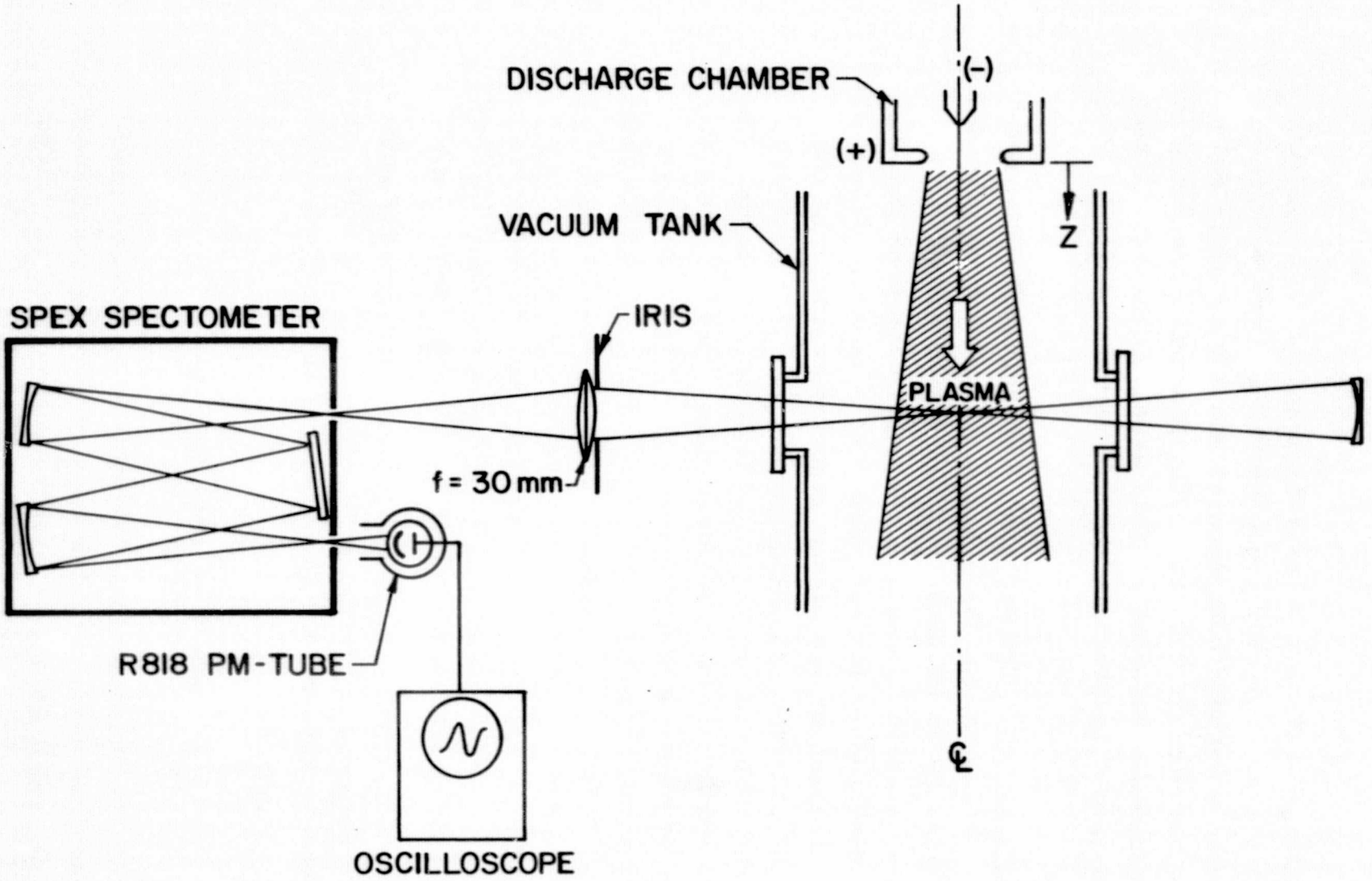

OPTICAL ARRANGEMENT

FIGURE 10
AP 25-5132

cathode which was 2.54 cm overall in length with a 1.27-cm-long conical tip. Injected argon propellant was equally divided between a cathode base annulus and a ring of 12 holes located at a radius of 3.81 cm in the boron nitride backplate. In the experiments reported in this section, the arc current was varied from 4 to 25 kA while mass flows of 6 and 12 g/sec were used.

Line Radiation. The radiance from selected argon neutral (AI), and argon ion (AII) transitions has been recorded photoelectrically 36 cm downstream of the accelerator, a location calculated to lie within the relaxation zone for recombination of doubly ionized argon, AIII to AII. Figure 11 shows oscillograms of the photomultiplier response to the 0.7503 μ AI line and the 0.4880 μ AII line. Also shown in the figure are the arc current and terminal voltage. It is evident that all traces attain a quasi-steady value, although the AI record shows a large initial transient hump associated with the propagation of the plasma front through the cold pre-discharge mass flow. In addition, while the AII trace decays to a negligible value at the same time as the current and voltage, an "afterglow" radiance of AI is seen. This radiance indicates the successive recombination stages of the excited argon following current cessation.

From the following simplified expression for the photomultiplier response current, it is possible to estimate the relative populations of the upper states of the two transitions:

$$P \propto \eta(V)\,\phi(\lambda)\,K_1\,I_t \qquad (2)$$

where $\eta(V)$ is the functional dependence of the photomultiplier response current to its applied voltage (calibrated separately), $\phi(\lambda)$ is the wavelength response of the photo-

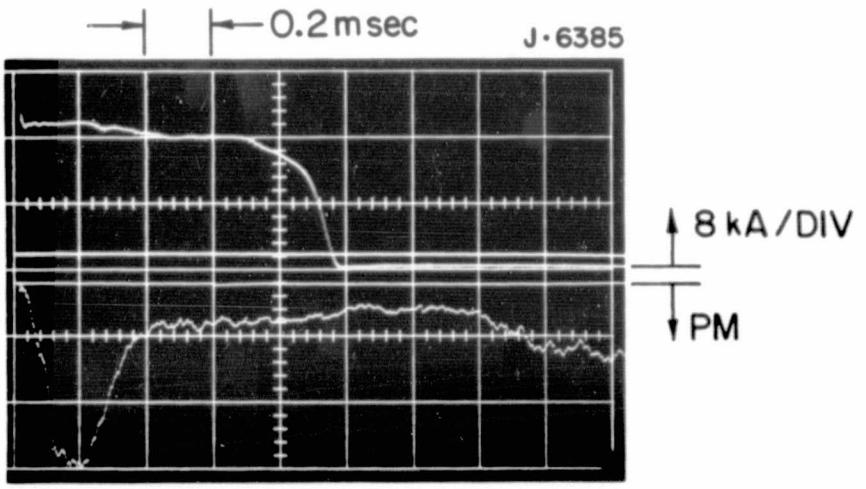

a) 0.7503 μ - AI

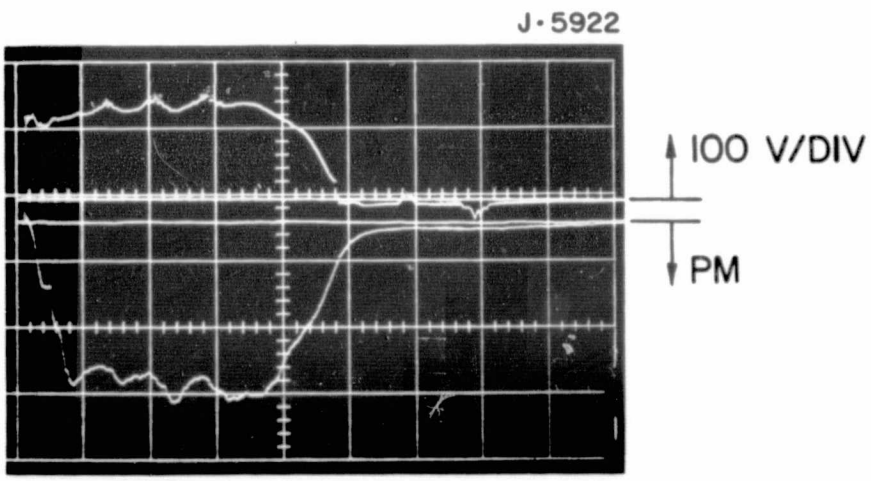

b) 0.4880 μ - AII

PM RESPONSE

FIGURE 11

cathode to incident radiation, K_1 is a geometrical factor which depends on the optical arrangement and is a constant for a given experiment, and I_t is the radiance integrated over the entire line profile. Furthermore, assuming no radial gradients, I_t can be related to the population densities of the upper atomic states by the following expression

$$I_t = \frac{n_j A_{jk} h\nu}{4\pi} B_{jk} L \qquad (3)$$

where A is the Einstein coefficient, L the effective path length, $h\nu$ the energy of the transition, n_j the population density of the upper state, and B_{jk} the radiation escape factor. Thus, combining equations 2 and 3, applying the appropriate atomic constants, and ratioing the two photomultiplier responses, the relative populations of the two upper states is obtained. For the data in Fig. 11, the ratio of the $(^3P)4p^2D^o_{5/2}$ AII state to the $4p'(1/2)_0$ AI state is found to be 15 ± 1.7.

In contrast, if local thermodynamic equilibrium is assumed, then the population ratio of these two states can be computed as a function of the electron number density and temperature by combining the Saha and Boltzmann equations:

$$\frac{n_1}{n_2} = \frac{2}{n_e} \left(\frac{2\pi m_e kT_e}{h^2} \right)^{3/2} \frac{g_1}{g_2} e^{-\left(\frac{\Delta E + I_{4p'}}{kT_e} \right)} \qquad (4)$$

where the subscripts 1 and 2 refer to the $^2D_{5/2}$ AII state and the $4p'(1/2)_0$ AI state, respectively, g is the degeneracy, ΔE the excitation energy of the $^2D^o_{5/2}$ AII state relative to ion ground (19.6 eV), and $I_{4p'}$, the ionization energy of the $4p'(1/2)_0$ AI state (2.53 eV). For an electron

temperature of 0.8 eV and an electron number density of $10^{13}cm^{-3}$, then

$$\frac{n_1}{n_2} = 2.3 \times 10^{-3}$$

Thus, the relative population of the excited levels inferred from line radiance measurements exceeds by a factor of more than 10^3 that calculated on the basis of LTE. This overpopulation of the excited ionic states is consistent with a recombination model in which the population is fed from higher lying states in the parent ion and the next higher degree of ionization. Measurements similar to those displayed here show that this overpopulation of the ionic states persists for distances up to 76 cm from the accelerator.

In order to determine the extent to which the background gas in the vacuum tank perturbs the observed radiance signals (e.g. by absorption of emitted radiation), the 0.7503 μ AI and 0.4880 μ AII lines were recorded photoelectrically for various vacuum tank prefill pressures. The prefill pressure ranged from 10^{-5} torr (the pressure normally achieved prior to each discharge) up to 7 torr. The arc current for these tests was maintained at 16 kA and the injected mass flow was 12 g/sec.

In Fig. 12, the radiance from the 0.7503 μ AI line along with the arc terminal voltage are compared for pressures of 10^{-5} and 7 torr. Oscillograms at intermediate pressures show that from 10^{-5} up to 3×10^{-2} torr, the signature of both the line radiance and the terminal voltage are identical to those in Fig. 12a. (The hump in the terminal voltage which appears at the end of the 1-msec current pulse in Fig. 12a is spurious and suggests a slight mismatch between the line and load impedances; it has no influence on the quasi-steady operation of the arc.) As the pressure is increased above 0.3 torr,

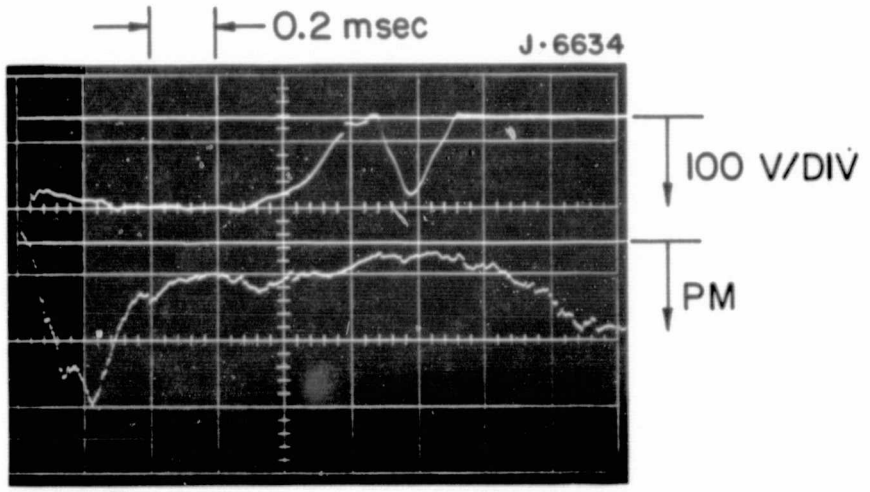

a) 10^{-5} torr

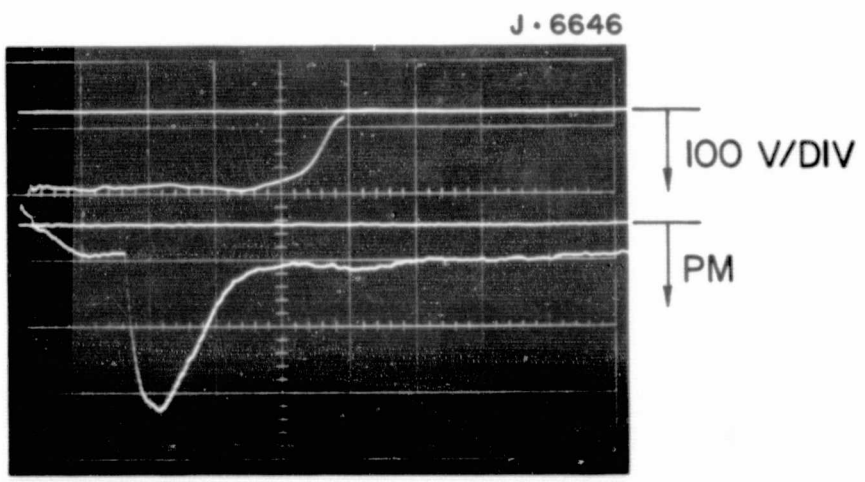

b) 7 torr

0.7503 μ - AI RADIANCE

AP 25 P 562 75

FIGURE 12

the arrival time of the plasma front is delayed due to its interaction with the ambient gas. Figure 12b shows that for a pressure of 7 torr, the delay in the radiance signal is accompanied by severe distortion in which a quasi-steady value can no longer be identified. In addition, the terminal voltage has dropped from 135 V to 112 V, a trend generally associated with higher mass flow through the discharge region.

Data for the 0.4880 μ AII transition are comparable to those displayed here, again with no effect observed until the fill pressure is increased beyond 3×10^{-2} torr.

These results are consistent with earlier data from steady state MPD accelerators where it was shown that back-pressures greater than 10^{-2} torr can cause spurious thruster operation.[A-14] Although considerably more data would be required to resolve the complex gasdynamic processes occurring in the present interaction of the exhaust flow with the ambient gas, sufficient data exists to conclude that for normal operation of the quasi-steady MPD device (background pressure $\approx 10^{-5}$ torr), the measured line radiance originates in the flowing plasma and is not perturbed by the background gas.

Optical Depth Measurements. Optical depth measurements of the 0.4880 μ AII line [$3p^5 4p(^3P)\,^2D^0_{5/2} \rightarrow 3p^5 4s(^3P)\,^2P_{3/2}$] were performed at an axial position 36 cm downstream of the anode for the following arc operating conditions: argon mass flow of 12 g/sec, and arc currents of 4, 8, 16, and 21 kA. This line was selected for the following reasons: 1) Due to the relatively high electron temperature ($\approx$ 0.8 eV), recombination from AIII to AII would be expected to predominate over that from AII to AI and thus the excited states of AII should be examined for inversions; 2) studies performed on hydrogenic plasmas using the collisional-radiative recombination model predict inversions between energy states similar to that involved in this transition; and 3) the line is

sufficiently isolated so that it can be recorded unambiguously by the spectrometer-photomultiplier detection system.

Figure 13 shows a few of the initial optical depth measurements for a mass flow of 12 g/sec and arc currents of 16 kA (Fig. 13a) and 4 kA (Fig. 13b). The photomultiplier response is shown for two consecutive discharges: one without the reflecting optics, I_1, and one with the reflecting optics, I_2. The traces show a delay after discharge initiation before the arrival at the 36-cm downstream location of the plasma front (approximately 40 and 300 μsec for the 16 and 4 kA conditions respectively). Following this plasma front, the radiance, like the previously measured plasma temperature, number density, and velocity, is usually steady with the exception of the lower currents where some time variation is observed.

From these data, the optical depth may be determined from

$$\tau = - \ln \left(\frac{I_2 - I_1}{r I_1} \right) \qquad (5)$$

where τ is the optical depth and r, the effective reflectivity of the reflecting optics. A negative optical depth thus implies a population inversion, while a positive optical depth signifies an uninverted distribution, though not necessarily Boltzmann. The accuracy of the optical depth determination depends in turn on the accuracy with which the effective reflectivity r of the reflecting optics is known. Measurements of the optically thin continuum near the 0.4880 μ line give $r = 0.65 \pm 0.01$.

From the measured optical depth, and assuming that radial gradients in number density and temperature are small, it is possible to calculate a value of the inversion density, Δn ,

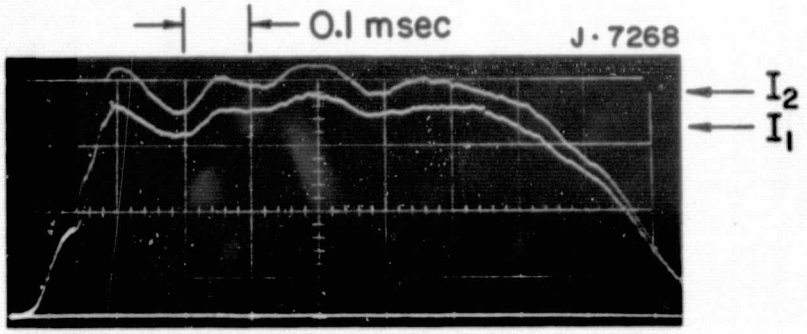

a) J = 16 kA

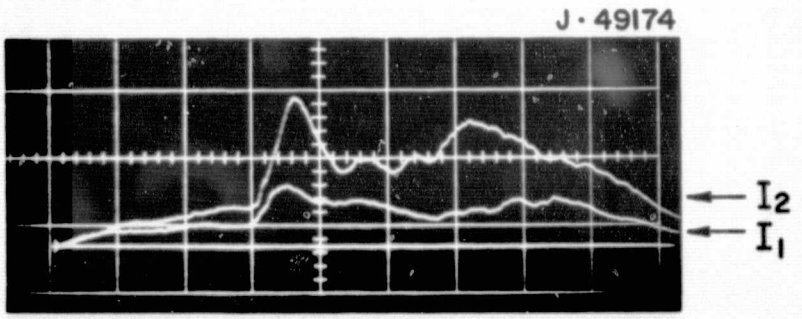

b) J = 4 kA

OPTICAL DEPTH MEASUREMENTS

FIGURE 13

from

$$\tau = -\frac{A_{21}\lambda^2}{8\pi}\frac{\Delta n}{\Delta \nu} L \qquad (6)$$

where

$$\Delta n = n_u - (g_u/g_\ell)\, n_\ell \qquad (7)$$

A_{21} is the Einstein coefficient, $\Delta\nu$ the full width at half-maximum, L the effective path length, and the subscripts u and ℓ refer to the upper and lower states respectively.

Table 1 lists the measurements of optical depth and the preliminary results of the inversion density for the 0.4880 μ line at different operating conditions and representative times after discharge initiation, t. The path length used in these calculations was taken from previous photographs of the discharge to be L = 15 cm.

TABLE 1

Optical Depth Measurements
$\dot{m}$ = 12 g/sec

J(kA)	t(μsec)	τ	Δn (cm^{-3})
21	250	0.64	-1.2×10^{11}
16	600	0.56	-1.1×10^{11}
8	600	0.62	-1.3×10^{11}
4	400	-0.72	3.2×10^{10}
4	600	-0.43	1.9×10^{10}
4	800	-0.43	1.9×10^{10}

The table shows that for the higher currents, population inversions do not appear at any time during the discharge.

However, the data also show that at the lowest current, a negative optical depth, indicative of a large population inversion, is maintained for approximately 500 μsec. A tentative explanation is that by decreasing the current, the electron temperature is reduced sufficiently for the collisional-radiative recombination mechanism to create population inversions among the excited electronic energy states. If such a large population inversion does occur in the recombining plasma, then it should readily show strong lasing in a cavity. Therefore, a qualifying experiment was performed to substantiate this measurement by placing an optically resonant cavity transverse to the flow at the same axial location. As has been the experience of other laboratories, initial results have proven negative which may be due to the following reasons: 1) the cavity was a marginally stable configuration, and 2) the region of the plasma sampled by the cavity had a height of approximately 600 μ at the axis compared to 3 cm in the optical depth measurements. Thus, the cavity may have been sampling a region of the plasma where inversions do not occur. Further experiments are in progress to examine the entire region observed in the optical depth measurements with a modified cavity.

B. MPD Discharge in a Laser Cavity (Dutt)

In the previous semi-annual report, the results of initial experiments with a unique 45-cm-wide discharge apparatus were described.[159] Resembling a two-dimensional version of a conventional MPD accelerator, the apparatus is designed to maximize the optical path transverse to the expanding plasma and thus allow a direct determination of whether lasing can be sustained in the discharge or exhaust regions. The exploratory experiments showed that the discharge current divided equally between the two anodes for operation in ambient argon, that the current distribution was reasonably uniform along the full width of the electrodes, and that a cold flow mass injection system could provide a uniform distribution of argon across the backplate of the accelerator with a 2 msec risetime.

However, these tests also highlighted certain characteristics of the apparatus and discharge which required modification before experiments including the optical cavity could begin. This report describes the consequent extensions and refinements in the discharge apparatus, the mass injection system and the resonant cavity.

Discharge Apparatus

Although the current distribution across the 45-cm electrode width showed no gross asymmetries, it was felt that the uniformity could be improved further by restraining the discharge laterally for a considerable distance downstream of the electrode region. To this end, thin Plexiglas plates, 40 cm high by 56 cm long, were attached to the existing sidewalls as shown in Fig. 14. To permit optical diagnostics at many locations, a matrix of holes were drilled through the side plates. Holes not in use may be closed by suitable plugs to confine the discharge to the fullest extent.

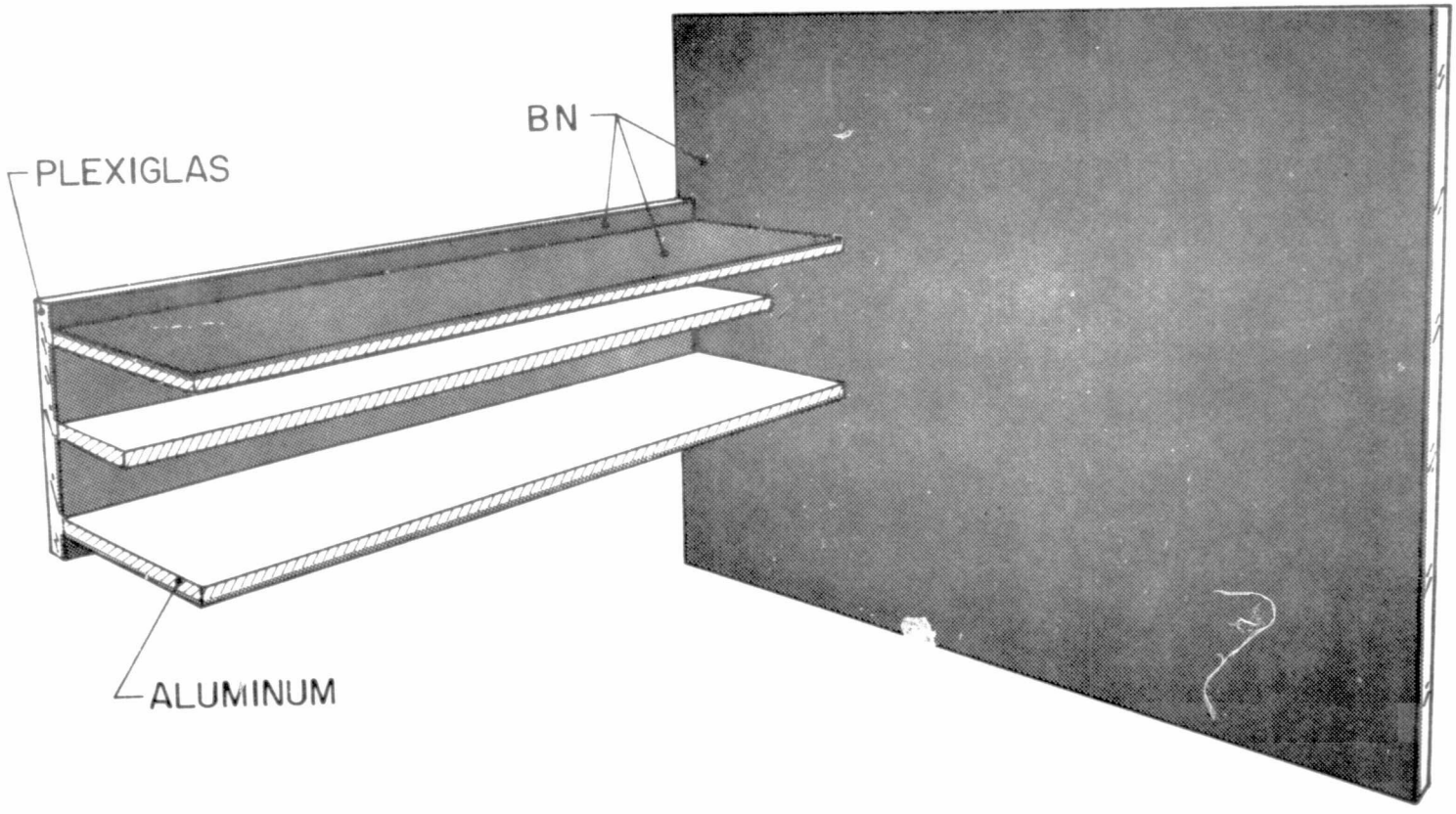

TWO DIMENSIONAL DISCHARGE APPARATUS

FIGURE 14
AP 25-5133

Another result of the previous magnetic field measurements was that about half of the current attachment at the anodes occurs on the outer surfaces. In order to increase the current density in the interelectrode space and thus enhance the compression and expansion of the argon plasma, insulation is required on the outer surfaces of the anodes.

Experiments reported by Boyle and others have indicated that the characteristics of the discharge can be significantly affected by the choice of insulator material.[151] It is thus desirable to choose a refractory insulating material in order to minimize the effect of insulator ablation. For the present application with large surface areas requiring insulation, a boron nitride paint was selected. Tests showed that adequate bonding of this paint to both aluminum and Plexiglas can be achieved provided that a) the surface to be coated is dry, and b) the coating is applied in thin layers (about 3 to 6×10^{-3} cm) and is allowed to air dry in an atmosphere of low humidity.

The boron nitride paint was applied to the confining sidewalls, the outside of the anodes and the Plexiglas backplate as shown in Fig. 14. Subsequent tests have shown that this boron nitride coating performs satisfactorily in the plasma environment.

Mass Injection System

Tests of the mass injection system described in the previous semi-annual report indicated that a reasonably well distributed mass pulse of fast risetime could be produced.[159] However, the upper limit of available argon mass flow was insufficient for the highest current operating conditions anticipated. Two causes for this deficiency were identified: the pressure loss in the supply line to the two Skinner

type V52 solenoid valves, and a current pulse too weak for proper opening of the valves at high pressures.

The pressure drop was minimized by installing a 500 cm^3 reservoir immediately upstream of the two valves. With this reservoir, the effective stagnation pressure at the valves decreases by less than 5% from the time the valves first begin to open until after a steady mass flow has been established and the arc discharge fired.

To allow valve operation at higher pressures, the power output from the pulsed valve driving circuit was increased by upgrading the energy storage capacitors and raising the charging voltage from 180 V to 350 V. The improved power supply allows simultaneous operation of the two valves at pressures up to 7 atmospheres, an increase of approximately a factor of three.

Following these changes, a mass flow calibration was conducted using a McLeod gauge to monitor the pressure rise in the vacuum tank after mass pulses of various durations. The mass flow rate was found to scale linearly with stagnation pressure, reaching a value of 60 g/sec for a stagnation pressure of 7 atmospheres. The orifice coefficient of the 18, 1.6-mm-diameter, choked injector holes was determined to be 0.82.

Optical Cavity

In the earlier alignment tests with the resonant optical cavity, the mirror supports were bolted to a single horizontal I-beam with a mirror separation of 67.5 cm. Using as the lasing medium a TRW argon ion laser with its own mirrors removed, this configuration was shown to be mechanically stable and capable of alignment with a He-Ne laser mounted external to the cavity. However, such a configuration cannot be used

in conjunction with the large 1-m-diameter vacuum tank. In this case, the mirrors need to be raised more than 55 cm above the supporting member which must pass below the vacuum tank, and the mirror separation must be increased to approximately 147 cm.

Figure 15 shows the modified optical configuration. The lowest aluminum I-beam is supported by an inverted V-frame at one end and by a vertical column at the other. Vibration pads and adjusting screws separate the legs from the floor. A new set of dielectric mirrors (radius of curvature = 147 cm) are mounted on additional sections of I-beams to bring the optical axis through the center of the discharge. The accuracy of alignment technique which uses a He-Ne laser mounted external to the cavity has been confirmed for this configuration by placing the TRW lasing medium between the mirrors and observing laser output.

The discharge apparatus, mass injection system, and resonant optical cavity are now ready for the optical experiments. The first locations to be examined will be various zones of the discharge chamber, with later tests to examine the compression and expansion regions of the plasma flow.

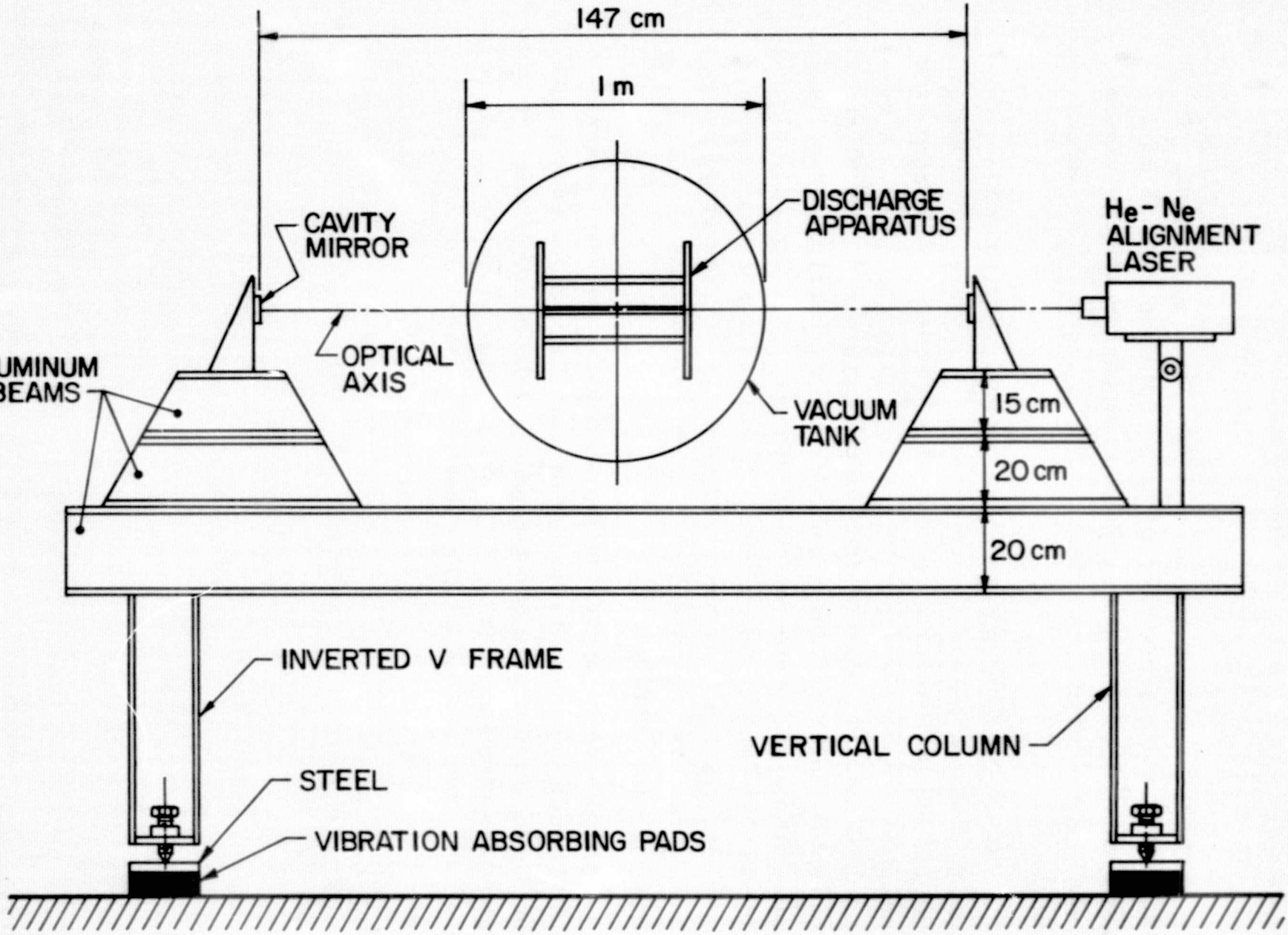

FIGURE 15
AP 25-5134

OPTICAL CAVITY STRUCTURE

IV. HOLLOW CATHODE STUDIES (Krishnan)

At the 11th Electric Propulsion Conference, to be held in New Orleans, Louisiana on March 19-21, 1975, a paper entitled "Hollow Cathode Characteristics in High Current Discharges," by M. Krishnan, W. F. von Jaskowsky, K. E. Clark and R. G. Jahn, will be presented which summarizes the Princeton hollow cathode program. Since this paper describes the most recent results as well as a concise review of previous and related work, it is presented here in full to provide a comprehensive picture of the hollow cathode program in this laboratory.

A. Introduction

Hollow cathodes were first used to advantage as early as 1916 in spectroscopic studies where they were shown to be capable of simultaneously providing high electron number density and relatively low temperature ions and neutrals in an essentially field-free cathode cavity.[A-15] More recently, hollow cathodes have been used as electron emitters in advanced ion thrusters where they exhibit a lower specific heating power and longer lifetime than oxide-coated or liquid-metal cathodes.[A-16] However, despite considerable research effort and developmental testing, which in isolated cases has extended cathode lifetime to beyond 9000 hours,[A-17,18] the hollow cathode still represents one of the main limitations of ion thruster system lifetime and reliability.[A-19] A detailed diagnostic study of the cavity plasma, which is clearly necessary in order to identify the dominant physical processes and ultimately to reduce the long-term wear characteristics to a tolerable level, has been precluded up to now by the small dimensions of these steady-state cathodes. As a result, the existing theories are incomplete and as yet have been unable to identify the scaling laws for proper hollow cathode operation.

In the present program a relatively large (2-cm-dia) hollow cathode has been incorporated in a high current, quasi-steady magnetoplasmadynamic (MPD) arc discharge where the large cavity permits the detailed study of the interior plasma by probing, photographic and spectroscopic observations. The objectives of this research program are: 1) to determine the conditions under which typical hollow cathode operation can be obtained in pulsed, multi-megawatt MPD discharges; 2) to take advantage of the large cavity dimensions and the low total energy in the pulsed operation to study the interior emission and ionization processes; 3) to compare the characteristics of pulsed hollow cathode operation to those of ion thruster hollow cathodes; and 4) to determine the nature and extent of scaling laws for characteristic hollow cathode operation.

This paper describes the influence of each of the three independent parameters — geometry, current, and mass flow — on the operation of large hollow cathodes. In the first part of the experimental section, the distributions of current and potential within and about various hollow cathode configurations are presented for a limited range of current and mass flow. The relative insensitivity of the interior plasma to electrode and insulator geometries leads to a second series of experiments wherein a particular cathode geometry is studied by several diagnostic methods over a wide range of current and mass flow. The interesting features of these experiments are presented in the second part of the experimental section. The relevance to several other researches is the subject of the discussion section.

B. Apparatus

Figure 16 shows a photograph of the experimental apparatus for hollow cathode studies, including a 45-cm-diameter x 90-cm-long glass vacuum tank, gas supply equipment, and associated electrical circuitry. A schematic of the apparatus is shown in Fig. 17. A

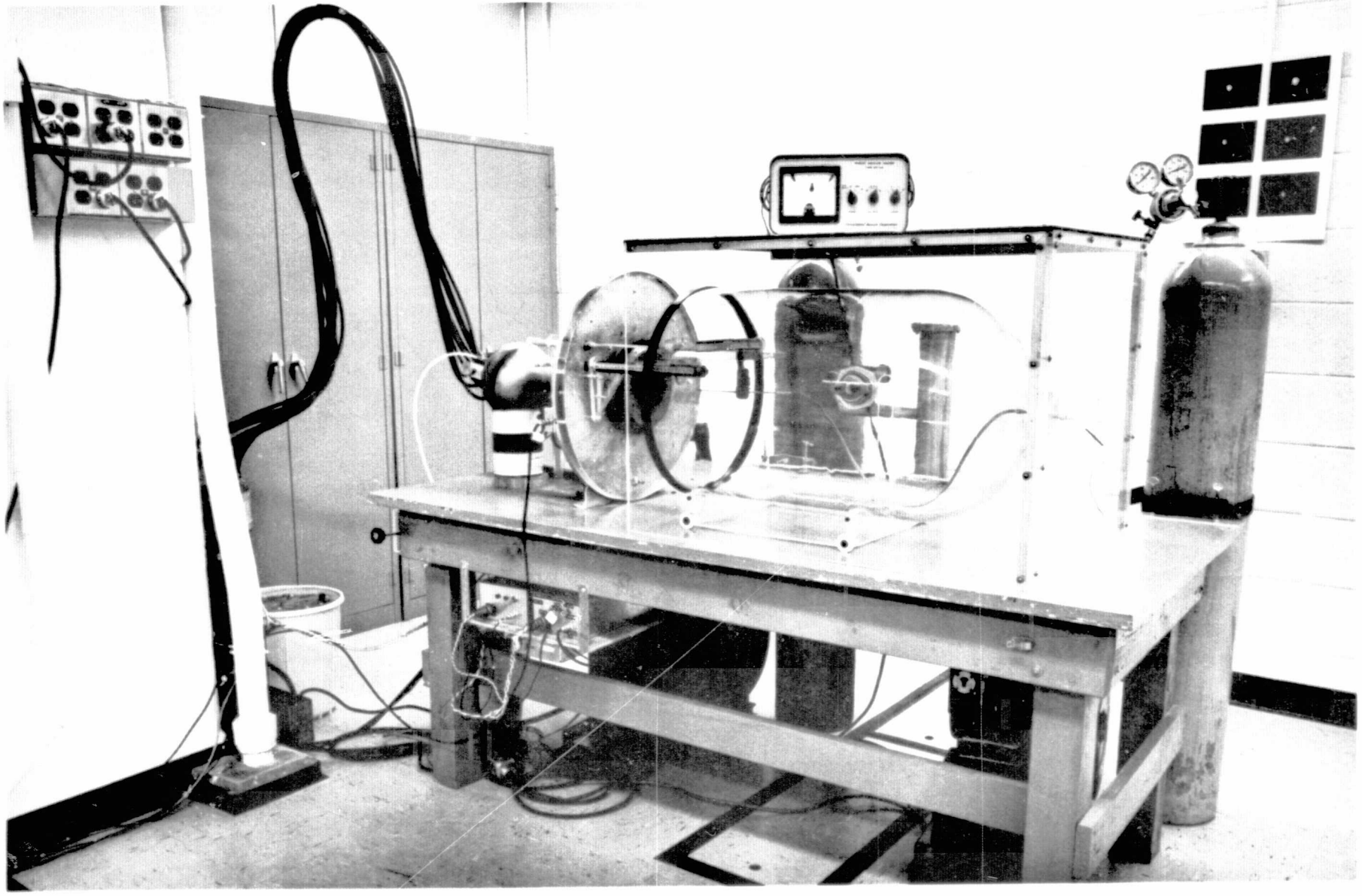

FIGURE 16
AP25-P-541

VIEW OF HOLLOW CATHODE FACILITY

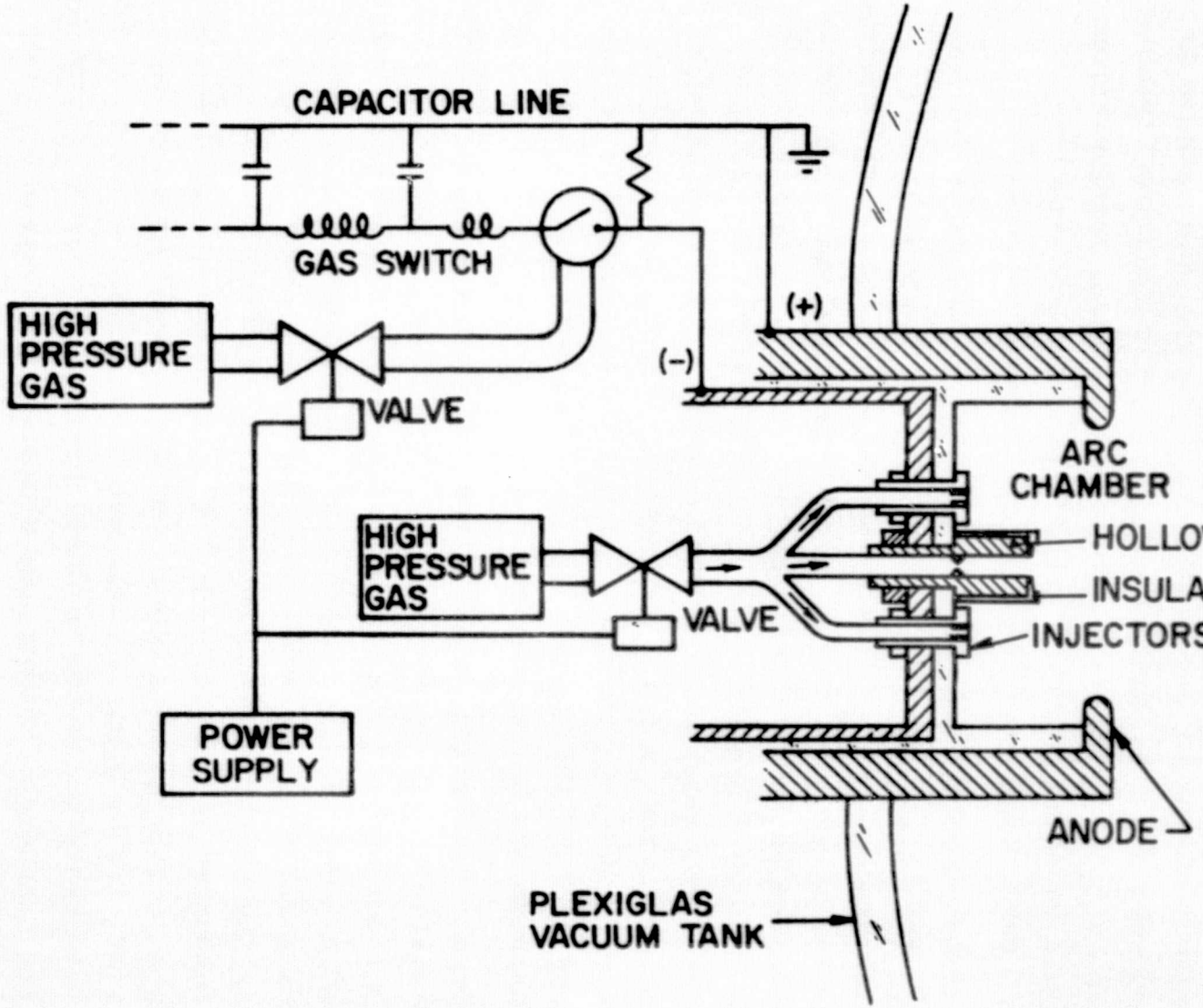

DISCHARGE APPARATUS

FIGURE 17
AP25-4681

typical thoriated tungsten hollow cathode, shown centrally located in the discharge chamber, is 3.2 cm in outer diameter, 3.3 cm long and has a 1.9-cm-diameter cavity. The cathode is screwed into the insulating backplate of the discharge chamber and can be fitted with many different insulator configurations. It should be noted that the cathode possesses no auxiliary heater, oxide-impregnated insert or keeper electrode.

Argon propellant was injected into the discharge chamber through the hollow cathode orifice and/or through six outer orifices arranged symmetrically at a radius of 2.54 cm from the centerline of the discharge. Since the propellant flow chokes at the seven inlet orifices, the mass flow rate is determined by the reservoir pressure and by the total area of the seven orifices. The fractional division of the total flow through the hollow cathode and the six outer injectors is controlled by the relative area of the orifice. Unless otherwise noted, the mass flow in the experiments reported here was injected only through the hollow cathode.

Power is supplied to the discharge from a network of four transmission lines, each assembled from 21 equal sections of 6.6-μH inductors and 27-μF capacitors. When connected in parallel and charged to 4 kV, these lines are capable of delivering a 20-kA x 0.5-msec current pulse into a load whose impedance matches the characteristic impedance of the transmission line. When connected in series, a 5-kA x 2-msec current pulse can be driven through a matched load. For the investigation of the effect of cathode geometry, the matching impedance was provided by an electrolytic cupric sulphate resistor connected in series with the discharge. Figure 18a shows an oscillogram of a 6-kA x 0.5-msec current pulse obtained with this arrangement. To extend the range of current to yet lower values, the electrolytic resistance was increased. The resulting current waveform, shown in Fig. 18b, is typical of a transmission line driving an impedance greater than its own characteristic impedance. When using this

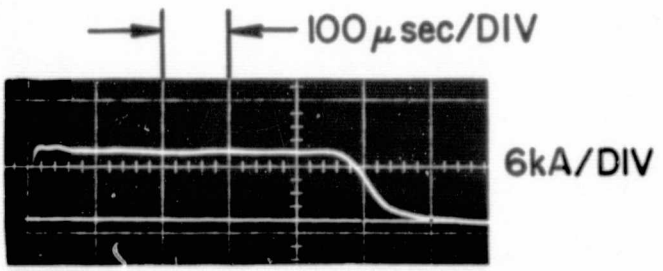

a) PARALLEL - MATCHED

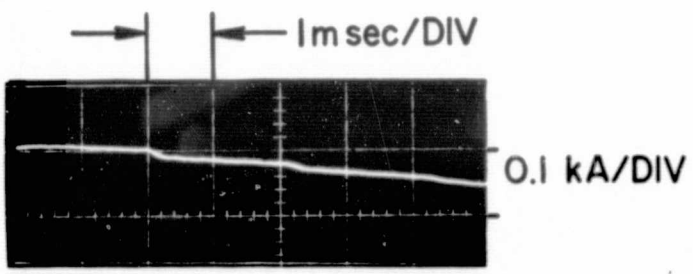

b) SERIES - UNMATCHED

DISCHARGE CURRENT

AP 25 P 554

FIGURE 18

current pulse, data was taken only during the first 2 msec, which is seen to be flat and of an amplitude as low as 180 A.

C. Experimental

Effects of Cathode Geometry

Early experiments with uninsulated and insulated hollow cathodes over a range of currents from 7 to 30 kA and argon mass flows from 0.04 to 6 g/sec demonstrated that quasi-steady hollow cathode operation can be achieved in multi-megawatt pulsed discharges without the assistance of auxiliary heating, low work function inserts, or keeper electrodes.[151] Probing of the cathode interior and exterior plasma indicated that at the given operating conditions, it was necessary to insulate the external surface and face of the hollow cathode in order to assure total current attachment inside the cavity. The current in these early cathodes attached in a relatively short zone at the downstream end of the cathode. Surveys of potential exhibited a nearly field-free region in the cavity coincident with the current attachment zone. This low axial field region was connected to the exterior discharge by a large electric field (up to 150 V/cm) in the insulated channel at the cathode tip.

To examine further the current attachment zone and its associated potential distribution, and to investigate the effects of cathode shape, orifice diameter, and tip thickness on the characteristics of the hollow cathode discharge, a variety of new hollow cathode configurations have been examined at a fixed current and mass flow of 7 kA and 4 g/sec respectively. These new cathodes, shown in Fig. 19, fall into two distinct groups. In the first, a fixed electrode geometry consisting of a 3.3-cm-long cylindrical thoriated tungsten hollow cathode with a 3.2-cm outer diameter and a 1.9-cm cavity diameter was fitted with several insulated orifice and channel configurations

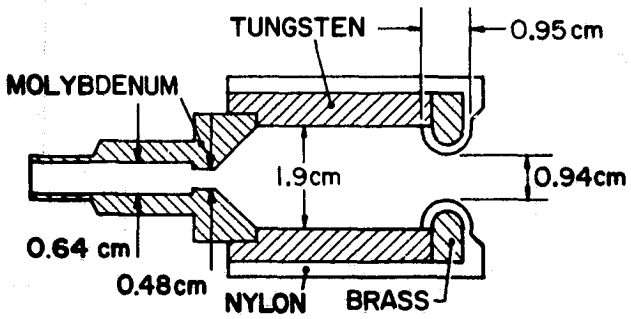

a) CATHODE IV

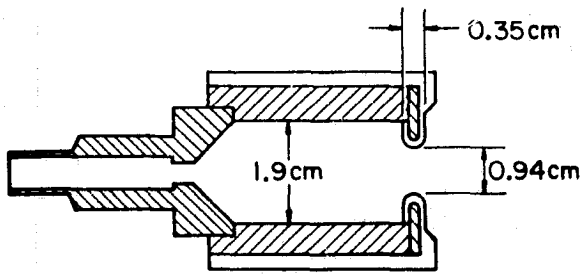

b) CATHODE V

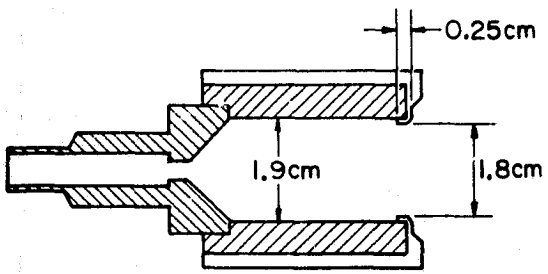

c) CATHODE VI

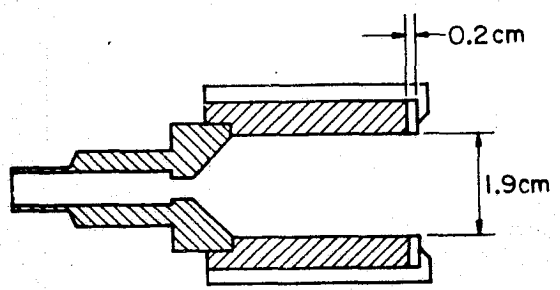

d) CATHODE VII

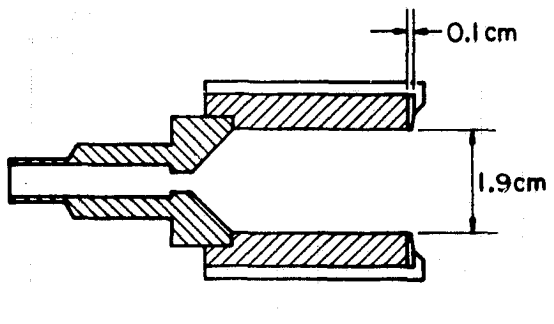

e) CATHODE VIII

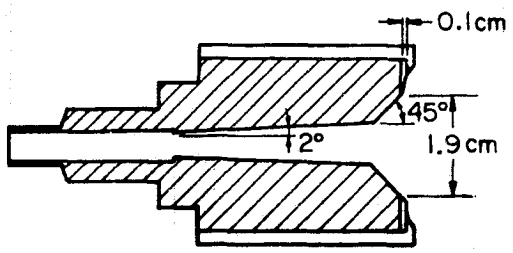

g) H.C. XI

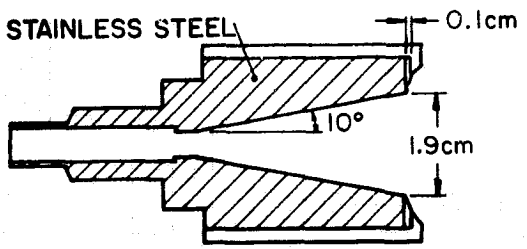

f) H.C. X

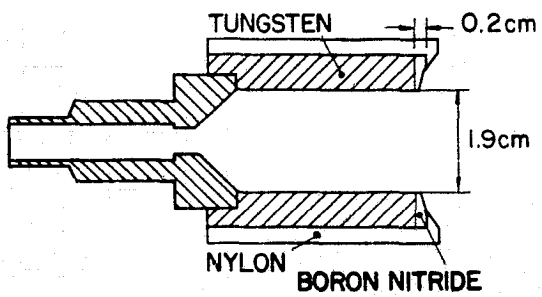

h) CATHODE XII

CATHODE CONFIGURATIONS

FIGURE 19
AP 25-5105

(HC-IV, V, VI, VII and VIII). The second group consists of two stainless steel cathodes, HC-X and HC-XI, with identical insulator configurations but conical electrode geometries. These right circular configurations with a 10° half-angle for HC-X and a 45° half-angle for HC-XI, may be considered as steps in the transition from a hollow cathode with a cylindrical cavity to a solid electrode with a flat face. Experiments with an additional configuration (not shown) have demonstrated that changing the cathode material from tungsten to stainless steel produces only marginal changes in the measured current and potential distributions.

Distribution of the current within the hollow cathodes is determined by a small magnetic field probe. This probe consists of a 0.1-cm-diameter coil in a thin glass tube to insulate it from the plasma. The coil generates a signal proportional to the change in magnetic flux which is then passively integrated at the oscilloscope to give the local magnetic field. This magnetic field is plotted in succeeding figures as the total enclosed current passing through a circular cross section whose radius equals the probe radial position in the discharge. The current distribution is obtained by traversing the probe axially at a fixed radius of 0.75 cm, and normalizing the measurements to the value obtained at the downstream end of the cavity.

Potential distributions within and around the cathode are obtained using a Langmuir probe consisting of an insulated 0.25-mm-diameter tungsten wire of which only the front 3 mm is exposed. The probe output is connected through a 100 MΩ P-6013A voltage probe to one input of a differential amplifier at the oscilloscope. The other input is the cathode potential, measured relative to the anode ground with an identical P-6013A probe. Thus, the oscilloscope displays the floating potential relative to the cathode surface, and since electron temperature effects

depress the floating potential below the true plasma potential, this differential signal is the minimum potential drop between the cathode and the probe tip.

Diagnostic study of the seven cathode geometries shown in Fig. 19 (HC-IV - VIII, X, XI) has revealed several characteristic features of high current, hollow cathode operation:

1) For all configurations, the discharge current attaches to the downstream portion of the cavity with a surface current density in excess of 1 kA/cm^2. The region over which 80% of the current attaches is 0.6 cm long, coincident with a weak axial electric field of less than 10 V/cm. Figure 20 shows typical current and potential distributions, plotted in this case for HC-VI which is shown in cross section at the top of the figure.

2) The electric field in the insulated channel connecting the cavity plasma with the exterior discharge is a function of the channel cross-sectional area regardless of the electrode shape. Figure 21 shows the measured electric fields of several cathode configurations plotted against their insulated channel cross-sectional areas. The observed inverse dependence of the electric field on the channel area for fixed current suggests that the current conduction through the channel plasma can be described by an Ohms law with constant conductivity. Using the data of Fig. 21, the calculated conductivity is approximately 1.2×10^4 mhos/m, a value which corresponds to an electron temperature of 2 to 4 eV at any substantial ionization level.[A-20]

3) Measured radial profiles of floating potential inside the cathode cavity indicate that the bulk of the potential drop occurs near the inner cathode wall, while the cavity interior is nearly field-free. Figure 22 shows HC-VI and the measured 28 V and 40 V equipotential contours. Since the contours represent floating potential relative to the cathode, the radial electric field is seen to increase as the radius increases. Within the 0.8-cm-diameter cylindrical region about the cavity axis, no further differences in potential could be resolved.

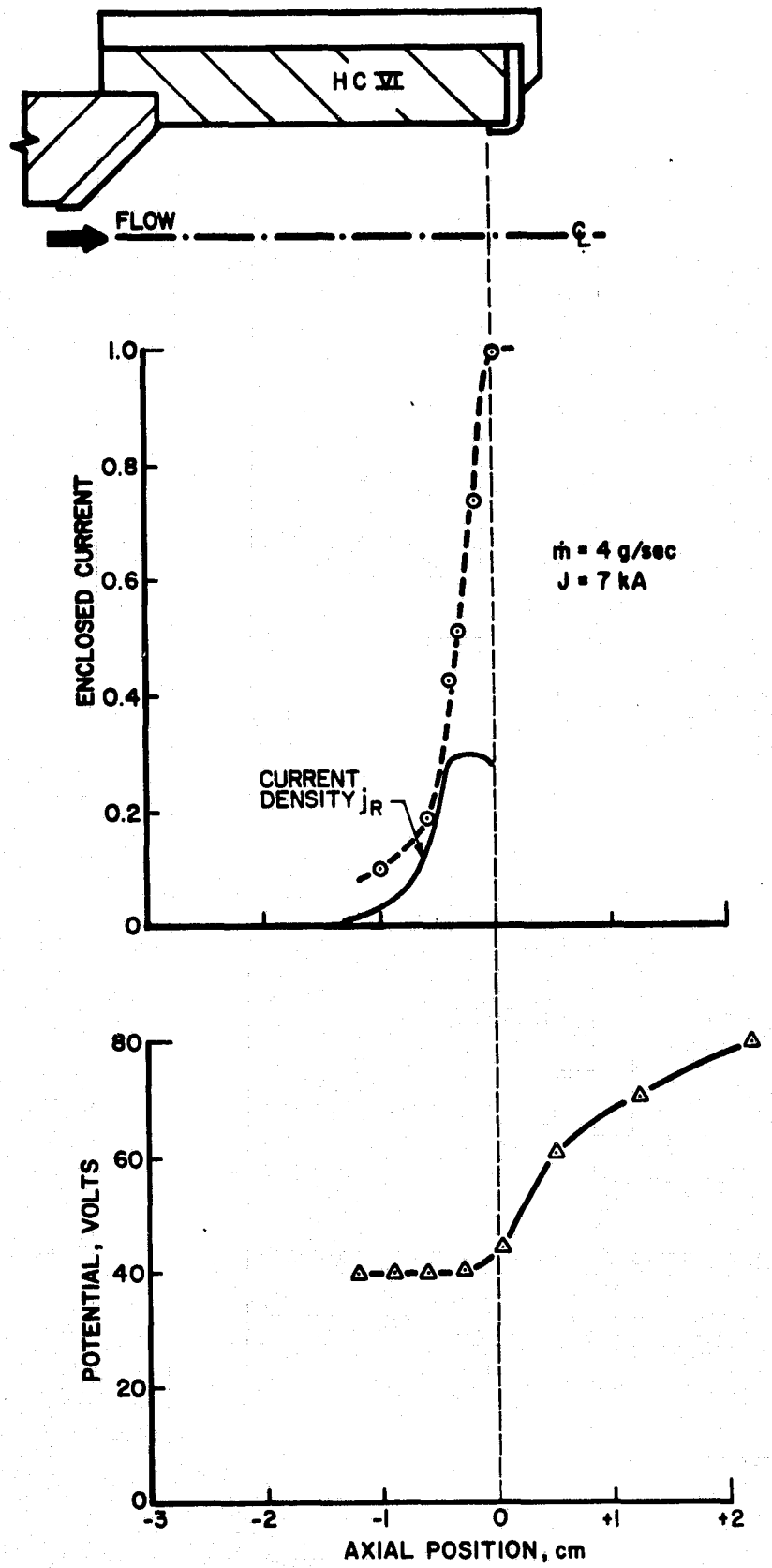

CURRENT AND POTENTIAL PROFILES

FIGURE 20
AP 25-5114

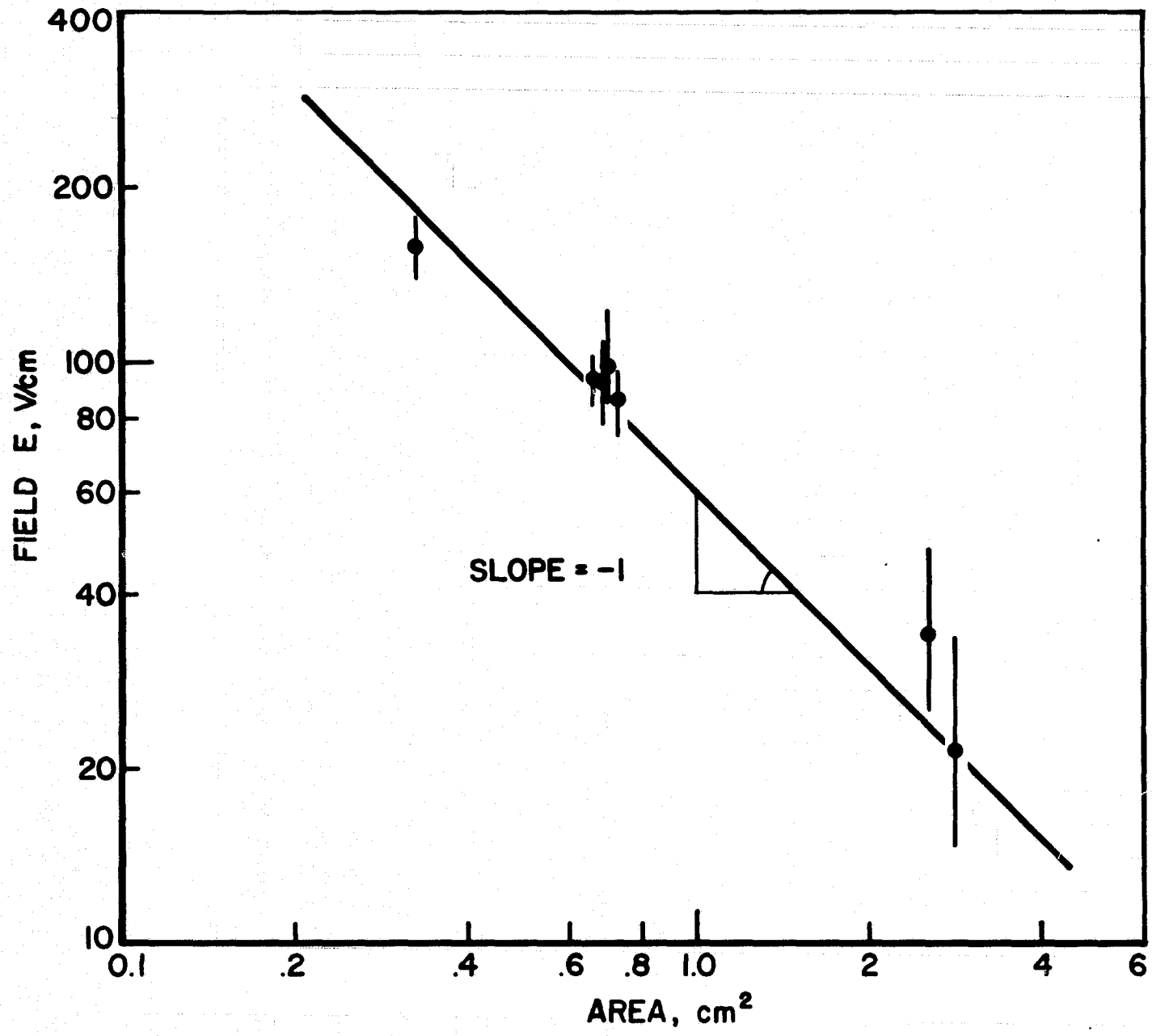

ELECTRIC FIELD IN INSULATED CHANNEL

FIGURE 21
AP 25-5109

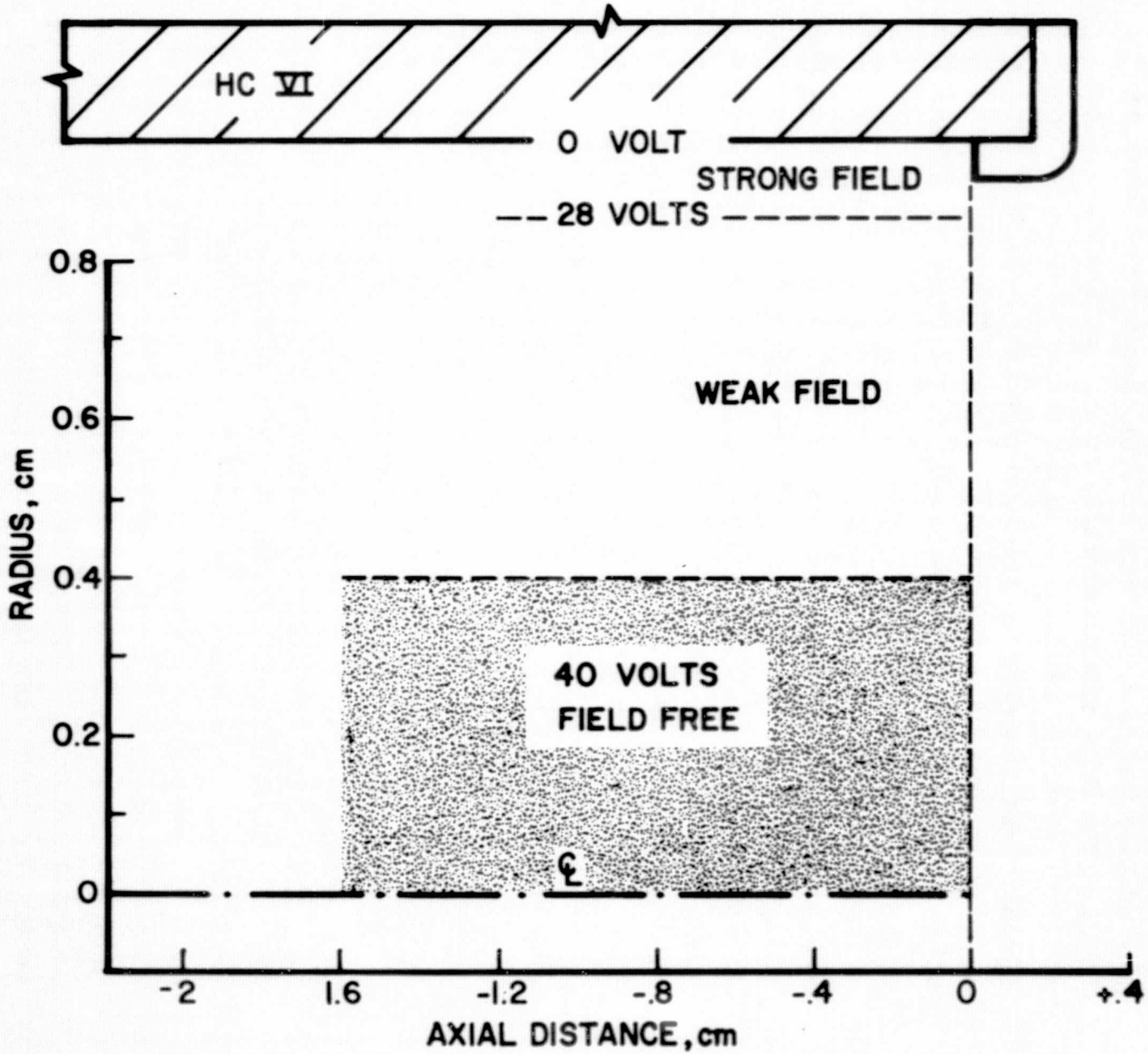

POTENTIAL DISTRIBUTION

FIGURE 22
AP 25-5108

4) Radial surveys of magnetic field show that the axial current density is uniformly distributed over the cavity opening. Figure 23 shows the results of a magnetic probe survey taken at the entrance to the insulated channel of HC-VI. The data are presented in terms of enclosed total current, which is readily obtained from the measured magnetic fields. For comparison, the enclosed total current for an assumed constant axial current density of $j = 2.8$ kA/cm^2 (7 kA ÷ 2.5 cm^2) is also presented and is seen to differ little from the measured values.

5) An interesting empirical observation is the change in texture of the tungsten surface of HC-VIII at the end of the cavity which further exhibits the pattern of current conduction in this hollow cathode. Figure 24 shows a perspective view of the insulated face and cavity of HC-VIII after a series of 7 kA discharges. The end of the conducting part of the cavity is clearly delineated as a bright edge, upstream of which there is an approximately 0.6-cm-wide band of clean metallic surface where 80% of the total current has been shown to attach (see Fig. 20). It is conjectured that ionic bombardment of the inner electrode surface in the primary current carrying region has produced this change in the cathode surface.

The insensitivity of the details of the current and potential distributions to cathode geometry and insulator configuration indicates that the measured distributions are characteristic of hollow cathode operation at these conditions. Despite a drastic change in electrode shape from a cylindrical to a 45^o conical geometry, and despite several different insulator channel lengths and orifice diameters, the current always attaches over approximately the first 0.6 cm of electrode, with an axial potential plateau coincident with the zone of attachment. The next step in the experimental program, therefore, was to select one particular cathode configuration that was most

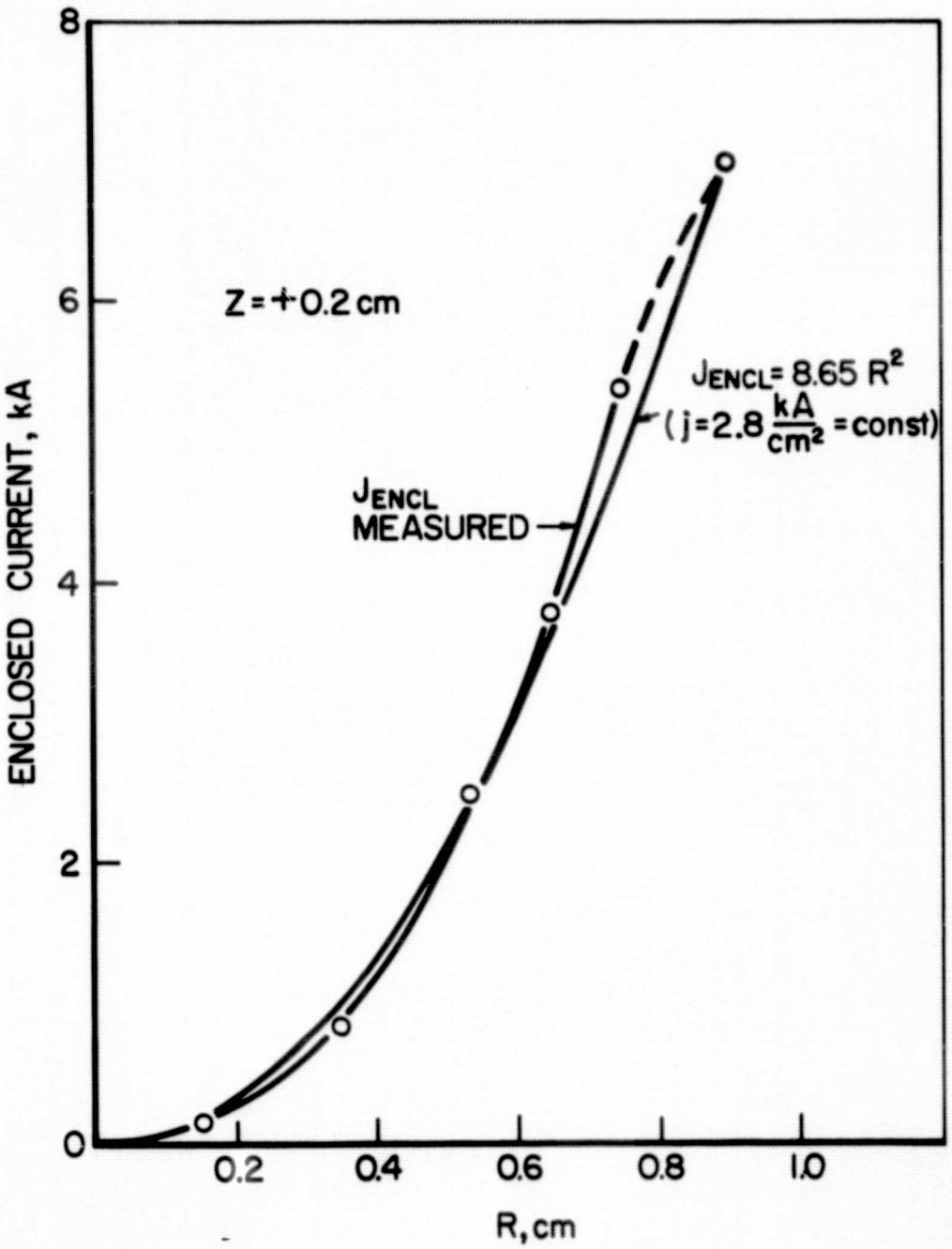

ENCLOSED CURRENT IN HC VI

FIGURE 23
AP25·4991

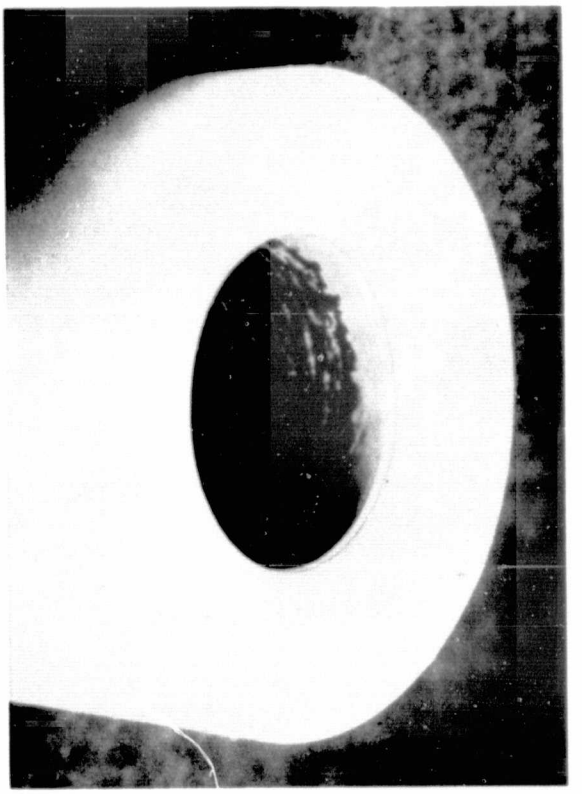

HOLLOW CATHODE VIII

FIGURE 24

amenable to diagnostics, and to study this cathode for wide variations in the two other independent variables, current and mass flow. The results of these investigations are presented in the next section.

Effect of Current and Mass Flow

The cathode design selected for detailed study is designated HC-XII and is shown in Fig. 19h. The electrode is identical to HC-VIII (Fig. 19e), but two changes were made to minimize wear of the insulators. First, the nylon disc insulating the front face of the cathode was replaced by a refractory boron nitride disc, 0.23-cm thick tapering down to 0.1-cm thick at the orifice. Second, the nylon outer sleeve which holds the disc pressed against the cathode face was coated with boron nitride paint to inhibit ablation of the nylon.

In the first series of experiments with this cathode, spectral photographs and near-infrared spectrograms of the discharge were taken. These optical diagnostics have proven capable of distinguishing subtle features of the discharge structure in the past, and were applied in this case to observe the gross effects of current and mass flow changes on the hollow cathode cavity plasma. Figure 25 shows selected spectrograms taken with the line-of-sight inclined 45° to the cavity axis for currents of 5 kA and 19 kA at argon mass flows of 0.4 g/sec (Fig. 25a) and 16 g/sec (Fig. 25b). Comparison of the spectra, particularly at the 5 kA current, reveals that mass flow has a striking effect on the distribution of radiance from the cavity. At a mass flow of 16 g/sec (Fig. 25b), the AII line radiation noticeably peaks at the outer portion of the cavity near the electrode surface. In contrast, the distribution of AII radiance at a mass flow of 0.4 g/sec (Fig. 25a) peaks in the center of the spectrogram, i.e. near the cavity axis. These spectra, as well as others taken end-on, indicate that as the

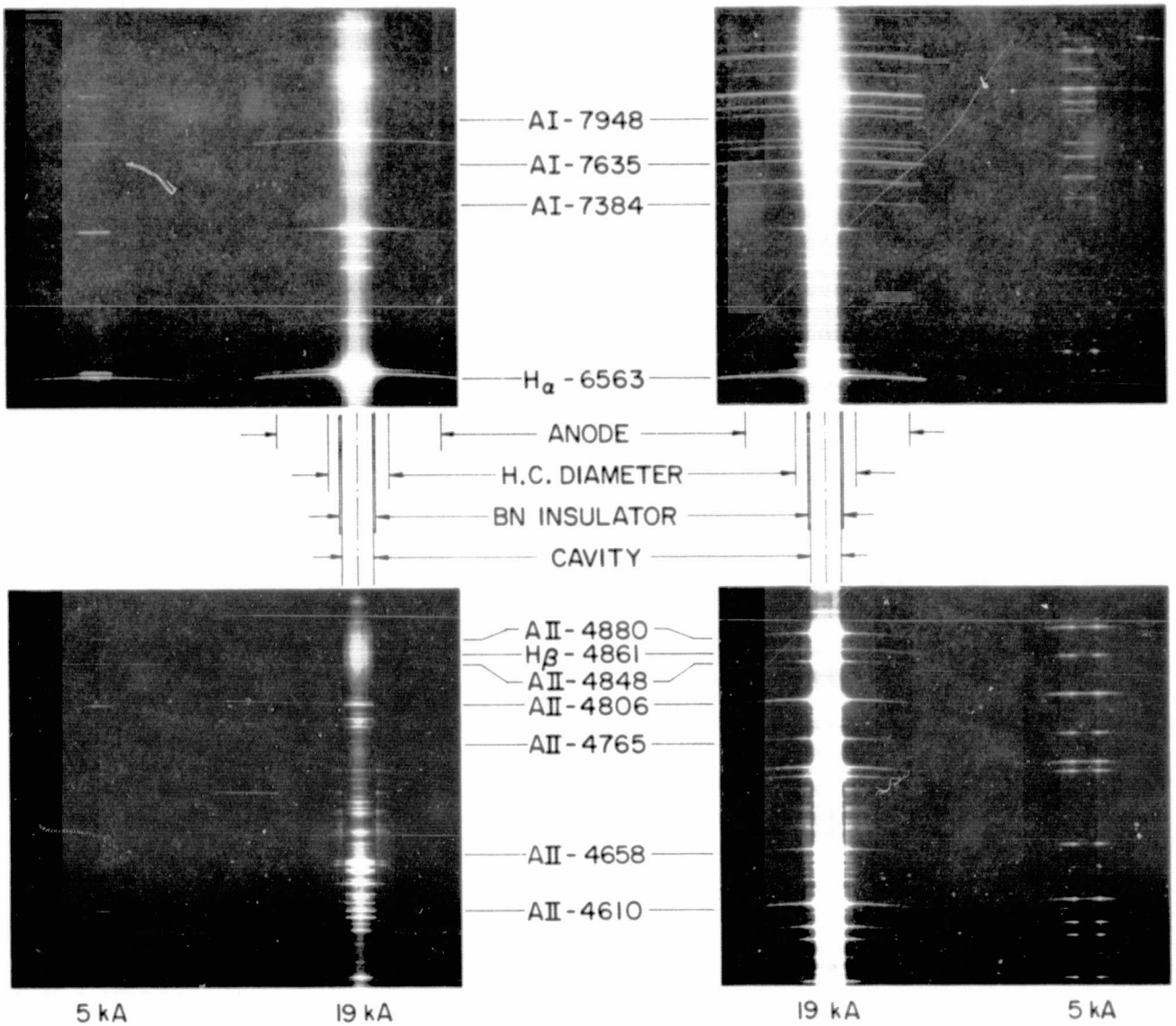

a) 0.4 g/sec

b) 16 g/sec

AP 25 P 564 75

SPECTRA OF HC DISCHARGES

FIGURE 25

mass flow decreases, the region of maximum AII radiance transforms from a relatively narrow, intense band near the surface of the cathode to a more uniform volume emission within the cavity.

This observation is supported by spectral photographs of the discharge for the same current and mass flow conditions. Figure 26 shows four photographs of the discharge taken from the same 45^{o} perspective through an interference filter which isolates the 4880 Å AII line. At the 16 g/sec mass flow (Fig. 26a,b), a bright ring is observed at the most downstream portion of the cathode surface, while at the 0.4 g/sec flow (Fig. 26c,d) the radiance emanates from across the entire cavity.

These spectrograms and photographs are manifestations of the participation of excited AII, coincident with a high electron number density, in the conduction process. At high mass flows, the radiance is concentrated in a sheath at the cathode surface which extends over a short axial region at the end of the cavity; at low mass flows, the bright radiance patterns next to the wall are absent indicating a more uniform distribution of the radiative processes.

To determine the current conduction pattern directly, magnetic probes were used in the cathode cavity for a range of currents from 0.9 to 7 kA and mass flows from 4.4×10^{-3} to 16 g/sec. The magnetic probe and technique used in this study are similar to that discussed previously, with the data acquired by translating the probe at a fixed radius of 0.75 cm. The current distributions are again presented as enclosed currents normalized to the value measured at the downstream end of the cavity.

In all cases, the stated mass flow is the flow injected through the hollow cathode into the discharge chamber. However, at the lower flow rates it was necessary to inject a small amount

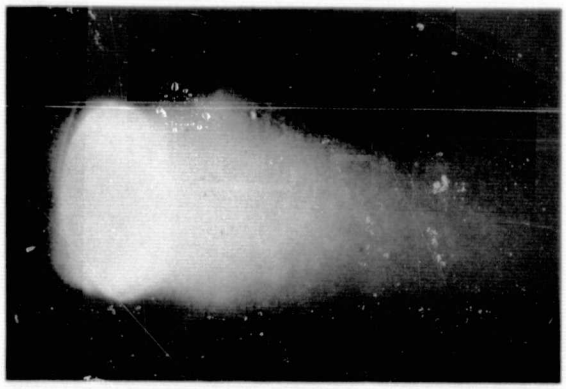

a) 19 kA

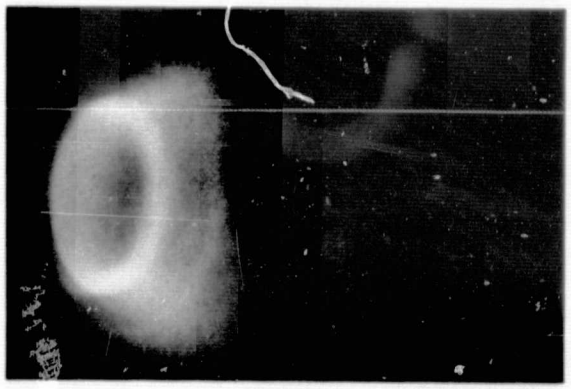

b) 5 kA

16 g/sec

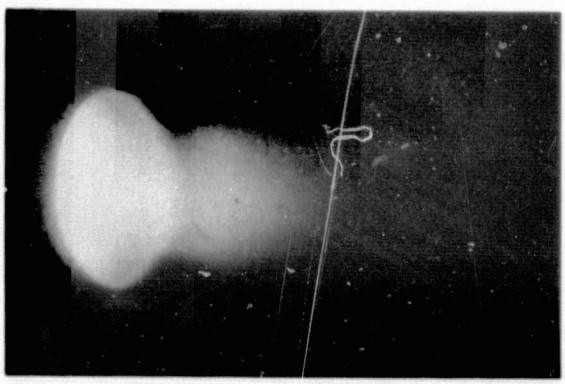

c) 19 kA

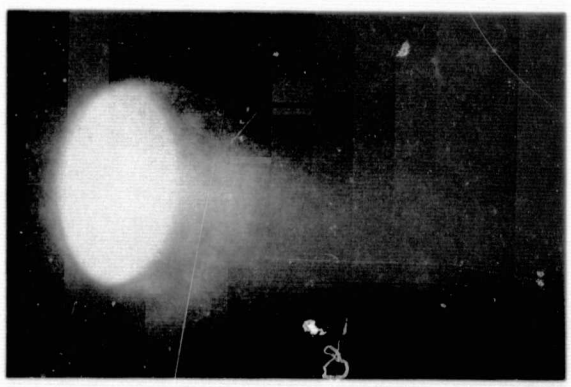

d) 5 kA

0.4 g/sec

HC XII DISCHARGES

AP 25 P 585 10

FIGURE 26

of gas through the outer six injectors in the discharge chamber backplate in order to maintain a satisfactory discharge in the chamber. Recent measurements of the plasma floating potential within and outside of the cathode cavity show that the cavity plasma is insensitive to changes in this external mass flow rate. Figure 27 shows the floating potential measured at three locations within the cavity and one downstream of the cathode for a fixed cathode mass flow of 4 g/sec and external mass flows of 0, 4 and 8 g/sec. These locations are shown in the inset of Fig. 27. Within the accuracy of the data, the potential distribution in the cavity is seen to be unaffected by the external flow.

The effects of current and mass flow on the enclosed current distribution inside the hollow cathode are shown in Fig. 28. Figure 28a shows normalized enclosed current profiles for currents of 0.9 and 7 kA at a fixed cathode mass flow of 0.4 g/sec, while Fig. 28b shows normalized profiles for several mass flows at a fixed current of 0.9 kA. Whereas changes in the cathode configuration had little effect on the current distribution within the hollow cathode, it is apparent that both current and mass flow have a first-order effect on the penetration of the current upstream into the cavity. In Fig. 28a, the 7 kA profile is seen by comparison with Fig. 20 to be identical to the profiles for all cathode configurations previously tested over a modest range of current and mass flow. However, reducing the current to 0.9 kA produces a drastic increase in the current penetration. This new current distribution is accompanied by a broadening of the cleaned metallic cathode surface from the 0.6-cm-wide band observed previously, Fig. 24, to a 1.5-cm-wide silvery area.

The dependence of the current distribution on mass flow for a fixed current is equally significant. Figure 28b shows that for the 0.9 kA current, a relatively high mass flow of 2 g/sec results in a current attachment of a few millimeters at the

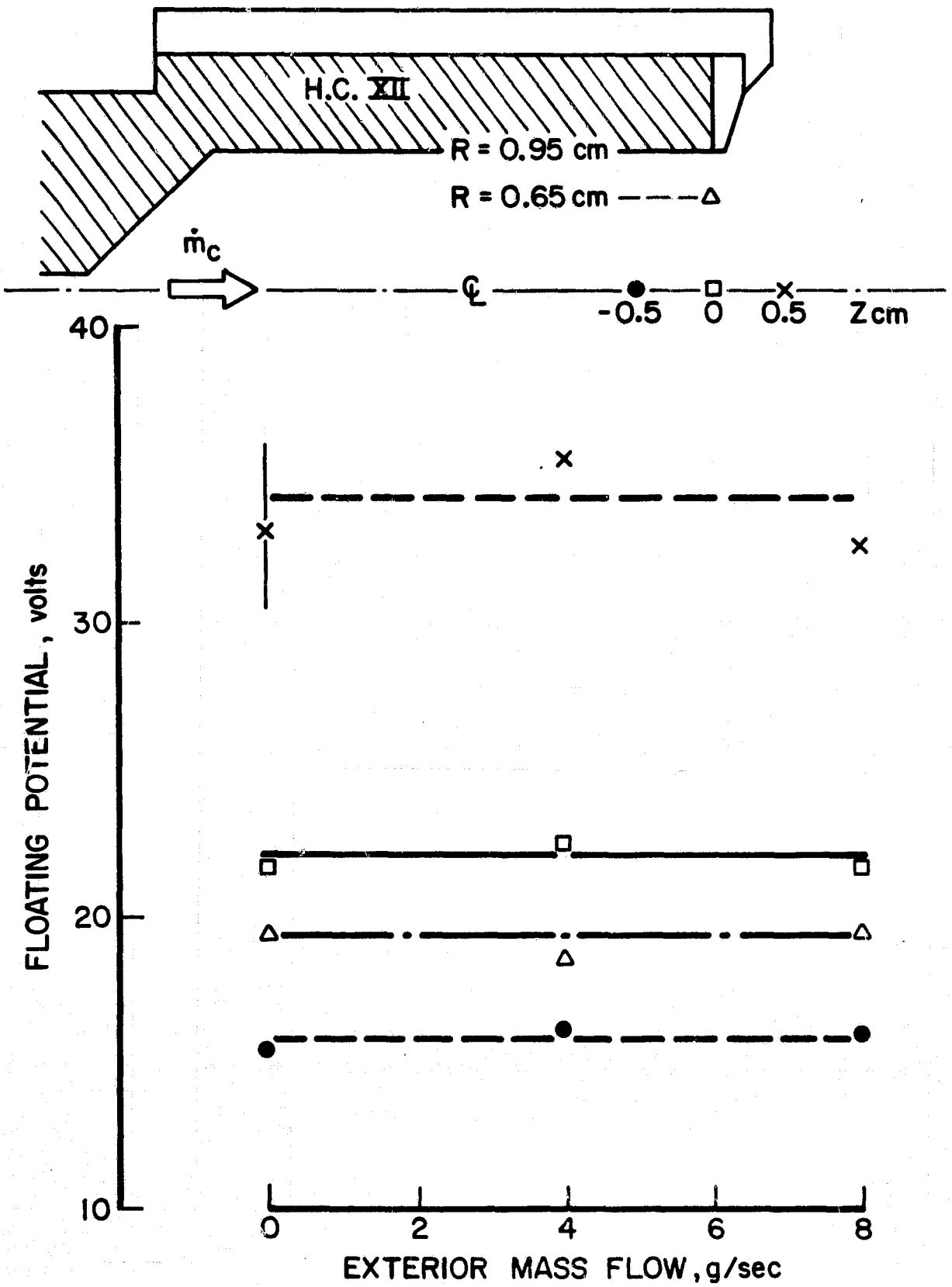

CAVITY POTENTIAL DEPENDENCE ON EXTERNAL FLOW

$\dot{m}_c$ = 4 g/sec ; J = 7 kA

FIGURE 27

AP 25-5135

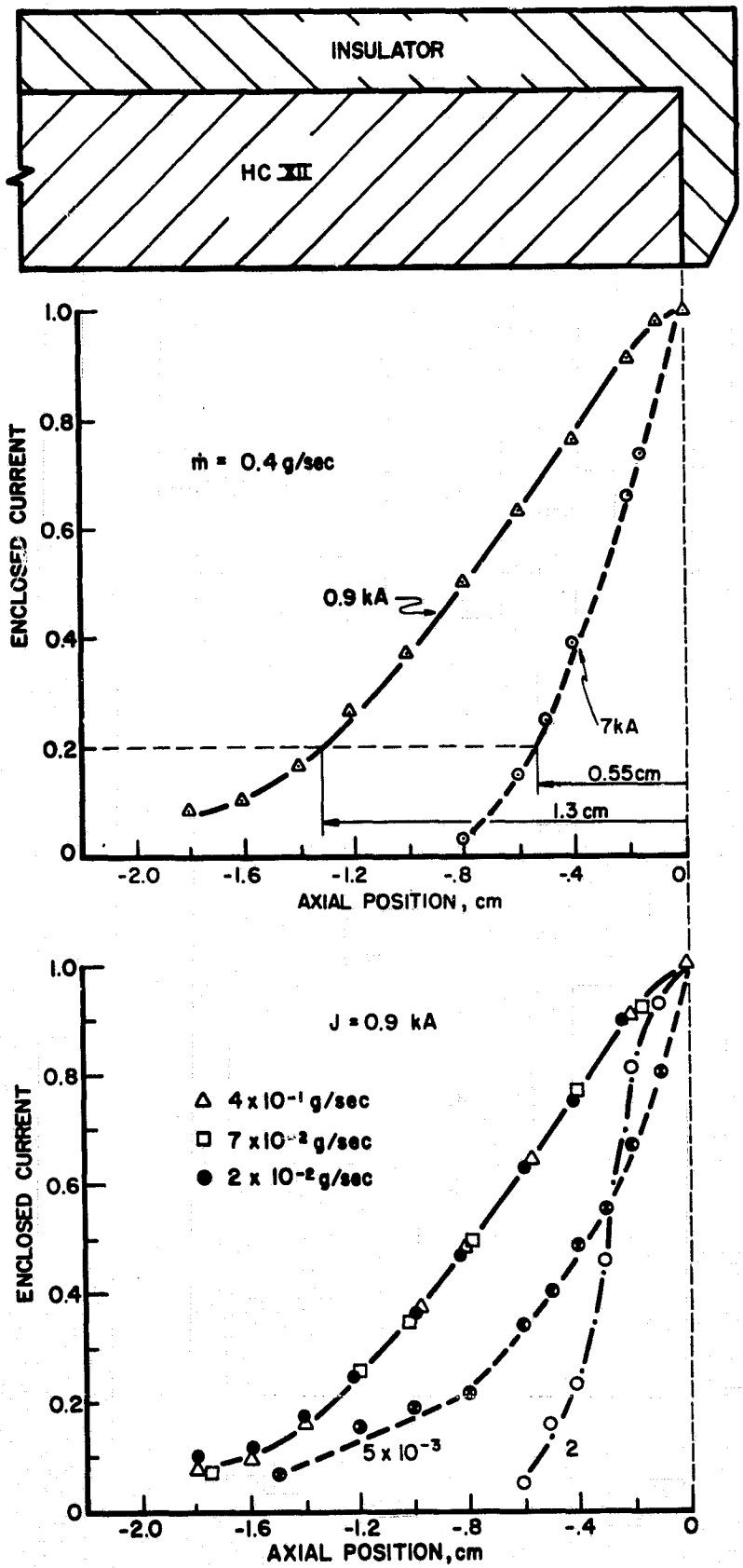

CURRENT DISTRIBUTIONS IN HC XII

FIGURE 28
AP 25-5112

downstream end of the cavity. As the mass flow is decreased, the current penetrates farther into the cavity, increasing its attachment area by more than a factor of three. However, further decrease in the mass flow to less than 10^{-2} g/sec produces a return of the current attachment to a narrow region at the end of the cavity.

For the purposes of comparing the relative penetration of the current for various operating conditions, it is useful to characterize the normalized current distribution by a single parameter, the active zone length, defined as the axial distance in the cavity over which 80% of the current is observed to attach. Figure 29 summarizes the variation in the experimentally determined active zone lengths over a wide range of current and mass flow. For a fixed mass flow of 0.4 g/sec (Fig. 29a), the active zone is seen to be relatively constant at the higher currents, but to increase by more than a factor of two as the current drops from 4.7 to 0.9 kA. The variation of the active zone length with mass flow is shown in Fig. 29b. As previously exhibited by the normalized distributions of current in Fig. 28b, the active zone is seen to achieve a maximum length over a restricted range of mass flow for a given current. The maximum penetration, as given by the active zone length shown in Fig. 29a, occurs for a mass flow of approximately 0.1 g/sec. Particularly interesting are the well-defined limits on mass flow for maximum current penetration. The lower limit appears to be independent of current at approximately 2×10^{-2} g/sec, while the upper limit increases somewhat with current, lying between 0.4 and 4.0 g/sec.

The measured active zone lengths displayed in Fig. 29b allow further interpretation of the spectra and luminosity photographs shown previously in Figs. 25 and 26. Recalling that for currents of 5 and 19 kA, these optical data reveal a luminous band at the downstream edge of the cathode cavity for a mass flow of 16 g/sec and a uniform luminosity at 0.4 g/sec, Fig. 29b shows that the 16 g/sec data is characteristic of a condition where the mass flow

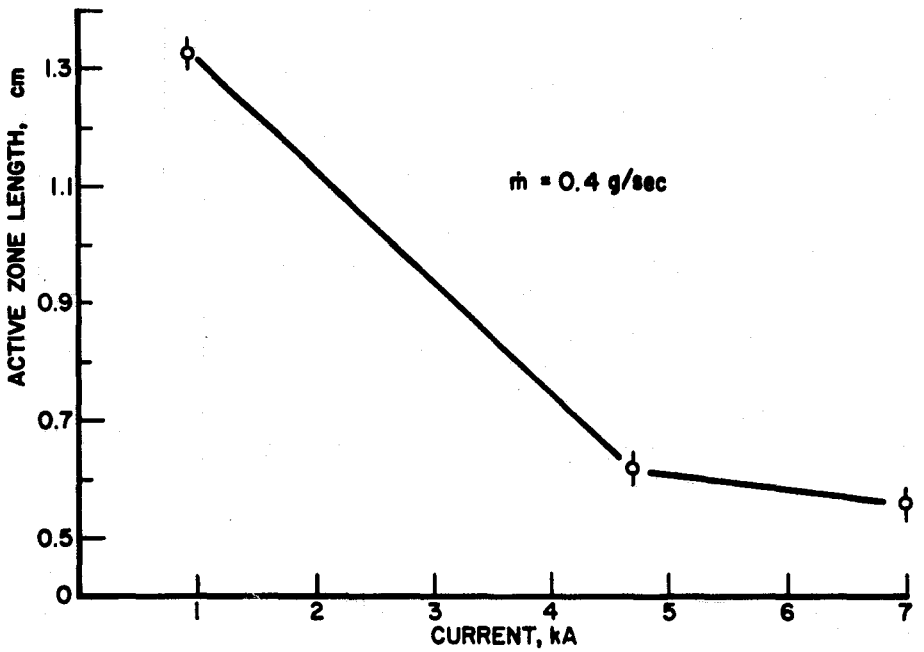

ACTIVE ZONE LENGTH

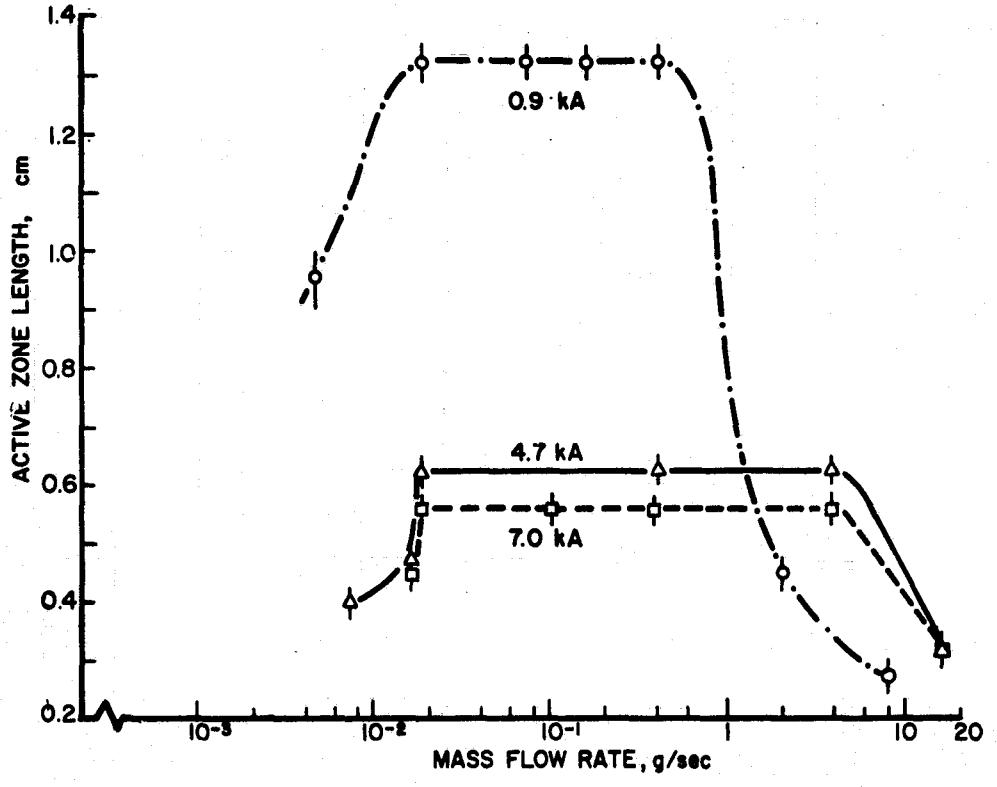

ACTIVE ZONE LENGTH

FIGURE 29
AP 25-5111

is greater than that for maximum current penetration. Thus, the band of radiance is associated with a high current density distribution at the downstream end of the cavity. Indeed, measurements of the axial extent of this band taken directly from the photographs give approximately 0.3 cm, in good agreement with the active zone length determined from magnetic probe data. In a similar way, the uniform radiance observed in the photographs at the lower mass flow typifies the deeper and more uniform current attachment deduced from the magnetic field measurements.

D. Discussion

It is instructive to compare the operating conditions at which the present results have been obtained with the working regimes of other hollow cathode researches. Since the choice of parameters for this comparison is somewhat arbitrary, the simplest combination of independent variables is selected: a mass flux $\dot{m}/S$ and a current density J/S, where S is the flow cross-sectional area at the cavity exit. Despite their previous use in the literature,[A-21] it is recognized that these parameters do not necessarily characterize hollow cathode operation; nevertheless they do provide a useful starting point for determining the proper scaling for these cathodes.

In Fig. 30, operating points and working regimes of several hollow cathode experimenters are displayed in the $\dot{m}/S$, J/S parameter plane. This plot is by no means a comprehensive summary of current research in hollow cathode discharges, but is instead a selection of operating conditions representative of the various programs. In the upper right corner lie the early MPD hollow cathode experiments.[154] The operating conditions for these tests were scaled to the early ion engine hollow cathode operating regime which lies in the upper right of the neighboring box. The mass flux and current density parameters for the ion engine hollow cathodes were calculated using the average cross-sectional area

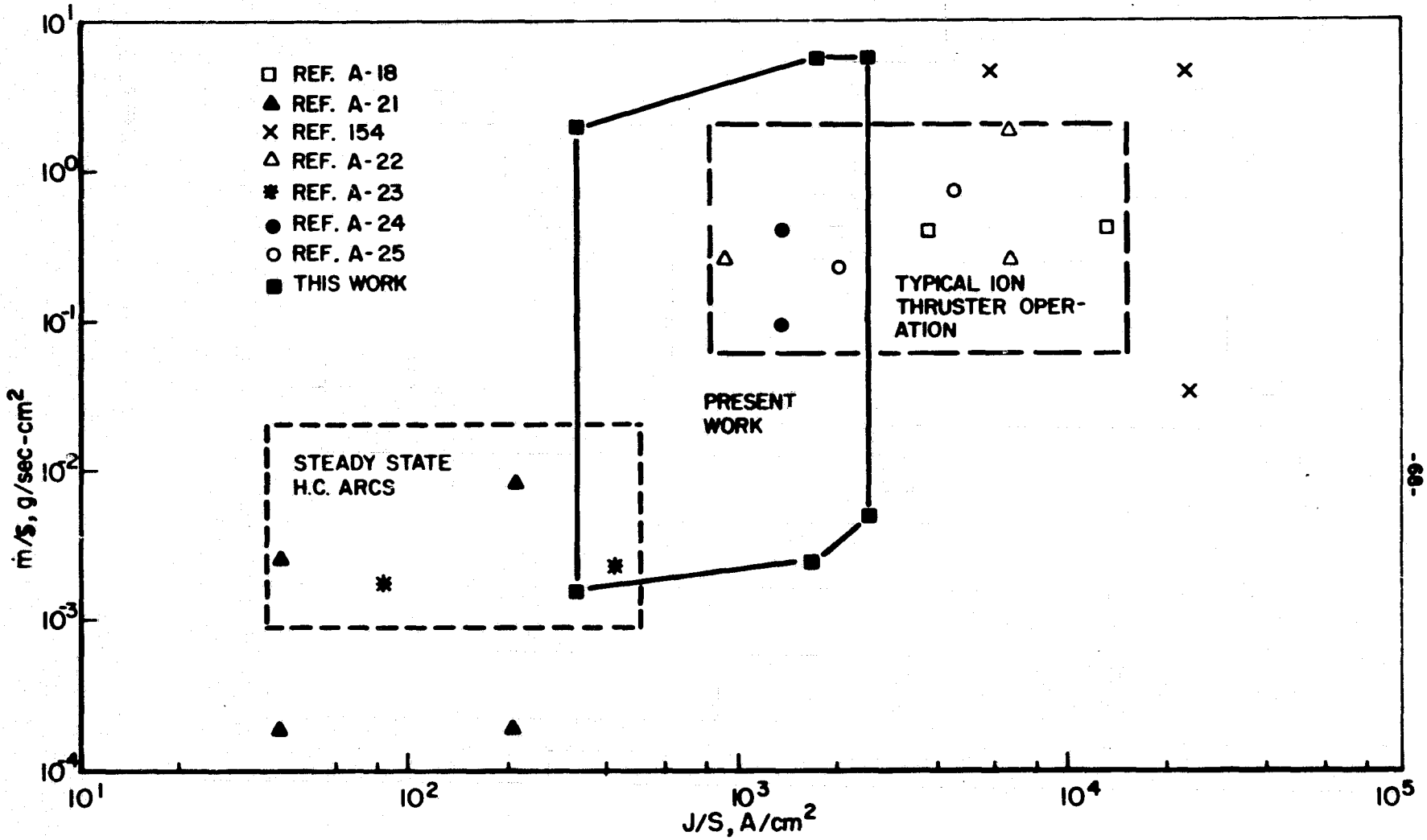

FIGURE 30
AP 25-5136

HC OPERATING REGIMES

of the tapered tungsten orifice at the downstream end of the cathode. The box in the lower left shows the so-called "normal" working regime of steady-state hollow cathode arcs.[A-21] This work focussed on the physics of hollow cathode operation with no constraints imposed by ion beam optics or ionization efficiency as in the case of the ion thrusters. The range of conditions examined in the present work is seen to bridge the steady-state and ion engine domains.

It is interesting to note that all of the three hollow cathode research areas outlined in Fig. 30 identify some restriction on mass flow for proper hollow cathode operation. For example, in the ion engine program, operation in the "spot" mode, which is more efficient than the higher voltage "plume" mode, typically requires mass fluxes greater than 0.3 g/sec-cm^2.[A-22] Similarly, experiments with steady-state hollow cathode arcs define a lower limit on mass flux below which the current attachment, as inferred from temperature measurements on the outside of the cylindrical cathode, moves from the interior of the cavity to the cavity lip.[A-21] An upper limit on mass flux is defined in this same work by a similar movement of the inferred current distribution. These limits are shown as the lower and upper boundaries of this operating regime on Fig. 30. For the present MPD hollow cathode work, the measured current distributions, summarized in Fig. 29, display larger and smaller values of the mass flux beyond which the active zone contracts to a higher current density attachment at the end of the cavity. The identification of mass flux limits in various hollow cathode experiments over a diverse range of operating conditions suggests that the same physical principles may be prevalent in each case. The difference in absolute values of the limits may be due to the choice of cathode cavity cross section as the scaling parameter for the mass flow and current. This simple scaling obviously neglects surface phenomena inside the cathode which may strongly influence the current emission and conduction processes.

E. Summary

Current and potential distributions have been measured in various large hollow cathodes for a range of currents from several hundred to several thousand amperes and mass flows from 10^{-3} to 16 g/sec. Whereas the current distribution within the cavity is uninfluenced by changes in the cathode configurations, varying the current and mass flow for a fixed configuration produces significant changes in the current conduction pattern. For a given current, a range of mass flows is determined for maximum current penetration into the cavity, with the amount of penetration increasing as current decreases. Spectroscopic and photographic evidence of AII and electron densities within the cavity confirm this attachment behavior. Comparison of these results with other hollow cathode researches provides insight into the scaling laws for hollow cathode arcs and indicates that despite the large range of currents and mass flows involved, similar physical phenomena may be guiding their operation.

PROJECT REFERENCES

[1]Jahn, R. G., Bernstein, I. B. and Kunen, A. E., "Proposed Studies of the Formation and Stability of an Electromagnetic Boundary in a Pinch," Proposal for NASA Research Grant NsG-306-63, Mar. 5, 1962, Princeton Univ., Princeton, N. J.

[2]Jahn, R. G. and von Jaskowsky, W. F., "Pulsed Electromagnetic Gas Acceleration," NASA NsG-306-63 progress report for the period 1 July 1962 to 31 December 1962, Aeron. Eng. Rept. No. 634, Jan. 1963, Princeton Univ., Princeton, N. J.

[3]Jahn, R. G. and von Jaskowsky, W. F., "The Plasma Pinch as a Gas Accelerator," A.I.A.A. Preprint 63013, A.I.A.A. Electric Propulsion Conference, Colorado Springs, Colo., 11-13 Mar. 1963.

[4]Jahn, R. G. and von Jaskowsky, W. F., "Pulsed Electromagnetic Gas Acceleration," NASA NsG-306-63 progress report for the period 1 January 1963 to 30 June 1963, Aeron. Eng. Report No. 634a, June 1963, Princeton Univ., Princeton, N. J.

[5]Jahn, R. G. and von Jaskowsky, W. F., "Structure of a Large-radius Pinch Discharge," A.I.A.A. Journal, Vol. 1, No. 8, Aug. 1963, pp. 1809-1814.

[6]Jahn, R. G., von Jaskowsky, W. F. and Casini, A. L., "A Gas-triggered Inverse Pinch Switch," NASA NsG-306-63, Aeron. Eng. Tech. Note No. 660, Aug. 1963, Princeton Univ., Princeton, N. J.

[7]Jahn, R. G., von Jaskowsky, W. F. and Casini, A. L., "Gas triggered Inverse Pinch Switch," The Review of Scientific Instruments, Vol. 34, No. 12, Dec. 1963, pp. 1439-1440.

[8]Jahn, R. G. and von Jaskowsky, W. F., "Pulsed Electromagnetic Gas Acceleration," (Paper delivered at the 4th NASA Intercenter Conference on Plasma Physics, Washington, D. C., 2-4 Dec. 1963), p. 8.

[9]Jahn, R. G. and von Jaskowsky, W. F., "Pulsed Electromagnetic Gas Acceleration," NASA NsG-306-63 progress report for period 1 July 1963 to 31 December 1963, Aeron. Eng. Rept. No. 634b, Dec. 1963, Princeton Univ., Princeton, N. J.

PROJECT REFERENCES

[10]Jahn, R. G. and von Jaskowsky, W. F., "Current Distributions in Large-radius Pinch Discharges," A.I.A.A. Preprint 64-25, A.I.A.A. Aerospace Sciences Meeting, New York, N. Y., 20-22 Jan. 1964.

[11]Jahn, R. G. and von Jaskowsky, W. F., "Current Distributions in Large-radius Pinch Discharges," A.I.A.A. Bulletin, Vol. 1, No. 1, Jan. 1964, p. 12.

[12]Jahn, R. G. and von Jaskowsky, W. F., "Pulsed Electromagnetic Gas Acceleration," NASA NsG-306-63 renewal proposal for 15-months extension, Jan. 15, 1964, Princeton Univ., Princeton, N. J.

[13]Jahn, R. G. and von Jaskowsky, W. F., "Pulsed Electromagnetic Gas Acceleration," NASA NsG-306-63 progress report for the period 1 January 1964 to 30 June 1964, Aeron. Eng. Rept. No. 634c, July 1964, Princeton Univ., Princeton, N. J.

[14]Jahn, R. G., von Jaskowsky, W. F. and Casini, A. L., "Gas-triggered Pinch Discharge Switch," NASA NsG-306-63, Aerospace and Mechanical Sciences Tech. Note No. 101, July 1964, Princeton Univ., Princeton, N. J.

[15]Corr, J. M., "Double Probe Studies in an 8" Pinch Discharge," M.S.E. thesis, Sept. 1964, Princeton Univ., Princeton, N. J.

[16]Jahn, R. G. and von Jaskowsky, W. F., "Exhaust of a Pinched Plasma From an Axial Orifice," A.I.A.A. Bulletin, Vol. 1, No. 10, Oct. 1964, p. 570.

[17]Jahn, R. G. and von Jaskowsky, W. F., "Current Distributions in Large-radius Pinch Discharges," A.I.A.A. Journal, Vol. 2, No. 10, Oct. 1964, pp. 1749-1753.

[18]Jahn, R. G., von Jaskowsky, W. F. and Casini, A. L., "Gas-triggered Pinch Discharge Switch", The Review of Scientific Instruments, Vol. 36, No. 1, Jan. 1964, pp. 101-102.

[19]Jahn, R. G. and von Jaskowsky, W. F., "Exhaust of a Pinched Plasma from an Axial Orifice," A.I.A.A. Paper 65-92, A.I.A.A. 2nd Aerospace Sciences Meeting, New York, N. Y., 25-27 Jan. 1964.

PROJECT REFERENCES

[20]Jahn, R. G. and von Jaskowsky, W. F., "Pulsed Electromagnetic Gas Acceleration," NASA NsG-306-63 progress report for the period 1 July 1964 to 31 December 1964, Aerospace and Mechanical Sciences Rept. No. 634d, Jan. 1965, Princeton Univ., Princeton, N. J.

[21]Wright, E. S., "The Design and Development of Rogowski Coil Probes for Measurement of Current Density Distribution in a Plasma Pinch," M.S.E. thesis, May 1965, Princeton Univ., Princeton, N. J.

[22]Jahn, R. G. and von Jaskowsky, W. F., "Pulsed Electromagnetic Gas Acceleration," NASA NsG-306-63 renewal proposal for 12-months extension, June 7, 1964, Princeton Univ., Princeton, N. J.

[23]Jahn, R. G. and Black, N. A., "On the Dynamic Efficiency of Pulsed Plasma Accelerators," A.I.A.A. Journal, Vol. 3, No. 6, June 1965, pp. 1209-1210.

[24]Black, N. A., "Linear Pinch Driven by a High-current Pulse-forming Network," A.I.A.A. Bulletin, Vol. 2, No. 6, June 1965, p. 309.

[25]Wright, E. S. and Jahn, R. G., "The Design and Development of Rogowski Coil Probes for Measurement of Current Density Distribution in a Plasma Pinch," NASA NsG-306-63, Aerospace and Mechanical Sciences Rept. No. 740, June 1965, Princeton Univ., Princeton, N. J.

[26]Rowell, G. A., "Cylindrical Shock Model of the Plasma Pinch," M.S.E. thesis, July 1965, Princeton Univ., Princeton, N. J.

[27]Black, N. A., "Linear Pinch Driven by a High-current Pulse-forming Network," A.I.A.A. Paper 65-336, A.I.A.A. 2nd Annual Meeting, San Francisco, Calif., 26-29 July 1965.

[28]Jahn, R. G. and von Jaskowsky, W. F., "Pulsed Electromagnetic Gas Acceleration," NASA NsG-306-63 progress report for the period 1 January 1965 to 30 June 1965, Aerospace and Mechanical Sciences Rept. No. 634e, July, 1965, Princeton Univ., Princeton, N. J.

[29]Jahn, R. G. and Ducati, A. C., "Design and Development of a Thermo-Ionic Electric Thrustor," 5QS 085-968 Interim Report, NASA Contract NASw-968, Aug. 1965, Giannini Scientific Corp., Santa Ana, Calif.

PROJECT REFERENCES

[30]Jahn, R. G., von Jaskowsky, W. F. and Burton, R. L., "Ejection of a Pinched Plasma From an Axial Orifice," A.I.A.A. Journal, Vol. 3, No. 10, Oct. 1965, pp. 1862-1866.

[31]Jahn, R. G. and Wright, E. S., "Miniature Rogowski Coil Probes for Direct Measurement of Current Density Distribution in Transient Plasmas," The Review of Scientific Instruments, Vol. 36, No. 12, Dec. 1965, pp. 1891-1892.

[32]Jahn, R. G. and von Jaskowsky, W. F., "Pulsed Electromagnetic Gas Acceleration," NASA NsG-306-63 progress report for the period 1 July 1965 to 31 December 1965, Aerospace and Mechanical Sciences Rept. No. 634f, Jan. 1966, Princeton Univ., Princeton, N. J.

[33]Burton, R. L. and Jahn, R. G., "Electric and Magnetic Field Distributions in a Propagating Current Sheet," A.I.A.A. Bulletin, Vol. 3, No. 1, Jan. 1966, p. 35.

[34]Rowell, G. A., Jahn, R. G. and von Jaskowsky, W. F., "Cylindrical Shock Model of the Plasma Pinch," NASA NsG-306-63, Aerospace and Mechanical Sciences Rept. No. 742, Feb. 1966, Princeton Univ., Princeton, N. J.

[35]Burton, R. L. and Jahn, R. G., "Electric and Magnetic Field Distributions in a Propagating Current Sheet," A.I.A.A. Paper 66-200, A.I.A.A. 5th Electric Propulsion Conference, San Diego, Calif., 7-9 Mar. 1966.

[36]Black, N. A., "Pulse-forming Networks for Propulsion Research," Proceedings of the 7th Symposium on Engineering Aspects of Magnetohydrodynamics, Princeton Univ., Princeton, N. J., Mar. 30-April 1, 1966, pp. 10-11.

[37]Jahn, R. G., "Electromagnetic Propulsion," Astronautics and Aeronautics, Vol. 4, No. 2, February, 1966, pp. 73-75.

[38]Black, N. A., "Dynamics of a Pinch Discharge Driven by a High-current Pulse-forming Network," Ph.D. thesis, May 1966, Princeton Univ., Princeton, N. J.

[39]Black, N. A. and Jahn, R. G., "Dynamics of a Pinch Discharge Driven by a High-current Pulse-forming Network," NASA NsG-306-63, Aerospace and Mechanical Sciences Rept. No. 778, May 1966, Princeton Univ., Princeton, N. J.

PROJECT REFERENCES

[40]Jahn, R. G., "Pulsed Plasma Propulsion," Proceedings of the 5th NASA Intercenter and Contractors Conference on Plasma Physics, Washington, D. C., 24-26 May 1966, pt. V, pp. 75-81.

[41]Jahn, R. G. and von Jaskowsky, W. F., "Pulsed Electromagnetic Gas Acceleration," NASA NsG-306-63 renewal proposal for 24-months extension, May 25, 1966, Princeton Univ., Princeton, N. J.

[42]Ducati, A. C., Jahn, R. G., Muehlberger, E. and Treat, R. P., "Design and Development of a Thermo-Ionic Electric Thrustor," FR-056-968 Final Report, NASA CR-54703, May 1966, Giannini Scientific Corp., Santa Ana, Calif.

[43]Jahn, R. G. and Clark, K. E., "A Large Dielectric Vacuum Facility," A.I.A.A. Journal, Vol. 4, No. 6, June 1966, p. 1135.

[44]John, R. R., Bennett, S. and Jahn, R. G., "Current Status of a Plasma Propulsion," A.I.A.A. Bulletin, Vol. 3, No. 5, May 1966, p. 264.

[45]John, R. R., Bennett, S. and Jahn, R. G., "Current Status of a Plasma Propulsion," A.I.A.A. Paper 66-565, A.I.A.A. 2nd Propulsion Joint Specialist Conference, Colorado Springs, Colo., 13-17 June 1966.

[46]Jahn, R. G. and von Jaskowsky, W. F., "Pulsed Electromagnetic Gas Acceleration," NASA NsG-306-63 progress report for the period 1 January 1966 to 30 June 1966, Aerospace and Mechanical Sciences Rept. No. 634g, July 1966, Princeton Univ., Princeton, N. J.

[47]Burton, R. L., "Structure of the Current Sheet in a Pinch Discharge," Ph.D. thesis, Sept. 1966, Princeton Univ., Princeton, N. J.

[48]Burton, R. L. and Jahn, R. G., "Structure of the Current Sheet in a Pinch Discharge," NASA NsG-306-63, Aerospace and Mechanical Sciences Rept. No. 783, Sept. 1966, Princeton Univ., Princeton, N. J.

[49]Jahn, R. G. and von Jaskowsky, W. F., "Pulsed Electromagnetic Gas Acceleration," NASA NsG-306-63 progress report for the period 1 July 1966 to 31 December 1966, Aerospace and Mechanical Sciences Rept. No. 634h, Jan. 1967, Princeton Univ., Princeton, N. J.

PROJECT REFERENCES

[50]Burton, R. L. and Jahn, R. G., "Structure of the Current Sheet in a Pinch Discharge," Bulletin of the American Physical Society, Vol. 12, Ser. II, Paper L1, May 1967, p. 848.

[51]Jahn, R. G., "Plasma Propulsion for Deep Space Flight," Bulletin of the American Physical Society, Vol. 12, Ser. II, Paper BC-1, May 1967, p. 646.

[52]Ellis, W. R., Jr., "An Investigation of Current Sheet Structure in a Cylindrical Z-Pinch," Ph.D. thesis, July 1967, Princeton Univ., Princeton, N. J.

[53]Ellis, W. R., Jr. and Jahn, R. G., "An Investigation of Current Sheet Structure in a Cylindrical Z-Pinch," NASA NsG-306-63, Aerospace and Mechanical Sciences Rept. No. 805, July 1967, Princeton Univ., Princeton, N. J.

[54]Jahn, R. G. and von Jaskowsky, W. F., "Pulsed Electromagnetic Gas Acceleration," NASA NsG-306-63 progress report for the period 1 January 1967 to 30 June 1967, Aerospace and Mechanical Sciences Rept. No. 634i, July 1967, Princeton Univ., Princeton, N. J.

[55]Clark, K. E. and Jahn, R. G., "The Magnetoplasmadynamic Arc," Astronautica Acta, Vol. 13, No. 4, 1967, pp. 315-325.

[56]Jahn, R. G., "The MPD Arc," NASA Contract NASw-1513, Aug. 1967, Giannini Scientific Corp., Santa Ana, Calif.

[57]Eckbreth, A. C., Clark, K. E. and Jahn, R. G., "Current Pattern Stabilization in Pulsed Plasma Accelerators," A.I.A.A. Bulletin, Vol. 4, No. 9, Sept. 1967, p. 433.

[58]Clark, K. E., Eckbreth, A. C. and Jahn, R. G., "Current Pattern Stabilization in Pulsed Plasma Accelerators," A.I.A.A. Paper 67-656, A.I.A.A. Electric Propulsion and Plasmadynamics Conference, Colorado Springs, Colo., 11-13 Sept. 1967.

[59]Jahn, R. G. and von Jaskowsky, W. F., "Pulsed Electromagnetic Gas Acceleration," NASA NsG-306-63 progress report for the period 1 July 1967 to 31 December 1967, Aerospace and Mechanical Sciences Rept. No. 634j, Jan. 1968, Princeton Univ., Princeton, N. J.

PROJECT REFERENCES

[60]Ducati, A. C., Jahn, R. G., Muehlberger, E. and Treat, R. P., "Exploratory Electromagnetic Thruster Research," TR 117-1513 Annual Report, NASA CR 62047, Feb. 1968, Giannini Scientific Corp., Santa Ana, Calif.

[61]Jahn, R. G., PHYSICS OF ELECTRIC PROPULSION, McGraw-Hill Book Company, New York, 1968.

[62]Burton, R. L. and Jahn, R. G., "Acceleration of Plasma by a Propagating Current Sheet," The Physics of Fluids, Vol. 11, No. 6, June 1968, pp. 1231-1237.

[63]Jahn, R. G. and von Jaskowsky, W. F., "Pulsed Electromagnetic Gas Acceleration," NASA NGR 31-001-005 step-funding renewal proposal for the period 1 October 1968 to 30 September 1971, June 1, 1968, Princeton Univ., Princeton, N. J.

[64]Jahn, R. G. and von Jaskowsky, W. F., "Pulsed Electromagnetic Gas Acceleration," NASA NsG-306/31-001-005 progress report for the period 1 January 1968 to 30 June 1968, Aerospace and Mechanical Sciences Rept. No. 634k, July 1968, Princeton Univ., Princeton, N. J.

[65]Wilbur, P. J., "Energy Transfer from a Pulse Network to a Propagating Current Sheet," Ph.D. thesis, Sept. 1968, Princeton Univ., Princeton, N. J.

[66]Wilbur, P. J. and Jahn, R. G., "Energy Transfer from a Pulse Network to a Propagating Current Sheet," NASA NGR 31-001-005, Aerospace and Mechanical Sciences Rept. No. 846, Sept. 1968, Princeton Univ., Princeton, N. J.

[67]Ducati, A. C., Jahn, R. G., Muehlberger, E. and Treat, R. P., "Exploratory Electromagnetic Thruster Research, Phase II," 2SS108-1513 Interim Report, NASA Contract NASw-1513, Oct. 1968, Giannini Scientific Corp., Santa Ana, Calif.

[68]Eckbreth, A. C., Clark, K. E. and Jahn, R. G., "Current Pattern Stabilization in Pulsed Plasma Accelerators," A.I.A.A. Journal, Vol. 6, No. 11, Nov. 1968, pp. 2125-2132.

PROJECT REFERENCES

[69]Eckbreth, A. C., "Current Pattern and Gas Flow Stabilization in Pulsed Plasma Accelerators," Ph.D. thesis, Dec. 1968, Princeton Univ., Princeton, N. J.

[70]Eckbreth, A. C. and Jahn, R. G., "Current Pattern and Gas Flow Stabilization in Pulsed Plasma Accelerators," NASA NGL 31-001-005, Aerospace and Mechanical Sciences Rept. No. 857, Dec. 1968, Princeton Univ., Princeton, N. J.

[71]York, T. M., "Pressure Distribution in the Structure of a Propagating Current Sheet," Ph.D. thesis, Dec. 1968, Princeton Univ., Princeton, N. J.

[72]York, T. M. and Jahn, R. G., "Pressure Distribution in the Structure of a Propagating Current Sheet," NASA NGL 31-001-005, Aerospace and Mechanical Sciences Rept. No. 853, Dec. 1968, Princeton Univ., Princeton, N. J.

[73]Eckbreth, A. C. and Jahn, R. G., "Current Pattern and Gas Flow Stabilization in Pulsed Plasma Accelerators," A.I.A.A. Bulletin, Vol. 5, No. 12, Dec. 1968, p. 730.

[74]Wilbur, P. J. and Jahn, R. G., "Energy Transfer From a Pulse Network to a Propagating Current Sheet," A.I.A.A. Bulletin, Vol. 5, No. 12, Dec. 1968, p. 730.

[75]Ellis, W. R. and Jahn, R. G., "Ion Density and Current Distributions in a Propagating Current Sheet, Determined by Microwave Reflection Technique," Rept. No. CLM-P-187, Dec. 1968, Culham Laboratory, Abingdon, Berkshire, Great Britain.

[76]Jahn, R. G. and von Jaskowsky, W. F., "Pulsed Electromagnetic Gas Acceleration," NASA NGL 31-001-005 progress report for the period 1 July 1968 to 31 December 1968, Aerospace and Mechanical Sciences Rept. No. 634, Jan. 1969, Princeton Univ., Princeton, N. J.

[77]Eckbreth, A. C. and Jahn, R. G., "Current Pattern and Gas Flow Stabilization in Pulsed Plasma Accelerators," A.I.A.A. Paper 69-112, A.I.A.A. 7th Aerospace Sciences Meeting, New York, N. Y., 20-22 Jan. 1969.

PROJECT REFERENCES

[78] Wilbur, P. J. and Jahn, R. G., "Energy Transfer From a Pulse Network to a Propagating Current Sheet," A.I.A.A. Paper 69-113, A.I.A.A. 7th Aerospace Sciences Meeting, New York, N. Y., 20-22 Jan. 1969.

[79] Ellis, W. R. and Jahn, R. G., "Ion Density and Current Distributions in a Propagating Current Sheet, Determined by Microwave Reflection Technique," Journal of Plasma Physics, Vol. 3, Pt. 2, 1969, pp. 189-213.

[80] York, T. M. and Jahn, R. G., "Pressure Distribution in the Structure of a Propagating Current Sheet," A.I.A.A. Bulletin, Vol. 6, No. 2, Feb. 1969, p. 75.

[81] Clark, K. E. and Jahn, R. G., "Quasi-steady Plasma Acceleration," A.I.A.A. Bulletin, Vol. 6, No. 2, Feb. 1969, p. 75.

[82] York, T. M. and Jahn, R. G., "Pressure Distribution in the Structure of a Propagating Current Sheet," A.I.A.A. Paper 69-264, A.I.A.A. 7th Electric Propulsion Conference, Williamsburg, Va., 3-5 Mar. 1969.

[83] Clark, K. E. and Jahn, R. G., "Quasi-steady Plasma Acceleration," A.I.A.A. Paper 69-267, A.I.A.A. 7th Electric Propulsion Conference, Williamsburg, Va., 3-5 Mar. 1969.

[84] Jahn, R. G. and Mickelsen, W. R., "Electric Propulsion Notebook," A.I.A.A. Professional Study Series, Williamsburg, Va., 1-2 Mar. 1969.

[85] Boyle, M. J., "Plasma Velocity Measurements with Electric Probes," B.S.E. thesis, April 1969, Princeton Univ., Princeton, N. J.

[86] Clark, K. E., "Quasi-steady Plasma Acceleration," Ph.D. thesis, May 1969, Princeton Univ., Princeton, N. J.

[87] Clark, K. E. and Jahn, R. G., "Quasi-steady Plasma Acceleration," NASA NGL 31-001-005, Aerospace and Mechanical Sciences Rept. No. 859, May 1969, Princeton Univ., Princeton, N. J.

PROJECT REFERENCES

[88]Boyle, M. J., "Plasma Velocity Measurements with Electric Probes," Paper No. 4 (Paper presented at the Northeastern Regional Student Conference, Princeton Univ., Princeton, N. J., 9-10 May 1969).

[89]Mickelsen, W. R. and Jahn, R. G., "Status of Electric Propulsion," A.I.A.A. Bulletin, Vol. 6, No. 6, June 1969, p. 257.

[90]Mickelsen, W. R. and Jahn, R. G., "Status of Electric Propulsion," A.I.A.A. Paper 69-497, A.I.A.A. 5th Propulsion Joint Specialist Conference, U. S. Air Force Academy, Colo., 9-13 June 1969.

[91]Ducati, A. C. and Jahn, R. G., "Electron Beam from a Magnetoplasmadynamic Arc," The Physics of Fluids, Vol. 12, No. 6, June 1969, pp. 1177-1181.

[92]Jahn, R. G. and von Jaskowsky, W. F., "Pulsed Electromagnetic Gas Acceleration," NASA NGL 31-001-005 progress report for the period 1 January 1969 to 30 June 1969, Aerospace and Mechanical Sciences Rept. No. 634m, July 1969, Princeton Univ., Princeton, N. J.

[93]Jahn, R. G. and von Jaskowsky, W. F., "Pulsed Electromagnetic Gas Acceleration," NASA NGR 31-001-005 step-funding renewal proposal for the period 1 October 1969 to 30 September 1970, July 1, 1969, Princeton Univ., Princeton, N. J.

[94]Jahn, R. G., Clark, K. E., Oberth, R. C. and Turchi, P. J., "Acceleration Patterns in Quasi-steady MPD Arcs," A.I.A.A. Bulletin, Vol. 6, No. 12, Dec. 1969, p. 701.

[95]Ducati, A. C. and Jahn, R. G., "Repetitively Pulsed, Quasi-steady Vacuum MPD Arc," A.I.A.A. Bulletin, Vol. 6, No. 12, Dec. 1969, p. 701.

[96]Jahn, R. G., von Jaskowsky, W. F. and Clark, K. E., "Pulsed Electromagnetic Gas Acceleration: Acceleration Processes in Quasi-steady Arcs," (Paper delivered at the 6th NASA Intercenter and Contractors Conference on Plasma Physics, NASA Langley Research Center, Hampton, Va., 8-10 Dec. 1969), pp. 8-15.

PROJECT REFERENCES

[97]Jahn, R. G., von Jaskowsky, W. F. and Clark, K. E., "Pulsed Electromagnetic Gas Acceleration," NASA NGL 31-001-005 progress report for the period 1 July 1969 to 31 December 1969, Aerospace and Mechanical Sciences Rept. No. 634n, Jan. 1970, Princeton Univ., Princeton, N. J.

[98]Eckbreth, A. C. and Jahn, R. G., "Current Pattern and Gas Flow Stabilization in Pulsed Plasma Accelerators," A.I.A.A. Journal, Vol. 8, No. 1, Jan. 1970, pp. 138-143.

[99]Jahn, R. G., Clark, K. E., Oberth, R. C. and Turchi, P. J., "Acceleration Patterns in Quasi-steady MPD Arcs," A.I.A.A. Paper 70-165, A.I.A.A. 8th Aerospace Sciences Meeting, New York, N. Y., 19-21 Jan. 1970.

[100]Ducati, A. C. and Jahn, R. G., "Repetitively Pulsed, Quasi-steady Vacuum MPD Arc," A.I.A.A. Paper 70-167, A.I.A.A. 8th Aerospace Sciences Meeting, New York, N. Y., 19-21 Jan. 1970.

[101]Wilbur, P. J. and Jahn, R. G., "Energy Transfer from a Pulse Network to a Propagating Current Sheet," A.I.A.A. Journal, Vol. 8, No. 1, Jan. 1970, pp. 144-149.

[102]Clark, K. E. and Jahn, R. G., "Quasi-steady Plasma Acceleration," A.I.A.A. Journal, Vol. 8, No. 2, Feb. 1970, pp. 216-220.

[103]York, T. M. and Jahn, R. G., "Pressure Distribution in the Structure of a Propagating Current Sheet," The Physics of Fluids, Vol. 13, No. 5, May 1970, pp. 1303-1309.

[104]Jahn, R. G., "Pulsed Electromagnetic Gas Acceleration," NASA NGL 31-001-005 step-funding renewal proposal for period 1 October 1970 to 30 September 1971, June 11, 1970, Princeton Univ., Princeton, N. J.

[105]Jahn, R. G., von Jaskowsky and Clark, K. E., "Pulsed Electromagnetic Gas Acceleration," NASA NGL 31-001-005, progress report for the period 1 January 1970 to 30 June 1970, Aerospace and Mechanical Sciences Rept. No. 634o, July 1970, Princeton Univ., Princeton, N. J.

PROJECT REFERENCES

[106]Turchi, P. J. and Jahn, R. G., "The Cathode Region of a Quasi-steady MPD Arcjet," A.I.A.A. Bulletin, Vol. 7, No. 9, Sept. 1970, p. 449.

[107]Clark, K. E., DiCapua, M. S., Jahn, R. G. and von Jaskowsky, W. F., "Quasi-steady Magnetoplasmadynamic Arc Characteristics," A.I.A.A. Bulletin, Vol. 7, No. 9, Sept. 1970, p. 449.

[108]Turchi, P. J. and Jahn, R. G., "The Cathode Region of a Quasi-steady MPD Arcjet," A.I.A.A. Paper 70-1094, A.I.A.A. 8th Electric Propulsion Conference, Stanford, Calif., 31 Aug.-2 Sept. 1970.

[109]Clark, K. E., DiCapua, M. S., Jahn, R. G. and von Jaskowsky, W. F., "Quasi-steady Magnetoplasmadynamic Arc Characteristics," A.I.A.A Paper 70-1095, A.I.A.A. 8th Electric Propulsion Conference, Stanford, Calif., 31 Aug.-2 Sept. 1970.

[110]Turchi, P. J., "The Cathode Region of a Quasi-steady Magnetoplasmadynamic Arcjet," Ph.D. thesis, Sept. 1970, Princeton Univ., Princeton, N. J.

[111]Turchi, P. J. and Jahn, R. G., "The Cathode Region of a Quasi-steady Magnetoplasmadynamic Arcjet," NASA NGL 31-001-005, Aerospace and Mechanical Sciences Rept. No. 940, Oct. 1970, Princeton Univ., Princeton, N. J.

[112]Oberth, R. C., "Anode Phenomena in High-Current Discharges," Ph.D. thesis, Dec. 1970, Princeton Univ., Princeton, N. J.

[113]Oberth, R. C. and Jahn, R. G., "Anode Phenomena in High-Current Discharges," NASA NGL 31-001-005, Aerospace and Mechanical Sciences Rept. No. 961, Dec. 1970, Princeton Univ., Princeton, N. J.

[114]Di Capua, M. S. and Jahn, R. G., "Voltage-Current Characteristics of Parallel-Plate Plasma Accelerators," A.I.A.A. Bulletin, Vol. 8, No. 1, Jan. 1971, p. 40.

[115]Oberth, R. C. and Jahn, R. G., "Anode Phenomena in High-Current Accelerators," A.I.A.A. Bulletin, Vol. 8, No. 1, Jan. 1971, p. 40.

[116]Di Capua, M. S. and Jahn, R. G., "Energy Deposition in Parallel-Plate Plasma Accelerators," A.I.A.A. Paper 71-197, A.I.A.A. 9th Aerospace Sciences Meeting, New York, N. Y., 25-27 Jan. 1971.

PROJECT REFERENCES

[117]Oberth, R. C. and Jahn, R. G., "Anode Phenomena in High-Current Accelerators," A.I.A.A. Paper 71-198, A.I.A.A. 9th Aerospace Sciences Meeting, New York, N. Y., 25-27 Jan. 1971.

[118]Jahn, R. G., Clark, K. E., Oberth, R. C. and Turchi, P. J., "Acceleration Patterns in Quasi-steady MPD Arcs," A.I.A.A. Journal, Vol. 9, No. 1, Jan. 1971, pp. 167-172.

[119]Jahn, R. G., von Jaskowsky, W. F. and Clark, K. E., "Pulsed Electromagnetic Gas Acceleration," NASA NGL 31-001-005, semi-annual report for period 1 July 1970 to 31 December 1970, Aerospace and Mechanical Sciences Rept. No. 634p, January 1971, Princeton University, Princeton, N. J.

[120]Jahn, R. G., von Jaskowsky, W. F. and Clark, K. E., "Pulsed Electromagnetic Gas Acceleration," NASA NGL 31-001-005 step-funding renewal proposal for the period 1 October 1971 to 30 September 1972, June 16, 1971, Princeton Univ., Princeton, N. J.

[121]Clark, K. E., Jahn, R. G. and von Jaskowsky, W. F., "Exhaust Characteristics of a Quasi-steady MPD Accelerator," DGLR Symposium on Electric Space Thruster System, Braunschweig, Germany, June 22-23, 1971, DLR Mitt. 71-21, Teil 1, pp. 81-100.

[122]Turchi, P. J. and Jahn, R. G., "Cathode Region of a Quasi-steady MPD Arcjet," A.I.A.A. Journal, Vol. 9, No. 7, July 1971, pp. 1372-1379.

[123]Jahn, R. G., von Jaskowsky, W. F. and Clark, K. E., "Pulsed Electromagnetic Gas Acceleration," NASA NGL 31-001-005, semi-annual report for period 1 January 1971 to 30 June 1971, Aerospace and Mechanical Sciences Dept. No. 634q, July 1971, Princeton University, Princeton, N. J.

[124]Cory, John S., "Mass,Momentum and Energy Flow from an MPD Accelerator," Ph.D. thesis, August 1971, Princeton University, Princeton, N. J.

PROJECT REFERENCES

[125]Cory, J. S. and Jahn, R. G., "Mass, Momentum and Energy Flow from an MPD Accelerator," NASA NGL 31-001-005, Aerospace and Mechanical Sciences Rept. No. 999, September 1971, Princeton University, Princeton, N. J.

[126]Jahn, R. G., von Jaskowsky, W. F. and Clark, K. E., "Quasi-steady Plasma Acceleration," International Symposium on Dynamics of Ionized Gases, University of Tokyo, September 1971.

[127]Di Capua, M. S., "Energy Deposition in the Parallel-Plate Plasma Accelerator," Ph.D. thesis, November 1971, Princeton University, Princeton, N. J.

[128]Di Capua, M. S. and Jahn, R. G., "Energy Deposition in Parallel-Plate Plasma Accelerators," NASA 31-001-005, Aerospace and Mechanical Sciences Rept. No. 1015, December 1971, Princeton University, Princeton, N. J.

[129]Parmentier, N., "Hollow Cathode, Quasi-steady MPD Arc," M.S.E. thesis, December 1971, Princeton University, Princeton, N. J.

[130]Parmentier, N. and Jahn, R. G., "Hollow Cathode, Quasi-steady MPD Arc," NASA NGL 31-001-005, Aerospace and Mechanical Sciences Rept. No. 1023, December 1971, Princeton University, Princeton, N. J.

[131]Jahn, R. G., von Jaskowsky, W. F. and Clark, K. E., "Pulsed Electromagnetic Gas Acceleration," NASA NGL 31-001-005, semi-annual report for period 1 July 1971 to 31 December 1971, Aerospace and Mechanical Sciences Report No. 634r, January 1972, Princeton University, Princeton, N. J.

[132]Oberth, R. C. and Jahn, R. G., "Anode Phenomena in High-Current Accelerators," A.I.A.A. Journal, Vol. 10, No. 1, January 1972, pp. 86-91.

[133]Clark, K. E., "Electric Propulsion," Astronautics and Aeronautics, Vol. 10, No. 2, February 1972, pp. 22-23.

[134]Hixon, T. L., "Near-Ultraviolet Spectroscopic Studies of a Quasi-Steady Magnetoplasmadynamic Arc,"B.A. thesis, April 1972, Princeton University, Princeton, N. J.

[135]Hixon, T. L., "Near-Ultraviolet Spectrographic Studies of AIII in an MPD Arc Discharge," Paper presented at the Northeastern Regional Student Conference, Rutgers University, New Brunswick, N. J., April 29, 1972.

PROJECT REFERENCES

[136]Clark, K. E., Jahn, R. G. and von Jaskowsky, W. F., "Distribution of Momentum and Propellant in a Quasi-Steady MPD Discharge," A.I.A.A. Bulletin, Vol. 9, No. 4, April 1972, p. 165.

[137]Bruckner, A. P. and Jahn, R. G., "Exhaust Plume Structure in a Quasi-steady MPD Arc," A.I.A.A. Bulletin, Vol. 9, No. 4, April 1972, p. 166.

[138]Clark, K. E., Jahn, R. G. and von Jaskowsky, W. F., "Measurements of Mass, Momentum and Energy Distributions in a Quasi-Steady MPD Discharge," A.I.A.A. Paper 72-497, A.I.A.A. 9th Electric Propulsion Conference, Bethesda, Md., 17-19 April 1972.

[139]Bruckner, A. P. and Jahn, R. G., "Exhaust Plume Structure in a Quasi-Steady MPD Arc," A.I.A.A. Paper 72-499, A.I.A.A. 9th Electric Propulsion Conference, Bethesda, Md., 17-19 April, 1972.

[140]Bruckner, A. P., "Spectroscopic Studies of the Exhaust Plume of a Quasi-steady MPD Accelerator," Ph.D. thesis, May 1972, Princeton University, Princeton, N. J.

[141]Bruckner, A. P. and Jahn, R. G., "Spectroscopic Studies of the Exhaust Plume of a Quasi-steady MPD Accelerator," NASA NGL 31-001-005, Aerospace and Mechanical Sciences Rept. No. 1041, May, 1972, Princeton University, Princeton, N. J.

[142]Jahn, R. G., von Jaskowsky, W. F. and Clark, K. E., "Pulsed Electromagnetic Gas Acceleration," NASA NGL 31-001-005 step-funding renewal proposal for the period 1 October 1972 to 30 September 1973, June 1972, Princeton University, Princeton, N. J.

[143]Jahn, R. G., von Jaskowsky, W. F. and Clark, K. E., "Pulsed Electromagnetic Gas Acceleration," NASA NGL 31-001-005, semi-annual report for period 1 January 1972 to 30 June 1972, Aerospace and Mechanical Sciences Report No. 634s, July 1972, Princeton University, Princeton, N. J.

[144]Kelly, A. J. and Clark, K. E., "Plasma Propulsion Systems," Aerospace and Mechanical Sciences Rept. No. 1074, September 1973, Princeton University, Princeton, N. J.

[145]Greco, R. V., Bliss, J. R., Murch, C. K., Clark, K. E., and Kelly, A. J., "Resistojet and Plasma Propulsion System Technology," AIAA Paper 72-1124 (1972).

PROJECT REFERENCES

[146]Jahn, R. G., von Jaskowsky, W. F. and Clark, K. E., "Pulsed Electromagnetic Gas Acceleration," NASA NGL 31-001-005, semi-annual report for period 1 July 1972 to 31 December 1972, Aerospace and Mechanical Sciences Report No. 634t, January 1973, Princeton University, Princeton, N. J.

[147]Fradkin, D. B., "Analysis of Acceleration Mechanisms and Performance of an Applied Field MPD Arcjet," Ph.D. thesis, March 1973, Princeton University, Princeton, N. J.

[148]Jahn, R. G., von Jaskowsky, W. F. and Clark, K. E., "Quasi-Steady Plasma Acceleration," in Dynamics of Ionized Gases, Proceedings of the International Symposium on Dynamics of Ionized Gases sponsored by the International Union of Theoretical and Applied Mechanics, Tokyo, Japan, September 13-17, 1971, University of Tokyo Press, 1973, Edited by M. J. Lighthill, I. Imai and H. Sato.

[149]von Jaskowsky, W. F., Jahn, R. G., Dutt, G. S. and Clark, K. E., "Impact Pressure Measurements in a Quasi-Steady MPD Discharge " Paper dedicated to Prof. H. Maecker, Technical University, Munich, Germany (April 1973).

[150]Jahn, R. G., von Jaskowsky, W. F. and Clark, K. E., "Pulsed Electromagnetic Gas Acceleration," renewal proposal for the period 1 October 1973 to 30 September 1974, June 1973, Princeton University, Princeton, N. J.

[151]Jahn, R. G., von Jaskowsky, W. F. and Clark, K. E., "Pulsed Electromagnetic Gas Acceleration, NASA NGL 31-001-005 semi-annual report for period 1 January 1973 to 30 June 1973, Aerospace and Mechanical Sciences Report No. 634u, July 1973, Princeton University, Princeton, N. J.

[152]Boyle, M. J., and Jahn, R. G., "Effects of Insulator Ablation on the Operation of a Quasi-Steady MPD Arc," A.I.A.A. Paper 73-1090, A.I.A.A. 10th Electric Propulsion Conference, Lake Tahoe, Nev., Oct. 31-Nov. 2, 1973.

[153]Saber, A. J. and Jahn, R. G., "Anode Power Deposition in Quasi-Steady MPD Arcs," A.I.A.A. Paper 73-1091, A.I.A.A. 10th Electric Propulsion Conference, Lake Tahoe, Nev., Oct. 31-Nov. 2, 1973.

PROJECT REFERENCES

[154] von Jaskowsky, W. F., Krishnan, M., Jahn, R. G. and Clark, K. E., "The Hollow Cathode in the Quasi-steady MPD Discharge," A.I.A.A. Paper 73-1092, A.I.A.A. 10th Electric Propulsion Conference, Lake Tahoe, Nev., Oct. 31-Nov. 2, 1973.

[155] Jahn, R. G., von Jaskowsky, W. F. and Clark, K. E., "Pulsed Electromagnetic Gas Acceleration," NASA NGL 31-001-005, semi-annual report for period 1 July 1973 to 31 December 1973, Aerospace and Mechanical Sciences Report No. 634v, Jan. 1974, Princeton Univ., Princeton, N. J.

[156] Saber, A. J., "Anode Power in the Quasi-steady MPD Thruster," Ph.D. thesis, May 1974, Princeton Univ., Princeton, N. J.

[157] Saber, A. J. and Jahn, R. G., "Anode Power in the Quasi-steady MPD Thruster," Aerospace and Mechanical Sciences Report No. 1128, May 1974, Princeton Univ., Princeton, N. J.

[158] Jahn, R. G., von Jaskowsky, W. F. and Clark, K. E., "Pulsed Electromagnetic Gas Acceleration," renewal proposal for the period 1 October 1974 to 30 September 1975, June 1974, Princeton Univ., Princeton, N. J.

[159] Jahn, R. G., von Jaskowsky, W. F. and Clark, K. E., "Pulsed Electromagnetic Gas Acceleration," NASA NGL 31-001-005, semi-annual report for the period 1 January 1974 to 30 June 1974, Aerospace and Mechanical Sciences Report No. 634w, July 1974, Princeton Univ., Princeton, N. J.

[160] Dutt, G. S. and Jahn, R. G., "Acoustics of the Piezoelectric Pressure Probe," Aerospace and Mechanical Sciences Report No. 1179, Aug. 1974, Princeton Univ., Princeton, N. J.

[161] Bruckner, A. P. and Jahn, R. G., "Exhaust Plume Structure in a Quasi-steady MPD Accelerator," A.I.A.A. Journal, Vol. 12, No. 9, Sept. 1974, pp. 1198-1203.

PROJECT REFERENCES

[162]Boyle, M. J., "Acceleration Processes in the Quasi-steady Magnetoplasmadynamic Discharge," Ph.D. thesis, Oct. 1974, Princeton Univ., Princeton, N. J.

[163]Boyle, M. J. and Jahn, R. G., "Acceleration Processes in the Quasi-steady Magnetoplasmadynamic Discharge," Aerospace and Mechanical Sciences Report No. 1188, Oct. 1974, Princeton Univ., Princeton, N. J.

[164]Clark, K. E., "Survey of Electric Propulsion Capability," A.I.A.A. Paper 74-1082, A.I.A.A./S.A.E. 10th Propulsion Conference, San Diego, California, October 21-23, 1974.

[165]Villani, D. D., Ph.D. thesis, Princeton Univ., Princeton, N. J., forthcoming.

GENERAL REFERENCES

A-1 Malliaris, A. C., John, R. R., Garrison, R. L. and Libby, D. R., "Performance of Quasi-steady MPD Thrusters at High Powers," AIAA Journal, Vol. 10, No. 2, February 1972, pp. 121-122.

A-2 Hügel, H., "Flow Rate Limitations in the Self-Field Accelerator," AIAA Paper No. 73-1094 (1973).

A-3 Kitaeva, V. F., Oduitsov, A. N. and Sobovev, N. J., "CW Argon Ion Lasers," Soviet Phys. Uspikhi 12, 1970.

A-4 Rhodes, C. K., "Review of Ultra-violet Laser Physics," J. Quant. Elec., Vol. QE-10, No. 2, Feb. 1974.

A-5 Bates, P. R., Kingston, A. E. and McWhirter, R. W. P., "Recombination Between Electrons and Atomic Ions," Proc. Roy. Soc., London A 267, 297 (1962).

A-6 Bohn, W. L., "Calculations of Inversions in a Decaying Plasma," Tenth International Conference on Phenomena in Ionized Gases, 1971.

A-7 Gudzenko, L. I. and Shelepin, L. A., "Radiation Enhancement in a Recombining Plasma," Soviet Physics-Doklady, Vol. 10, No. 2, August 1965.

A-8 Goldfarb, V. M. and Lukyanov, C. A., "Use of a Plasma Jet to Amplify Radiation," Soviet Physics—Technical Physics, Vol. 13, No. 10, April 1969.

A-9 Bowen, S. W. and Park, C., "Computer Study of Non-equilibrium Excitation in Recombining Nitrogen Plasma Flows," AIAA Journal, Vol. 9, No. 3, March 1971.

A-10 Goldfarb, V. M., Ilina, E. V., Kostygova, I. E. and Lukyanov, C. A., "Spectroscopic Investigation of Supersonic Plasma Jets," Soviet Physics-Doklady, April 1968.

A-11 Bowen, S. W. and Park, C., "Population Inversion of Atomic Carbon in Recombining Plasma Flow," AIAA Journal, Vol. 10, No. 4, April 1972.

GENERAL REFERENCES--cont'd

A-12 Hoffman, P. and Bohn, W. L., Z. Naturforsch. 27a, 5 (1972).

A-13 Irons, F. E. and Peacock, N. J., "Experimental Evidence for Population Inversion in C^{5+} in an Expanding Laser-Produced Plasma," J. Phys. B: Atom. Molec. Phys., Vol. 7, No. 9, 1974, p. 1109.

A-14 Connolly, D. J. and Sovie, R. J., "The Effect of Background Pressure and Magnetic Field Shape on MPD Thruster Performance," AIAA Paper 69-243 (1969).

A-15 Paschen, F., Ann.d. Physik, 50, 901 (1916): Schuler, H., Z. Physik, 35, 323 (1926).

A-16 Byers, D. C., "Performance of Various Oxide Magazine Cathodes in Kaufman Thrusters," NASA TM X-68132.

A-17 Nakanishi, S. and Finke, R. C., "A 9700-hr Durability Test of a 5-cm-diam Ion Thruster," AIAA Paper 73-111 (1973).

A-18 Rawlin, V. K. and Kerslake, W. R., "Durability of the SERT II Hollow Cathode and Future Applications of Hollow Cathodes," NASA TM X-52532 (1969).

A-19 Nakanishi, S., "Durability Tests of a Five-Centimeter Diameter Ion Thruster System," JSR, Vol. 10, No. 9, September 1973, p. 608.

A-20 Nighan, W. L., "Electrical Conductivity of Partially Ionized Noble Gases," The Phys. Fluids, 12, January 1969, pp. 162-171.

A-21 Delcroix, J. L. and Trindade, A. R., "Hollow Cathode Arcs," in Advances in Electronics and Electron Physics, edited by L. Marton, Vol. 35, Academic Press, 1974.

A-22 Csiky, G. A., "Measurements of Some Properties of a Discharge from a Hollow Cathode," NASA TND-4966, (1969).

GENERAL REFERENCES--cont'd

A-23 Lidsky, L. M., Rothleder, S. D., Rose, D. J., Yoshikawa, A., Michelson, C. and Mackin, Jr., R. J., "Highly Ionized Hollow Cathode Discharge," Journal of Applied Physics, Vol. 33, No. 8, 1962.

A-24 Byers, D. C. and Banks, B. A., "Survey of Electron-Bombardment Thruster Research," IEEE Transactions on Plasma Science, Vol. PS-2, No. 2 (June 1973).

A-25 Philip, C. M., "A Study of Hollow Cathode Discharge Characteristics," Royal Aircraft Establishment, Farnborough, England, 1969.

APPENDIX A: Semi-annual Statement of Expenditures

PULSED ELECTROMAGNETIC GAS ACCELERATION
NASA NGL 31-001-005

1 July 1974 to 31 December 1974

DIRECT COSTS

I.	Salaries		
	Professional	$19,925	
	Technicians	14,022	
	Students	5,918	
	Supporting Staff	2,353	
			$42,218
II.	Employee Benefits (22½%)		8,167
III.	Materials and Services		6,473
IV.	Travel		1,550
V.	Tuition		1,200
	TOTAL Direct Costs		$59,608

INDIRECT COSTS

VI.	Overhead (80%, 86½%)		33,956
		TOTAL	$93,564

C-2